Binding and Signaling Differences between Prostaglandin E_1 and E_2 Mediated by Prostaglandin E Subtype Receptors

---

A Dissertation Presentation to

The Department of Pharmacological and Pharmaceutical Sciences

University of Houston

In Partial Fulfillment of

The Requirement for the Degree

Doctor of Philosophy

By

Annirudha Jaikaran Chillar

August 2010

BINDING AND SIGNALING DIFFERENCES BETWEEN PROSTAGLANDIN E_1 AND E_2 MEDIATED BY PROSTAGLANDIN E SUBTYPE RECEPTORS

A dissertation for the degree Doctor of Philosophy

By

_____

Annirudha Jaikaran Chillar

Approved by Dissertation Committee:

_____

Dr. Ke-He Ruan, MD, Ph.D. Professor of Medicinal Chemistry & Pharmacology Director of the Center for Experimental Therapeutics and Pharmacoinformatics ,PPS

_____

Dr. Diana Chow Ph.D, Committee Member, Professor of Pharmaceutics,
Director, Institute for Drug Education and Research

_____

Dr. Xiaolian Gao, Ph.D, Committee Member
Professor, Department of Biology and Biochemistry

_____

Dr. Louis Williams, Ph.D, Committee Member
Associate Professor of Medicinal Chemistry, PPS

_____

Dr. Joydip Das, Ph.D, Committee Member
Assistant Professor of Medicinal Chemistry, PPS

_____

Dr. F. Lamar Pritchard, Dean
College of Pharmacy

August 2010

ACKNOWLEDGEMENTS

I would like to thank Dr. Ke-He Ruan for being my advisor and giving me the freedom to think freely. I would also like to thank my committee member Dr. Chow for being the most loving faculty and giving me support when I needed it the most. I would also like to thank my committee member Dr. Williams for being there as a wonderful ear and shoulder on which I could relentlessly cry on. I would also like to thank my committee member Dr. Gao who's encouragement made me work hard in the lab. I would also like to thank my committee member Dr. Das for his friendly support as a neighboring lab. I would also like to thank Dr. Bond for making me realize that the system is at fault, when I was finding faults with myself. I would also like to thank Dr. Lokhandwala for telling me that I could become anything I wanted to if I was capable enough. I would also like to thank Dr. Alkadhi for teaching me how to become steadfast. I would also like to thank Dr. MariVi for being the pleasant psychologist who I always felt knew and understood everything. I would also like to thank Dr. Pedemonte for telling me that everyone has a choice to either become a worker bee or a thinker. I would also like to thank Dr. Knoll for his humility and his faith that some day the system will improve. I would also like to thank Dr. Eikenburg for making me realize that a friendly childlike innocence can challenge the world and never wilt. I would also like to thank Dr. Schwarz for her profusely positive atmosphere which I cherished all throughout. I would also like to thank Dr. Szilagyi for making me realize the value of the sense of belonging. I would also

like to thank Dr. Lemke for his carefree adventurous persona. I would also like to thank Dr. Hussain for making me realize the strength in simplicity. I would also like to thank Dr. Hu for teaching me that one can be an island if one wants to. I would also like to thank Dr. Lau for maintaining the atmosphere and keeping the oxygen flowing. I would also like to thank Dr. Antel and Dr. Khator for being the channel that connects me to my universe.

I would like to thank all the graduate students for their continuous love and support. I would also like to thank Alice and Vanessa for being the most wonderful and cooperative lab colleagues that I could hope for. I would like to thank Jaixin for his help in the NMR data. I would also like to thank Alice for designing the hybrid enzyme. Above all I would like to thank my family who never gave me thoughts but always gave me freedom to think. I thank everyone for sharing that freedom with me.

Binding and Signaling Differences between Prostaglandin E_1 and E_2 Mediated by

Prostaglandin E Subtype Receptors

A Dissertation Presentation to
The Department of Pharmacological and Pharmaceutical Sciences
University of Houston

In Partial Fulfillment of
The Requirement for the Degree
Doctor of Philosophy

By
Annirudha Jaikaran Chillar
August 2010

ABSTRACT

Prostaglandin E_1 (PGE_1) and E_2 (PGE_2) are ligands for the prostaglandin E_2 receptor (EP) family, which consists of four subtype receptors, designated as EP_1, EP_2, EP_3 and EP_4. Interestingly, PGE_2 mediates inflammation whereas PGE_1 acts as an anti-inflammatory factor. However, the molecular basis of their opposite actions on the same set of EP receptors is poorly understood. To study the ligand recognition differences, a potential high throughput mutagenesis and constrained peptide was used. A peptide constrained to a conformation of the second-extracellular loop of human prostaglandin-E_2 (PGE_2) receptor subtype 3 (hEP_3) was synthesized. The contacts between the peptide residues at S211 and R214, and PGE_2 were first identified by NMR spectroscopy. The results were used as a guide for site-directed mutagenesis of the hEP_3 protein. The S211L and R214L mutants expressed in HEK293 cells lost binding to [^{3}H]PGE_2. This study found that the non-conserved S211 and R214 of the hEP_3 are involved in PGE_2 recognition. The mutant S211L was able to give a calcium signal with PGE_1, but not with PGE_2. This implied that the corresponding residues in other subtype receptors could be important in distinguishing the different configurations of PGE_2 and PGE_1 ligand recognition sites.

Direct transfection of point mutants in the EP_1 receptor extracellular loop (using PCR products) was evaluated in HEK293 cells. Twenty-four EP_1 extracellular loop mutants (alanine scan) were generated using phosporylated primers and ligase. The PCR product was directly transfected into HEK293 cells and the [^{3}H]-PGE_2 binding and PGE_1

and PGE_2 calcium signaling assay evaluated. Three mutants, A104G, P105A and P184A, showed reduced [^{3}H]PGE_2 binding, but could not differentiate between PGE_1 and PGE_2 in the calcium signaling assay. However, we propose that this novel high throughput mutagenesis approach using direct PCR product transfection can be integrated into a high throughput screening machine in the future.

The PGE_1 and PGE_2 binding affinity on the four human recombinant EPs expressed in the live HEK293 as stable cell lines was determined by [^{3}H]PGE_2 binding. The PGE_1 and PGE_2 signaling on the four EPs was determined by the calcium (Ca^{2+}) and cyclic AMP signaling. The Kd for [^{3}H]PGE_2 was calculated using saturation kinetic experiments. The IC50 of PGE_2 and PGE_1 were calculated from [^{3}H]PGE_2 displacement experiments using cold PGE_2 and PGE_1, respectively. PGE_2 showed higher affinity or preference for EP_3 and EP_4 as compared to that of EP_1 and EP_2. PGE_1 also showed a higher Ca^{2+} signal in EP_1 as compared to that of PGE_2. There was a two-log concentration difference between PGE_2 and PGE_1 for generation of Ca^{2+} signal in EP_4. There was no difference in cAMP accumulation with PGE_1 and PGE_2. Leukotriene C4/D4/E2 levels were higher in the EP_1 stable cell line upon stimulation with PGE_2, but not PGE_1. An anti-inflammatory molecule, 20 hydroxy lipoxin B4, peak was observed using mass spectroscopy with PGE_1 and not PGE_2.

We also used a newly engineered hybrid enzyme (COX-2-10aa-mPGES-1) linking COX-2 and mPGES-1 together thus adopting the full biological activity of COX-2 and

mPGES-1 in directly converting AA to PGE_2. This enzyme was genetically introduced into HEK293 cells. These cells expressing the COX-2-10aa-mPGES-1 were producing higher level of PGE_2 using endogenous AA as confirmed by LC/MS analysis. A new mouse model of cancer was developed by subcutaneous injection of these cells into Balb/c/nu/nu mice. A 100% (8 out 8) occurrence rate of cancer mass was detected in these cells. In contrast, 30% occurrence of cancer mass were determined for the groups of the cells co-expressing the individual COX-2 and mPGES-1. The presence of EP_1 and EP_2 stable cell line growth around these tumor masses confirmed their involvement in cancer.

In conclusion, the Ca^{2+} signal indicated that the EP_1 is likely the dominant and ligand-differentiating receptor in terms of signaling in tissues that co-express the EPs (cancer cells). PGE_2 is likely to cause inflammation through leukotrienes and PGE_1 is likely to be anti-inflammatory due to its ability to produce Lipoxin B4. High throughput mutagenesis for producing multiple-point mutations using direct PCR product transfection is a promising new method for the future. The experiments on nude mice indicated that the sole coupling of COX-2 to mPGES-1 is a powerful cancer-advancing factor, which implies that the coupling of COX-2 to mPGES-1 is a promising target for anti-cancer drug development. EP_1 and EP_2 receptors were identified as the likely receptors, to induce cancer. This study provides a molecular basis to understand the biological functions of PGE_1 and PGE_2 through their binding and signaling properties.

TABLE OF CONTENTS

LIST OF ABBREVIATIONS

$[^{14}C]AA$	Tritium labeled arachidonic acid
AA	Tritium labeled arachidonic acid
Akt	Protein kinase B
BALB/c nu/nu	The autosomal recessive nude gene in homozygous (nu/nu) mice causing immune deficiency.
Ca^{2+}	Calcium
cAMP	Cyclic adenosine monophosphate
CD	Circular Dichroism Spectroscopy
COX	Cyclooxygenase
COX-2-10aa-mPGES-1	Hybrid enzyme (cyclooxygenase 2 -10 amino acid - microsomal Prostaglandin E synthase
cPGES	Cytosolic Prostaglandin E synthase
CREB	cAMP responsive element binding protein
CYP1B1	Cytochrome 1B1
D_2O	Deuterium oxide
DLD1	Colorectal adenocarcinoma
DP	Prostaglandin D_2 receptor
DQF-COSY	Double-quantum filtered correlated spectroscopy
EIA	Enzyme immunoassay
eLP_2	Second extracellular loop

EP_1	Prostaglandin E subtype 1 receptor
EP_2	Prostaglandin E subtype 2 receptor
EP_3	Prostaglandin E subtype 3 receptor
EP_4	Prostaglandin E subtype 4 receptor
ERK	Extracellular signal- regulated kinase
FP	Prostaglandin $F_{2\alpha}$ receptor
GPCR	G protein coupled receptors
GSK-3β	Glycogen synthase kinase-3β
HCC1954	Ductal carcinoma of the breast
HEK293 cells	Human embryonic kidney cells
IP	Prostacyclin receptor
LC/MS/MS	Liquid chromatography-mass spectrometry-mass
MAPK	Mitogen-activated protein kinase
MCP-1	Monocyte chemoattractant protein-1
mPGES-1	Microsomal Prostaglandin E synthase
Myeov	MYEloma OVerexpressed gene
N217L	Asparagine 217 mutated to Leucine
NF-IL-6	Nuclear factor- interleukin-6
NMR	Nuclear magnetic resonance
NOESY	Nuclear Overhauser effect (NOE)
NSAIDs	Nonsteroidal anti-inflammatory drugs

PCR	Polymerase chain reaction
PGE_1	Prostaglandin E_1
PGE_2	Prostaglandin E_2
PGES	Prostaglandin E synthase
PI3K	Phosphoinositide-3-kinase
PKA	Protein kinase A
PLA_2	Phospholipase A_2
PLC	Phospholipase C
$[^3H]PGE_2$	Tritium labeled PGE_2
R214L	Arginine 214 mutated to Leucine
S211L	Serine 211 mutated to Leucine
SAR	Structure activity relationship
STAT	Signal transducer and activator of transcription
TM	Transmembrane
TOCSY	TOtal Correlation SpectroscopY
TP	Thromboxane A_2 receptor
Trp	Tryptophan
VEGF	Vascular endothelial growth factors

LIST OF TABLES

LIST OF FIGURES

1. INTRODUCTION AND STATEMENT OF PROBLEM

Prostaglandin (PG) E_2 and PGE_1 exert actions by acting on a group of EP receptor subtypes designated EP_1, EP_2, EP_3 and EP_4. EP subtype knock-out mice have identified the role of each EP subtype in various physiological and pathophysiological responses (Narumiya et al., 1999). For example, the EP_3 receptor mediates the pyrogenic response (Ushikubi et al., 1998), EP_1 and EP_3 mediate release of corticotropin-releasing hormone (Matsuoka et al., 2003), EP_2 facilitates ovulation and fertilization (Hizaki et al., 1999) and EP_2 and EP_4 mediate collagen-induced arthritis (Miyauchi, 1994). This highlights the discreet function of the individual receptors. However, the endogenous ligand, PGE_2, acts as an inflammatory molecule, whereas PGE_1 acts as an anti-inflammatory molecule; nevertheless, both act on the same set of EP receptors albeit with different affinities (Murota et al., 2008; Sobota et al., 2008). PGE_1 is being used clinically for treating collagen disease-related skin ulcers (Murota et al., 2008) and prevents apoptotic cell death in superficial dorsal horn of rat spinal cord with anticipated beneficial role in Alzheimer's and Parkinson's disease (Kawamura et al., 1997).

The agonists in EP receptors induce a signaling cascade inside the cell which seems to have similarities and yet show different signaling outcomes. EP_1 receptors mediate signaling by activation of phospholipase C (PLC), protein kinase Cα and c-Src with upregulation of endothelial growth factor-C (Su et al., 2004) and epidermal growth factor receptor (Han and Wu, 2005, Watanabe, 1999). The EP_2 and EP_4 are linked to

cAMP/protein kinase A (PKA) and phosphoinositide-3-kinase (PI3K) signaling (Okuyama, et al., 2002). The EP_3 receptors however couple to multiple G proteins such as the Gi subunits, resulting in the inhibition of adenylyl cyclase and Gs subunit resulting in cAMP production (Katoh et al., 1998; Tamma et al., 2003). This fact led us to choose EP_3 as our primary receptor for ligand residue interaction identification studies as the probability of recognizing differences in ligand recognition would be higher. EP_3 receptors can also activate the Ras signaling pathway leading to cancer (Yano et al., 2002).

Many studies demonstrate that the second extracellular loop of the receptor is involved in prostanoid-ligand recognition in the rabbit EP_3 receptor. Site-directed mutagenesis of seven conserved residues in the second extracellular loop of EP_3 (EP_3 eLP_2), in transfected HEK293 cells was assessed for their ability to decrease intracellular cAMP (Audoly and Breyer, 1997). However, we hypothesized that the differences in ligand recognition and ultimately the functional effect must logically lie in the non-conserved region as these EP receptors have multiple common ligands showing different effects; ie. PGE_2 acts as an inflammatory molecule, whereas PGE_1 acts as an anti-inflammatory molecule and both act on the same set of EP receptors with different affinities (Murota et al., 2008; Sobota et al., 2008; Miyauchi, 1994).

Thus, in order to understand the EP receptors, it is important to uncover how the eight prostanoid receptors distinguish between the similar prostanoids, which are synthesized from the same precursor, PGH_2. Using the TM (transmembrane) domains of

the working model for the EP_3 receptor, the constrained peptides mimicking the EP_3 eLP_2 was synthesized and purified. The residues in the EP_3 eLP_2 interacting with PGE_2 in solution were determined by NMR spectroscopy. This method will help us recognize the fundamental differences that give quality to a receptor and can be used to benefit therapeutics.

We used various integrated approaches including constrained peptide, mutagenesis, CD/fluorescence (FL), and molecular modeling. Other than these we will use a novel high throughput mutagenesis approach using DNA fragments for identification of residues involved in ligand recognition. Another approach to identify ligand specific residues is to create point mutations in receptors using PCR products. Studies have shown that double stranded (ds) DNA molecules as PCR products could mimic promoter or enhancer sequences which can be used for manipulating the transcriptional machinery of a specific gene. These PCR fragments can be easily captured by the cells and has been postulated as a potential therapeutic tool to control disease-related genes (Santori et al., 2006). Also, PCR products using biotinylated primers can be conveniently used to introduce a site-directed mutation, which obviates the need for cloning or plasmid purification (Penolazzi et al., 2007; Piva et al., 1998). Thus residues involved in ligand recognition can be studied using PCR products for generating receptors with point mutation. These point mutated PCR products can be directly transfected into HEK293 cells for evaluation.

These EP receptors signal mainly through activation or inhibition of calcium (Ca^{2+}) and cyclic AMP (cAMP) signaling. Many studies have identified the Ca^{2+} and cAMP signal for the EP receptors but none have quantified the signal nor evaluated the ligands' likely choice of a dominant EP receptor. Therefore, by comparing the binding affinities of the ligands with their signaling intensity we might be able to understand better the differences between PGE_1 and PGE_2 and their receptors.

The spatial and temporal properties of intracellular Ca^{2+} signals are important (Berridge et al., 2000) because a large number of cellular processes are dependent on the Ca^{2+} signal. For example, gene transcription in T cells (Li et al., 1998; Dolmetsch et al., 1998), and the exocrine function of acinar cells of the pancreas and salivary glands are examples of spatially and temporally localized signals (Maruyama et al., 1993; Giovannucci et al., 2002). These Ca^{2+} signals are shaped by the concomitant activation of additional signal transduction pathways, such as the cAMP concentrations. The crosstalk between Ca^{2+} and cAMP has also been demonstrated by the fact that Ca^{2+} can affect components of the cAMP signaling machinery. Calcium can either activate or inhibit different subtypes of adenylyl cyclase which produce cAMP (Cooper et al., 1995; Mons et al., 1998) and different subtypes of phosphodiesterase which degrade cAMP (Kakkar et al., 1999).

Therefore, by quantifying the Ca^{2+} and cAMP signal generated by PGE_1 and PGE_2 we expect to better understand the signaling patterns that might help us determine the

reason for their opposite action. Since PGE_2 is involved in promotion of various cancer growths (Chen et al., 2007; Thorat et al., 2007; Gustafsson et al., 2007; Chang et al., 2005; Shoji et al., 2004; Chell et al., 2006), it will be interesting to evaluate the choice of dominant EP receptor that it is likely to be used for its action by correlating the binding affinity with the signaling intensity.

Since these EP receptors are co-expressed in various organ systems, we have expressed them individually as recombinant receptors in HEK293 cells. We have shown the binding affinity differences of PGE_1 and PGE_2 on EP receptors in whole live cells. We have also shown how the binding affinity of PGE_1 and PGE_2 reflects on the efficacy (intensity of Ca^{2+} and cAMP signaling). This has helped us determine the likely dominant EP receptor as a potential target site for cancer proliferation and differentiation. The importance lies in the fact that it helps us recognize the dominant EP receptor and differentiate between PGE_1 and PGE_2 which are similar in their structure, and yet have opposite functions.

Endogenous prostaglandin E_2 (PGE_2) is known to play an important role in cell functions such as stem cell proliferation and tissue and bone regeneration (Murakami et al., 2002). Prostaglandin (PG) E_2 is the major prostanoid produced in several cancers and has been implicated in the development of colorectal cancer. PGE_2 has been shown to promote colon cancer cell survival in vitro and tumorigenesis and angiogenesis in vivo (Sheng et al., 2001; Levy, 1997; Reinhart et al., 1983). Use of certain nonsteroidal anti-

inflammatory drugs (NSAIDs) causing PGE_2 deficiency could produce stomach ulcers and possibly affect stem cell development (North et al., 2007). However, PGE_2 in disease states acts as a pro-inflammatory and cancer promoting molecule (Murakami and Kudo, 2006). PGE_2 is produced from arachidonic acid (AA) and requires the catalytic activity of two enzymes (cyclooxygenase (COX) and prostaglandin E synthase (PGES)) (Ruan and Dogne, 2006; Ruan, 2004). COX-2 overexpression has also been shown in various cancer cells and tissues (Subbaramaiah et al., 1996; Kargman et al., 1995). Inhibition of this COX-2 with Non-steroidal anti-inflammatory drugs, have been shown to reduce the incidence of colorectal cancer (Marnett, 1992; Rao et al., 1995; Sheng et al., 1997). Experiments on Apc mutant mice (a model for human familial adenomatous polyposis) have shown that Gene disruption of COX-2 (Oshima et al., 1996) results in reduction of the number and size of intestinal polyps.

Similarly, PGES catalyzes the conversion of PGH_2, to PGE_2. There are at least three PGES enzymes, which include cytosolic PGES (cPGES) (Tanioka et al., 2000), microsomal PGES (mPGES) -1 (Jakobsson et al., 1999; Murakami et al., 2000; Mancini et al., 2001), and mPGES-2 (Tanikawa et al., 2002). Among these, it is the microsomal PGES-1 (mPGES-1) which is induced by pro-inflammatory stimuli, and is functionally coupled dominantly with COX-2 in comparison to COX-1 (Jakobsson et al., 1999; Murakami et al., 2000; Mancini et al., 2001). mPGES-1 is also over expressed in a variety of cancers along with COX-2 (Yoshimatsu et al.,2001; Jabbour et al., 2001; Yoshimatsu et

al.,2001). Many pathophysiological events involving COX-2-derived PGE_2, such as rheumatoid arthritis (Stichtenoth et al., 2001), fever (Yamagata et al., 2001), fertility (Filion et al., 2001; Lazarus et al., 2002), bone metabolism (Murakami et al., 2000), and Alzheimer's disease (Satoh et al., 2000), show an induced expression of mPGES-1. This induced expression of mPGES-1 is regulated by the NF-IL-6 pathway (Uematsu et al., 2002) or the mitogen-activated protein kinase pathway (Han et al.,2002), which stimulates the mPGES-1 gene transcription (Naraba et al., 2002).

We have engineered a hybrid enzyme, "Tri-Cat enzyme," inducible COX isoform-2 (COX-2) linked to inducible microsomal PGES-1, which can specifically convert AA into PGE_2 in the cells transfected with the cDNA of the Tri-Cat Enzyme (Ruan et al., 2006, 2008, 2008). We are thus able to re-direct and control the outcome of AA utilization by the COX pathway and the downstream enzymes in cells. The COX-2-10aa-mPGES-1 hybrid enzyme is thus able to produce excess PGE_2. We have used this novel hybrid enzyme that links human COX-2 and mPGES-1 through a well-defined transmembrane (TM) domain of 10 amino acids called COX-2-10aa-mPGES-1 to produce tumors in immune deficient Balb/c/nu/nu mice.

To date, there have been no animal tumor models designed for testing the anti-proliferative activity of COX-2 and mPGES-1 inhibitors. Our proposed model is target-specific for COX-2 and mPGES-1. This is important because the direct shifting of the results from the lab and non-specific animal studies to human clinical trials has created

many risks with damages to the patients during the human use of NSAIDs in the past. Vioxx has been the most recent typical case of this type (Konstam et al., 2001). The proposed tumor mice model that over-expresses COX-2-10aa-mPGES-1 (to produce excess PGE_2) could be a sufficiently sensitive animal model for anti-inflammation and anti-tumor efficacy tests. We propose that screening the COX-2 and mPGES-1 inhibitors for their anti-proliferative activity or ability to suppress tumor formation and reduce inflammatory PGE_2 production can be studied. We also propose that the tumors produced as a result of COX-2-10aa-mPGES-1 over expressed in HEK293 cells can be used to evaluate the EP receptors involved in cancer generation. The PGE_2 produced from the tumor can diffuse into the surrounding tissue and stimulate the EP receptor stable cell lines, thereby causing them to produce tumors as well. We propose that this strategy of using a primary tumor source for producing an inflammatory ligand, and a peripheral tumor for receptor studies, can be applied to other pathways as well.

The results from this study will advance the understanding of the structure/function relationship of GPCR receptors that share common ligands and yet exhibit opposite pathophysiological functions. They will also enhance the understanding of other GPCRs in general. The ligand preference in the EP receptors could also be used for selectively targeting cancers and stem cells whose proliferation and differentiation is influenced by EP receptor signaling (Han and Wu, 2005; Okuyama et al., 2002; Chen et al., 2007). The importance of our objective lies in the fact that it will help us recognize

the fundamental differences that give quality to a receptor and its ligand and can be used for the future benefit of therapeutics (Figure 1).

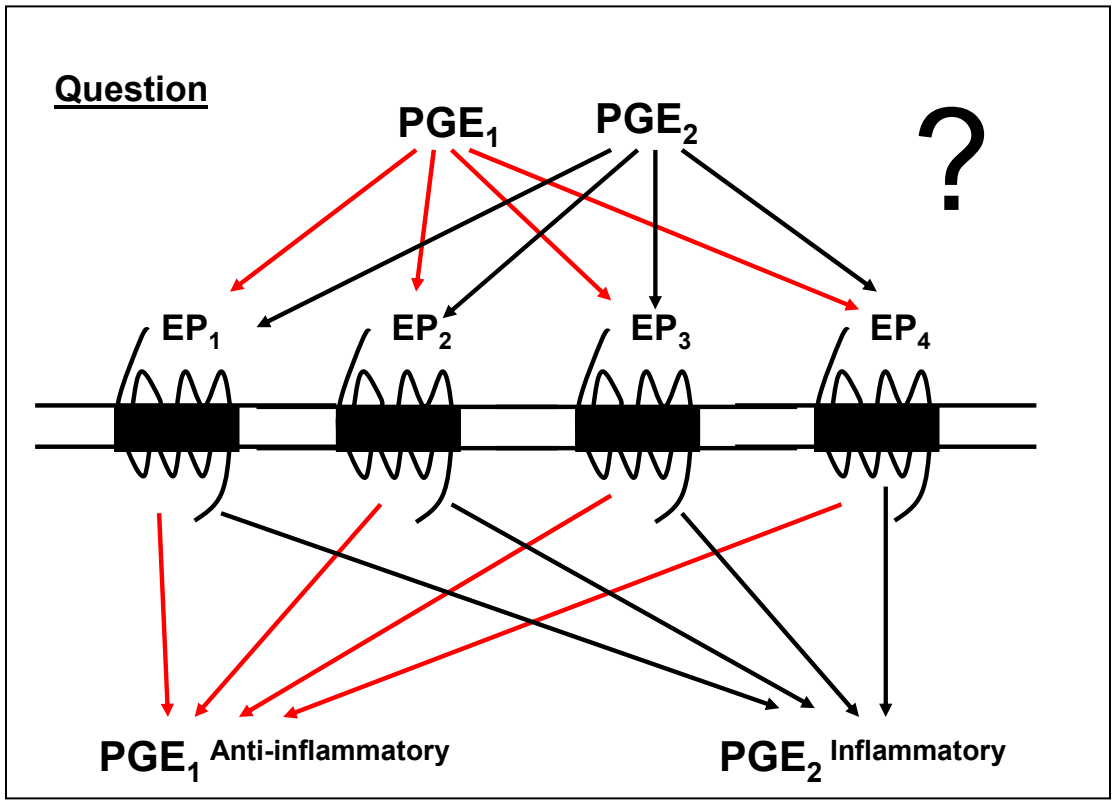

Figure 1: The schematic of the introduction to the statement of problem. PGE_1 and PGE_2 are ligands common to a set of EP receptors called EP_1, EP_2, EP_3 and EP_4, however PGE_1 is anti-inflammatory whereas PGE_2 is an inflammatory molecule. Therefore our statement of problem is to determine how two ligands activating the same set of receptors are able to produce opposite functions.

2. REVIEW OF LITERATURE

2.1. Prostaglandin E_2 subtype EP receptors

PGE_2 is the most abundant naturally occurring prostanoid and is derived de novo from arachidonic acid. (Campbell, 1990; Davies and MacIntyre, 1992). It has autocrine and paracrine function and is released in response to a variety of stimuli in many tissues, where they participate in a broad spectrum of physiological and pathophysiological events (Coleman et al., 1989). This has been implicated in a number of disease processes (Abramovitz and Metters, 1998). PGE_2 primarily produces its effect through interaction with four distinct prostanoid receptors: EP_1, EP_2, EP_3, and EP_4 (Coleman et al., 1994). They are members of the G-protein coupled receptor superfamily called as integral serpentine plasma membrane proteins (Boie et al., 1995). The signaling pathways involved in the four EP receptor subtypes are: EP_1 couples to $[Ca^{2+}]$ (Funk et al., 1993), EP_2 (Regan et al., 1994) and EP_4 (Bastien et al., 1994) cause an increase in intracellular cAMP accumulation, and EP_3 causes a decrease in intracellular cAMP levels (Boie et al., 1997; Jin et al., 1997) (Figure 2).

When all eight prostanoid receptors are aligned, including the four EP receptor subtypes (TP, Hirata et al, 1991; FP, Abramovitz et al., 1994; IP, Boie et al., 1994; DP, Boie et al., 1995), two subgroups are formed. These two subgroups can be easily differentiated by the signal transduction pathway to which the receptors couple, rather than their ligand interaction: thus, EP_1, FP, TP, and EP_3 receptors couple to Gαq/Gαi,

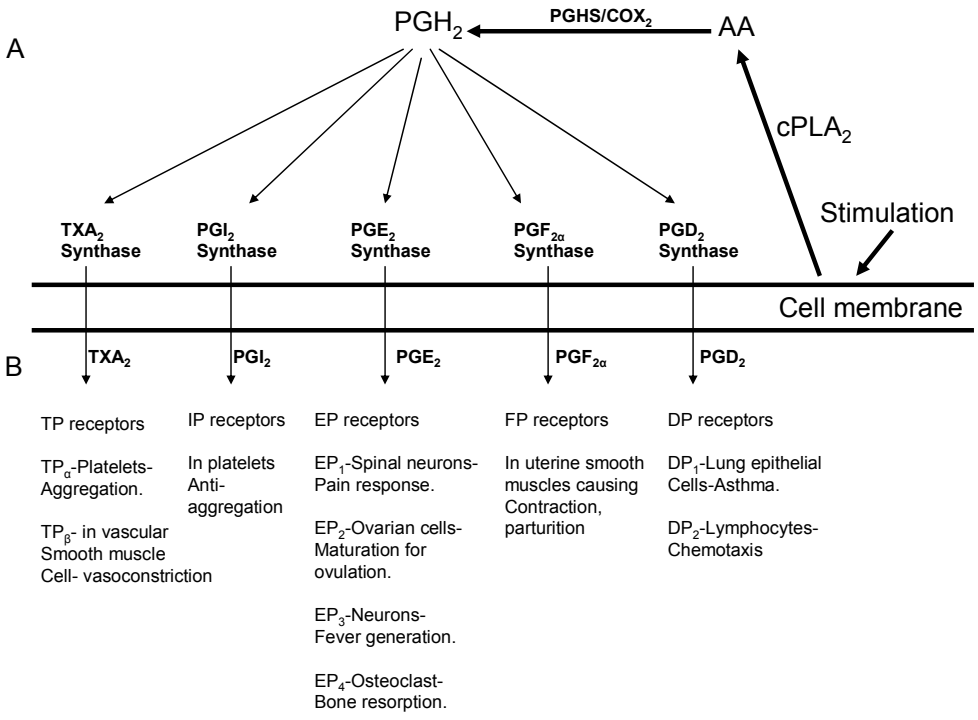

Figure 2: Simplified cascade of the prostanoid pathway. (A) Shows the enzymes and substrates involved starting from arachidonic acid (AA) being formed by stimulation of the cell membrane with the help of cytosolic phospholipase A_2 ($cPLA_2$). This AA is the substrate for Prostaglandin H synthase (PGHS also called cyclooxygenase COX) which produces prostaglandin H_2 (PGH_2). PGH_2 is the substrate for the various synthases producing their respective prostaglandins (Thromboxane A_2 (TXA_2) , Prostacyclin (PGI_2), Prostaglandin $F_{2\alpha}$ ($PGF_{2\alpha}$), Prostaglandin D_2 (PGD_2) and Prostaglandin E_2 (PGE_2). (B) Panel shows the various effector systems and functions of the prostaglandins produced.

whereas the EP_2, EP_4, DP, and IP receptors couple to Gαs (Boie et al., 1995; Toh et al., 1995). Preliminary molecular models of the EP receptors show a few common residues found in the putative ligand binding pocket which are also present in one or more of the non-EP prostanoid receptors (Yamamoto and Imai, 1996). A number of SAR studies of

prostanoids and prostanoid analogs, using tissues with mixed expression of populations of two or more receptors, have been performed with limiting interpretation of the results (Lawrence et al., 1992). Detailed SAR studies are currently being performed using recombinant systems expressing individual prostanoid receptors. The cloning of the prostanoid receptor family (Coleman et al., 1994; Boie et al., 1995) has opened the pathway for evaluation of compounds on all eight prostanoid receptors (Kiriyama et al., 1997; Abramovitz et al., 2000). Characterization of the EP receptors has been performed on bovine chondrocytes (Fernandes et al., 1996) and mouse podocytes (Bek et al., 1999).

The four EP receptors are encoded in separate genes and are well conserved throughout the mammalian system. Phylogenetic analysis of the amino-acid sequence indicates that they were all sequentially derived from a primitive PGE receptor by gene duplication (Toh et al., 1995). EP_3 and EP_1 receptor isoforms generated by alternative splicing of their mRNA have been reported (Irie et al., 1993; Namba et al., 1993; An et al., 1994; Breyer et al., 1994; Regan et al., 1994; Schmid et al., 1995; Okuda et al., 1996; Pierce and Regan, 1998; Oldfield et al., 2001). All EP receptor subtypes are expressed on the plasma membrane. EP_3 and EP_4 receptors also have nuclear membrane localization (Bhattacharya et al., 1998, 1999).

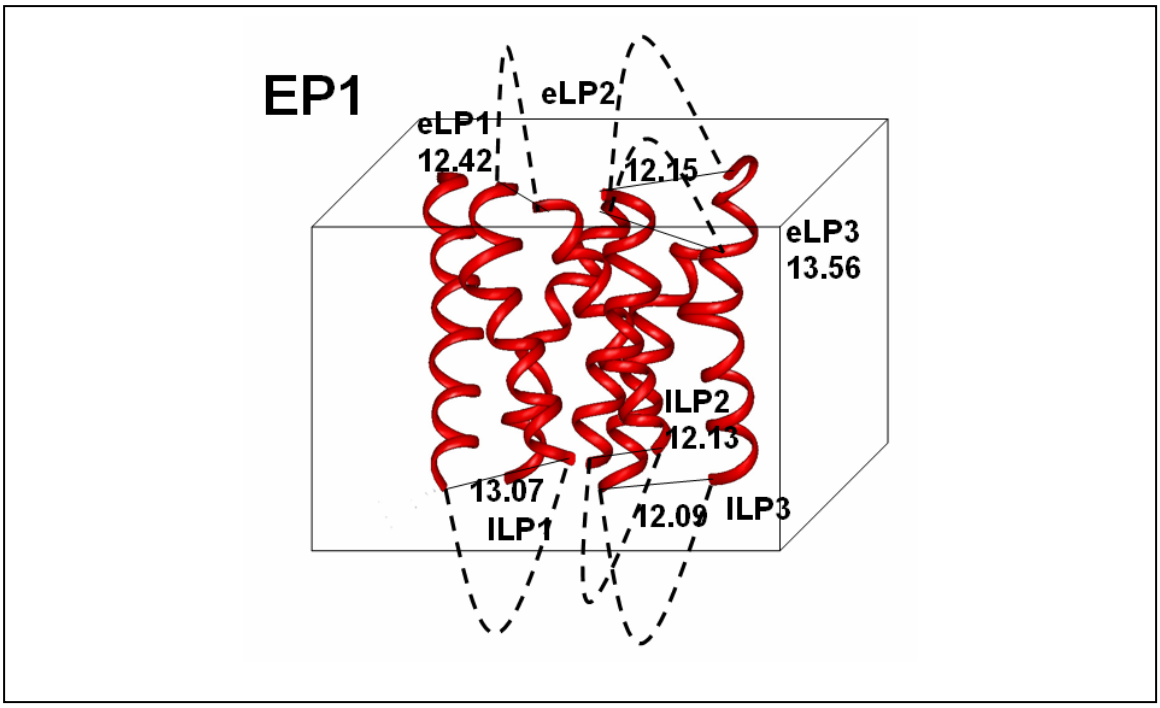

Figure 3: Homology model of the EP_1 receptor using the β2 adrenergic receptor as the template. Felix 2000 software was used to align the residue sequence of the β2 adrenergic receptor with the EP_1 receptor sequence and generate the model. The distance between the transmembrane loops is shown in angstrom units (Å).

2.2. EP_1 receptor

The EP_1 receptor has been cloned from humans and rodents (Funk et al., 1993; Watabe et al., 1993; Okuda et al., 1996). EP_1 has two splice variants (Okuda et al., 1996). EP_1 has the least affinity for PGE_2 among the four subtypes of EP receptors, (dissociation constant (KD) of 16–25 nM. The human EP_1 receptor has 402 residues with a predicted molecular mass of 41,858 and is functionally coupled to intracellular calcium (Figure 3). EP_1 binds to PGs in the order of $PGE_2 > PGE_1 > PGF_{2\ alpha} > PGD_2$ (Funk et al., 1993). A few

selective agonists for EP_1 like ONO-DI-004 and 17-phenyl trinor PGE_2 are available. Other agonists such as sulprostone, carbacyclin and enprostil exhibit the highest affinity for EP_1, but are also very potent EP_3 agonists. Antagonists such as ONO-AE-829, ONO-8711, ONO-8713, SC-19220 and AH6809 are available for the EP_1 receptor but possess a weak antagonist activity (Woodward et al., 1995, 2005)(Figure 3).

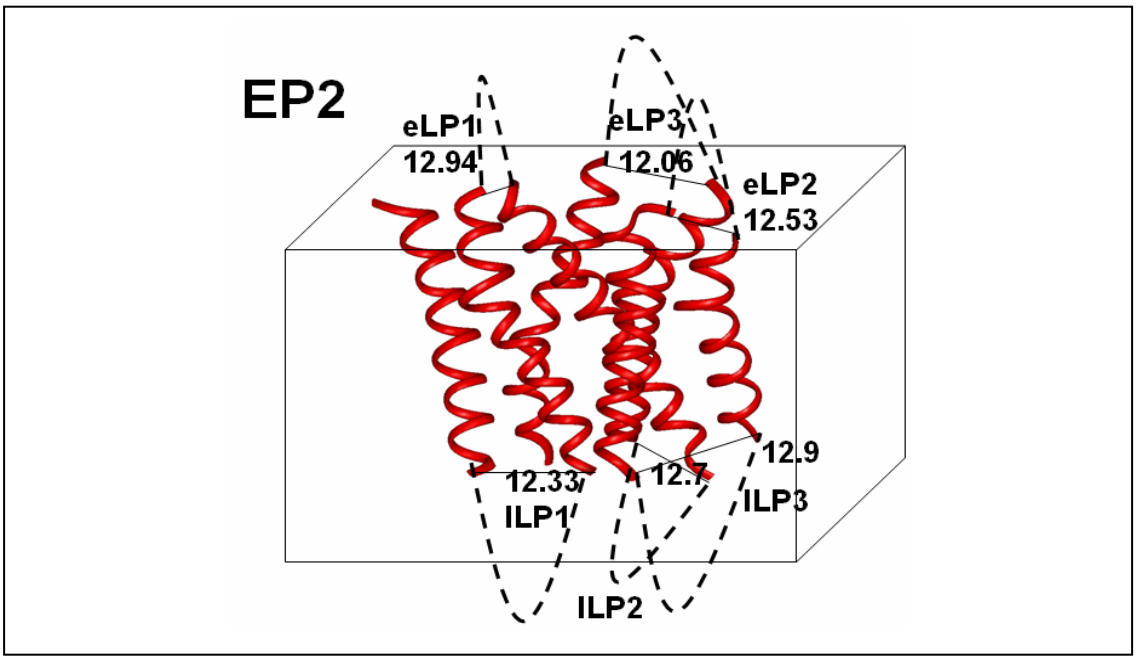

Figure 4: Homology model of the EP_2 receptor using the β2 adrenergic receptor as the template. Felix 2000 software was used to align the residue sequence of the β2 adrenergic receptor with the EP_2 receptor sequence and generate the model. The distance between the transmembrane loops is shown in angstrom units (Å).

2.3. EP_2 receptor

The cloned EP_4 receptor was referred to as EP_2 (Bastien et al., 1994; Regan et al., 1994) before the discovery of the EP_2 receptor in 1994. The EP_2 receptor is a 53 kDa

protein that has been cloned and expressed from various species (humans, bovine, rabbits, rodents and several other) (An et al., 1993; Katsuyama et al., 1995; Guan et al., 1996; Nemoto et al., 1997; Arosh et al., 2003). The human EP_2 consists of 358 residues. EP_2 is functionally coupled to the cAMP (Regan et al., 1994). The affinity of PGE_2 for EP_2 receptor differs greatly across species. The human EP_2 receptor binds PGE_2 and PGE analogues with a rank order of PGE_2>PGE_1>16, 16-dimethyl-PGE_2 >11-deoxy-PGE_1>butaprost,1-OH-PGE_1, M&B-28767 >sulprostone. AH-6809 is a well-known EP_2 antagonist (Dey et al., 2006) (Figure 4).

2.4. EP_3 receptor

The EP_3 receptor has been successfully cloned and expressed from humans and rodents (Sugimoto et al., 1992; Yang et al., 1994). The EP_3 is unique because it has multiple alternatively spliced variants that can activate contrasting second messenger signaling (Pierce and Regan, 1998). The human EP_3 has eight alternatively spliced variants with a predicted molecular mass of between 40 to 45 kDa. EP_3 binds to PGs in the order of PGE_2 = PGE_1 >> $PG_{F2\ alpha}$ = PGI_2 > PGD_2 >> U46619. EP_3 is functionally coupled to the Ca^{2+} mobilization and reduces cAMP production (Adam et al., 1994). The EP_3 receptor has a relatively higher affinity for PGE_2 as evidenced by a very low KD value of 0.33–2.9. L826266 is an EP_3 antagonist (Dey et al., 2006) (Figure 5).

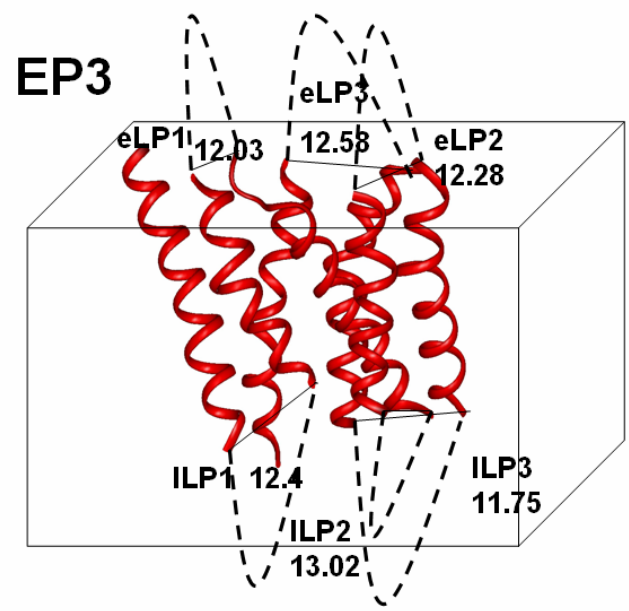

Figure 5: Homology model of the EP_3 receptor using the β2 adrenergic receptor as the template. Felix 2000 software was used to align the residue sequence of the β2 adrenergic receptor with the EP_3 receptor sequence and generate the model. The distance between the transmembrane loops is shown in angstrom units (Å).

2.5. EP_4 receptor

The EP_4 receptor cDNA encodes a 487–513 amino-acid polypeptide that has been cloned and expressed from various species (human, rodents, rabbit, bovine and others) (An et al., 1993; Honda et al., 1993; Breyer et al., 1996; Boie et al., 1997). EP_4 is functionally coupled to cAMP production (Nishigaki et al., 1995). Their affinity for PGE_2 is very high, with a KD value of 0.59–1.27. The rank order of affinity of PGE ligands for the mouse EP_4 receptor was PGE_2, PGE_1>11-deoxy-PGE_1, 16, 16-dimethyl-PGE_2,

misoprostol>1- OH-PGE1 and M&B-28767. Very few selective agonists or antagonists are available for EP_4 (Figure 6).

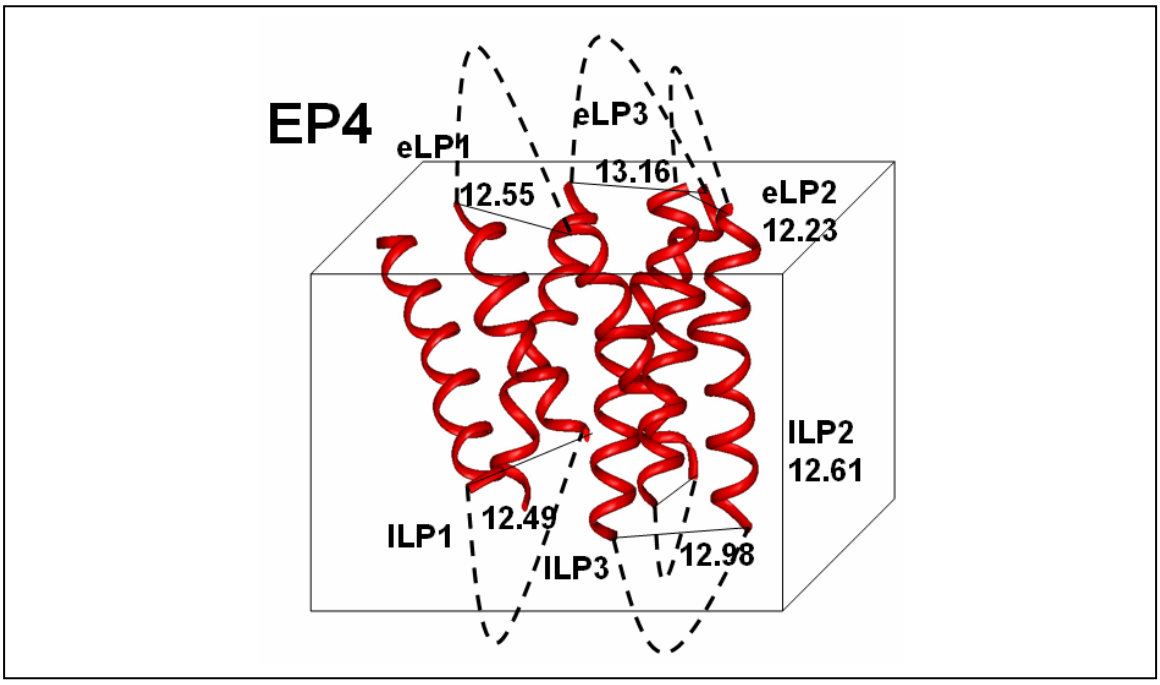

Figure 6: Homology model of the EP_4 receptor using the β2 adrenergic receptor as the template. Felix 2000 software was used to align the residue sequence of the β2 adrenergic receptor with the EP_4 receptor sequence and generate the model. The distance between the transmembrane loops is shown in angstrom units (Å).

2.6. EP receptor signaling and functions

The factors governing the outcome of EP receptor signaling are diverse. These differences are structural, pharmacological or functional. Structural differences related to the length and composition of amino acids in the extracellular, as well as the intracellular domains, are associated with variations in receptor signaling. e.g. Differences in the length of C-termini of EP_3 isoforms are associated with their

differential activation of a variety of second messenger pathways (Pierce and Regan, 1998). Similarly the extracellular sequence of the EP_2 receptor determines its structure and function (Stillman et al., 1999). Likewise, a cluster of hydrophobic aromatic amino acids in the second intracellular loop of EP_2 is essential for activation of Gαs subunit (Sugimoto et al., 2003, 2004). Pharmacologically the affinity of these receptors to its principal ligand, PGE_2, greatly varies between receptor subtypes. The affinity of PGE_2 to its receptor depends on the state of coupling of G protein subunits.

Differences in agonist-induced desensitization have been observed in EP receptors. e.g. the EP_4 receptor is easily desensitized in comparison to the EP_2 receptor (Nishigaki et al., 1996). Likewise, there are reported differences in ligand-induced internalization of EP receptors. e.g. EP_4 and EP_3 isoform-1 are readily internalized, whereas EP_2 and EP_3 isoforms (III and IV) are not (Desai et al., 2000; Bilson et al., 2004). Functionally, the differences among EP receptors also directly correlates with the type of signal it produces. e.g. an intracellular Ca^{2+} signal is associated with smooth muscle contraction, whereas an increase in cytoplasmic cAMP levels is associated with smooth muscle relaxation. Though the EP_1 receptors increase intracellular Ca^{2+} levels and EP_2 and EP_4 increase cytoplasmic cAMP, there are diverse factors involved. Signaling via EP_3 receptors causes a decrease in cAMP levels (Narumiya et al., 1999).

2.7. Signaling pathways affected by EP receptors

PGE_2 coupling to its specific receptors results in their activation and induces a signaling cascade inside the cell. However, signaling through different subtypes of EP receptors seems to overlap and yet have different signaling outcomes. The EP_1 receptor mediates signaling by activation of phospholipase C and elevation of inositol triphosphate, diacylglycerol and Ca^{2+}. PGE_2 also activates protein kinase Cα and c-Src via the EP_1 receptor. Indirectly, the signaling through EP_1 can also transactivate HER's-2/Neu tyrosine kinase receptor, which is mediated by c-Src resulting in an upregulation of vegetative endothelial growth factor-C (Su et al., 2004). The c-Src also mediates the transactivation of epidermal growth factor receptor by the EP_1 receptors through activation of protein kinase B (Akt) that also promotes cell proliferation and invasion (Han and Wu, 2005). Thus the EP_1 receptor knockout mouse has been implicated to play a role in colon carcinogenesis (Watanabe et al., 1999).

The EP_2 and EP_4 receptors produce their action by the stimulation of cAMP/protein kinase A (PKA) signaling through the sequential activation of Gαs and adenylate cyclase. This signaling pathway has been implicated in growth and proliferation. Increased cAMP production has been shown to have an anti-proliferative effects in human gastric carcinoma cell lines (Okuyama et al., 2002). A study has directly linked EP_2 receptor to cellular proliferation. Upon activation the Gαs subunit of EP_2 receptors can directly associate with the regulator of G protein signaling domain of Axin,

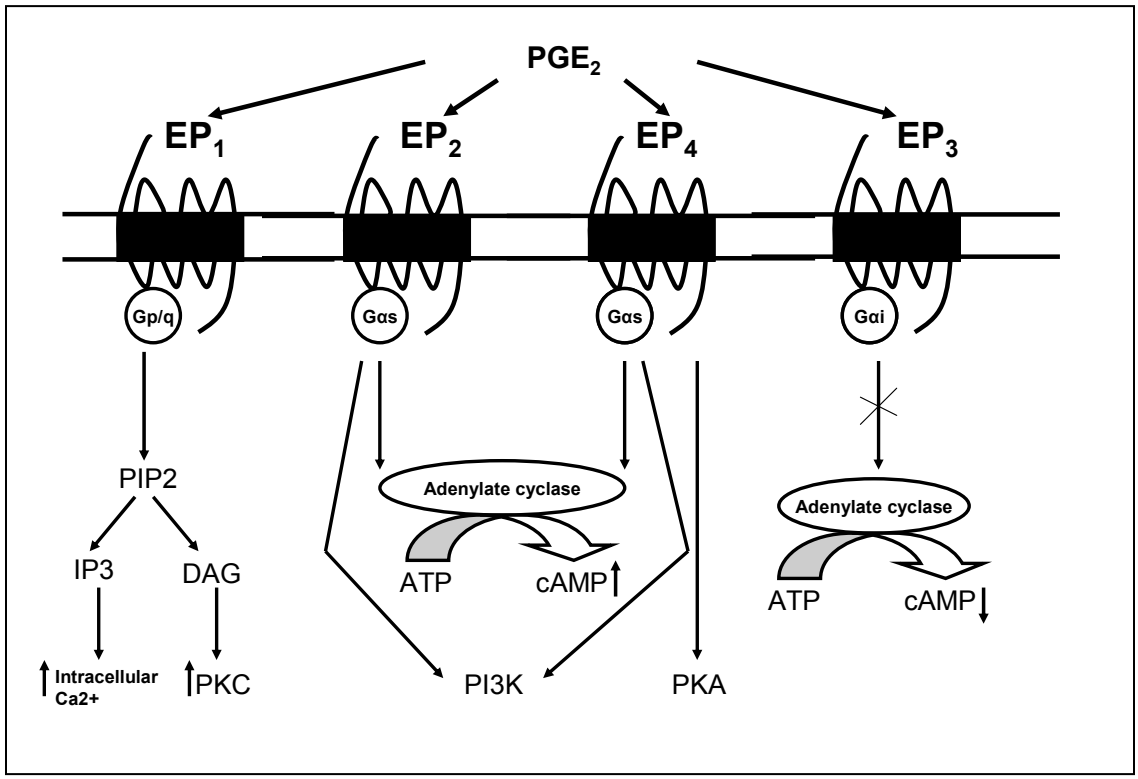

Figure 7: PGE2-EP receptor signaling pathways. Four major types of EP receptors are involved in the signaling pathway mediated via different G proteins (p/q, αs and αi) using different second messenger. PGE2 induces intracellular Ca^{2+} or cAMP when it couples and signals through EP1 or EP2/4 receptors respectively. However, it reduces intracellular cAMP when it signals through EP3 receptors. Several different kinases are involved in PGE2 induced signaling pathways. AC, adenylate cyclase; DAG, diacylglycerol; IP3, inositol triphosphate; PIP2, phosphatidylinositol diphosphate; PKA, protein kinase A; PKC, protein kinase C; PI3K, phosphoinositide-3-kinase; ↑, up regulated; ↓, down regulated; X, inhibition (Dey et al., 2006).

which inactivates and releases glycogen synthase kinase-3β (GSK-3β) from the Axin complex causing β -catenin activation and nuclear translocation (Castellone et al., 2005). PGE_2, via the EP_2 receptors, can activate both PI3K and Akt by using the free βγ subunit of G-protein (Castellone et al., 2005) (Figure 7).

A receptor-specific signaling outcome has also been observed with EP_2 and EP_4 receptors. e.g. When PGE_2 stimulates the EP_4, receptor but not EP_2, it leads to the phosphorylation of the extracellular signal-regulated kinases (ERKs) by a PI3K-dependent mechanism and induces the expression of early growth response factor-1 (Fujino et al., 2003). Both EP_2 and EP_4 receptors mediate the phosphorylation of cAMP responsive element binding protein (CREB) by different signaling pathways (Fujino et al., 2005).

The EP_3 receptors are different because of their ability to couple to multiple G proteins. The Gi subunit coupling results in the inhibition of adenylyl cyclase. The activation of Gs subunit results in cAMP production. The EP_3 receptor can also activate the small G protein, Rho, and its target p160 Rho-A binding kinase ROK α (Katoh et al., 1998; Tamma et al., 2003). EP_3 receptors have also been implicated in the activation of Ras signaling pathway leading to cancer (Yano et al., 2002). It was because of these reasons we chose the EP_3 receptor for our initial NMR study.

2.8. Identification of residues involved in the formation of the ligand-binding pocket of Prostaglandin E_2 subtype 3 (EP_3) receptor

Many studies demonstrate that the second extracellular loop of the receptor is involved in prostanoid ligand recognition. Site-directed mutagenesis of seven conserved residues in the second extracellular loop of EP_3 (in transfected HEK293 cells) was

assessed by the cells' ability to decrease intracellular cAMP (Audoly and Breyer, 1997, So et al., 2003).

The ligand-binding domain of the EP_3 receptor was essentially uncharacterized, but putatively the ligand-binding pocket resides in the TM α-helical domains. (Audoly and Breyer, 1997) considered that the conserved amino acid residues unique to the prostanoid receptor family are likely to be essential determinants of receptor structure, ligand binding, and/or signal transduction. e.g. Using molecular modeling the interactions of an agonist with its receptor inducing specific conformational changes within and between the helices of a receptor with eventual transfer of energy causing activation of G proteins was studied. The postulated reason for the behavior of residue D338 showing no loss of binding but loss of signaling is that the seventh hydrophobic domain is in an α-helical conformation, and D338 is located 180° to R329. If R329 is oriented towards the ligand-binding cleft, then D338 faces the lipid environment. This could be the reason that D338 does not appreciably affect high affinity binding of agonists to the EP_3 receptor yet abolishes the signaling cascade.

This phenotype may result from a number of effects:

i) Intrahelical flexibility necessary for hinge-bending conformational changes supporting receptor activation may be disrupted.

ii) D338 may represent a point of interaction between an adjacent helix or helices suggesting that these interactions represent an essential component of a

hydrogen bond network. This is postulated to be necessary for the proper transfer of energy between helices required for G protein activation.

iii) It could also mean that D338 may interact directly with Gi (Audoly and Breyer, 1997).

2.9. Direct transfection of PCR products into cells

Recombinant DNAs, small RNAs, and antisense oligonucleotides have been transfected into cells to study molecular biology and pharmacology (Scanlon et al., 1995). Various transfection methods (Sambrook et al., 1989) such as calcium phosphate, DEAE-dextran, electroporation modified viruses, liposomes, and dendrimers (Kukowska et al., 1996) have been used. New systems for improvements in delivery and transfection strategies are still in great demand regarding single-stranded synthetic oligonucleotides, which may enter mammalian cells by endogenous uptake pathways such as pinocytosis and endocytosis (Crooke, 1992, Wagner, 1994). Penolazzi et al., 1996 report a direct transfection of DNA fragments obtained by polymerase chain reaction (PCR) into the human cultured MCF7 cells using an ultrafiltration technique with ethidium bromide (EtdBr) as an indicator. This method was able to deliver small double-stranded (ds) DNA fragments. It was also able to evaluate the efficiency of DNA transfection into the cells. They introduced two PCR-generated ds DNA fragments: a 96-bp human genomic fragment in the 5* region of estrogen receptor (ER) gene (Green,

1986, Piva, 1993) and a 150-bp plasmid DNA fragment [pGEX-2TK (Nilsson, 1985)]. Fluorescent dye-labeled DNA and the corresponding retained-EtdBr fractions were transfected into the MCF7 cultured cells.

2.10. Anti-inflammatory activity of PGE_1

Sobota et al., 2008 have investigated the inhibitory activity of PGE_1 on IL-6- (interleukin-6) induced MCP-1 (monocyte chemotactic protein-1) expression. They showed that PGE_1 does not affect IL-6-induced STAT (signal transducer and activator of transcription) 3 activation, but does affect ERK (extracellular signal- regulated kinase) 1/2 activation which is crucial for IL-6- dependent expression of MCP-1. They discovered a specific cross-talk between the adenylate cyclase cascade and the IL-6-induced MAPK (mitogen-activated protein kinase) cascade. They then investigated its impact on IL-6-dependent gene expression because IL -6 exerts pro- as well as anti-inflammatory activity. IL-6 is the major inducer of acute phase proteins in the liver and acts as a differentiation factor for blood cells. It also acts as a migration factor for T-cells and is a potent inducer of the chemokine MCP-1 (monocyte chemoattractant protein-1) (Bode et al., 2001; Andus et al., 1988; Sobota et al., 2008).

2.11. Lipo PGE_1 in cutaneous ulcers

Intractable cutaneous ulcer is a common disease in which the inflammatory phase of the wound healing process is prolonged. This prevents the cells from growing at the local site. Cytokines such as VEGF and IL-6 (vascular endothelial growth factors), have been seen and implicated in these ulcers (Papps et al., 1995; Cianfarani et al., 2006). PGE_1 has been used for the treatment of cutaneous ulcers but has the disadvantage of rapid inactivation thus requiring a large dose of drug. Therefore lipid microspheres containing PGE_1 (Lipo-PGE_1) were developed to avoid the disadvantages of PGE_1. The efficacy of Lipo-PGE_1 (3 μg) in patients with peripheral vascular diseases was better when compared to 40–60 μg of PGE_1-cyclodextrin clathrated treatment group. Also, on evaluating the effects of ulcer reduction with the inflammatory markers, a positive correlation between IL-6 level, CRP (C reactive protein) value and changes in serum VEGF levels due to Lipo-PGE_1 administration was observed (Mizushima et al., 1983).

2.12. Lipo- PGE_1 preparation for diabetic neuropathy with leg ulcers

PGE_1 incorporated in lipid microspheres (lipo-PGE_1) (10 ug/day) that are designed to accumulate at vascular lesions were compared with placebo and free PGE_1 preparation (PGE_1-CD, 40 pg/day) in two studies (double-blind and well-controlled). The studies were done in 364 diabetic patients with neuropathy and/or leg ulcers. The route

of administration was intravenously (bolus or drip infusion) for 4 weeks. Clinical improvement was noted in 61.6% of the lipo-PGE_1 group and 30.0% of the placebo group and 37.1% in the PGE_1-CD group. Leg ulcers and diabetic neuropathy greatly improved in the lipo-PGE_1 groups with minimal side effects (Toyota et al., 1993).

2.13. Inflammatory activity of PGE_2 causing cancer

Evidence suggests that PGE_2 produced via the cyclooxygenase (COX)-2-dependent pathway plays a crucial role in the development of colorectal cancer and possibly other cancers (Williams et al., 1992). Non-steroidal anti-inflammatory drugs, which inhibit COX-2, have been shown to reduce the incidence of colorectal cancer (Marnett, 1992; Rao et al., 1995). The major prostanoid implicated in several types of cancer is PGE_2. It is produced by three biosynthetic reactions involving phospholipase A_2 (PLA_2), COX, and PGE_2 synthase (PGES). It promotes survival and motility of colon cancer cells and helps promote tumorigenesis and angiogenesis (Sheng et al., 2001; Levy, 1997). This has been demonstrated by the high expression of COX-2 which had been found in various cancer cells and tissues (Subbaramaiah et al.; 1996, Kargman et al., 1995). Study methods employing overexpression, antisense suppression, and specific inhibitors of COX-2 have shown that COX-2 contributes to the progression of several types of cancer (Liu et al., 2001; Tsujii et al., 1998). One study has demonstrated that co-transfection of COX-2 and mPGES-1 into HEK293 cells results in a cellular transformation

manifested by colony formation in soft agar culture and tumor formation when implanted subcutaneously into nude mice (Kamei et al., 2003).

The Myeov (MYEloma OVerexpressed gene) expression is enhanced in colorectal cancer (CRC) and is known to promote CRC cell proliferation and invasion. Prostaglandin E_2 (PGE_2) is a known factor in promoting CRC carcinogenesis. The role of PGE_2 in modulating Myeov expression has also not been defined. After Myeov knockdown there was a significant reduction in CRC cell migration, observable as early as within 12 hours when compared to the control at 36 hours. This Myeov expression was, however, enhanced after treatment with PGE_2. Lawlor et al., 2010 thus demonstrated that, in addition to promoting CRC proliferation and invasion, Myeov stimulates CRC cell migration, and its expression is likely to be PGE_2-dependent (Lawlor et al., 2010).

Kim et al., 2010 showed that PGE_2 acts on the EP_4 receptor to promote the migration of A549 lung cancer cells. They demonstrated that PGE_2 enhances tyrosine kinase c-Src activation, and blockade of c-Src activity represses the PGE_2-mediated lung cancer cell migration. After the knockdown of betaArrestin1 expression with short hair pin RNA (shRNA) there was a significantly impaired the PGE_2 induced c-Src activation and cell migration. This supports the idea that increased expression of the COX-2, which in turn produces high amounts of PGE_2, in the lung tumor microenvironment, may initiate a mitogenic signaling cascade. This cascade is composed of EP_4, betaArrestin1, and c-Src which mediate cancer cell migration (Kim et al., 2010).

Prostaglandin E_2 also induces CYP1B1 expression via ligand-independent activation of the estrogen receptor alpha pathway in human breast cancer cells (Han et al., 2010). Studies also support the associations between adenoma risk and genetic variability related to PGE_2, which suggest gene-environment interactions with anti-inflammatory exposures (Poole et al., 2010).

2.14. Tumor model

In 1969, came the first report of the growth of a human tumour in an immunodeficient ‘‘nude’’ (athymic) mouse (Rygaard et al., 1969). Since then, human tumour xenografts grown in nude (Giovanella et al., 1972) or in mice with severe combined immunodeficiency (SCID) (Boxma et al., 1983) have covered all of the major tumour types and represented the mainstay of preclinical anticancer drug development testing in vivo. Steel and colleagues established s.c. xenografts from a variety of tumour types (actually in conventional CBA mice that had been immuno-suppressed by thymectomy, cytosine arabinoside treatment and whole-body irradiation) and recorded that ‘‘human tumour xenografts broadly maintain the level of chemotherapeutic responsiveness of the source tumours in man’’ (Steel et al., 1983).

Background features in these mice include the features of the background strain, such as *H2* haplotype, behavior, and disease susceptibility. e.g., the NOD strain is

susceptible to diabetes, and is deficient in natural killer (NK), macrophage, antigen presenting cell (APC), and complement activity.

Table 1: Comparison of background features of a few immune deficent mice strains.

Background	Innate Immunity(NK, B, APC cells; complement activity)	SCID-associated leakiness	
BALB Substrains	Normal	High	
C57BL/6	Normal	High	
NOD/LtSz	impaired	Low	
NU/J	Normal	na	(Steel et al., 1983)

However a versatile and ideal mouse model should have the following features.

- No functional B and T cells
- No leakiness with age
- No Natural killer (NK) cell activity
- Lymphoma-resistant and long-lived
- Enables long-term experiments
- Superior ability to be humanized: excellent engraftment and differentiation of human hematopoietic stem cells (HSCs) into mature human lymphoid and myeloid cells

- Superior for HIV and other infectious disease research: can essentially be engrafted with a human immune system
- Adoptive transfer of diabetic T cells without irradiation
- Superior for transplantation research
- Breeds better
- Lives longer
- Hairless: subcutaneously transplanted tumors are easily visible
- Athymic, so no need for thymectomy (Steel et al., 1983; Giovanella et al., 1972).

3. METHODS AND MATERIALS

3.1. Peptide synthesis and purification

A peptide mimicking human EP_3 receptor eLP_2 (residues 189-227) with homocysteine added at both ends was synthesized using the fluorenylmethoxycarbonyl-polyamide solid phase method. After cleavage with TFA, the peptide was purified by HPLC on a Vydac C4 reversed phase column with a gradient from 0 to 80% acetonitrile in 0.1% TFA. The purified peptide was dissolved in 1 mL of DMSO, and added to H_2O at a final concentration of 0.02 mg/mL for cyclization (by disulfide bond formation) (Figure 8). The solution is adjusted to pH 8.5 using triethylamine, and stirred overnight at room temperature. It is then lyophilized and purified by HPLC on the C4 column (Ruan et al., 2001).

3.2. Fluorescence spectroscopic studies with the purified peptide (EP_3 eLP_2)

0.75 mL (0.1 mg/mL) of the purified peptide (EP_3 eLP_2) in a constrained loop form was dissolved in 0.01M phosphate buffer, pH 7.2, with 0.1M NaCl, and incubated with various concentrations of PGE_2. The crude (non-cyclised) EP_3 eLP_2 peptide was also used to assess the importance of cyclisation. The distance between the homocysteine residues for the disulphide bond used for cyclisation was between 12-14A^0 which was similar to the distance between the transmembrane loops in the homology models of the EP receptors (Figure 8A). The excitation wavelength was set at 292 nm to measure the

intrinsic signal of Trp residues. An emission scanning from 310-500 nm was monitored during the ligand titration to the peptide at room temperature in a 1.0-cm-path-length cell (Zhang et al., 2005). Fluorescence spectra were acquired with an SLM SPF500C spectrofluorometer (Ruan et al., 2001) (Figure 10).

3.3. Concentration dependant decrease in [^{3}H]PGE_2 binding in presence of peptide EP_3eLP_2

To further confirm the functional activity of the EP_3eLP_2 peptide the EP3 stable cell line was incubated with increasing concentration (0.1, 0.32 and 0.5µg) of peptide EP_3eLP_2 in the presence of [^{3}H]PGE_2. The thromboxane A2 (TP) and prostacyclin receptor (IP) eLP_2 were used as controls (Figure 11).

3.4. NMR Sample Preparation of the purified peptide (EP_3 eLP_2)

4mg of the purified and constrained peptide was dissolved in 0.5 mL, pH 5.5, 10mM sodium phosphate buffer with 10% D_2O, pH 6.0, at a final concentration of 2.43 mM. Next 0.5 mg of PGE_2 was dissolved in 50µl ethanol-d_6 and then added to 0.45 mL of sodium phosphate buffer (20 mM) containing 10% D_2O (Callihan et al., 1996).

3.5. NMR experiments of purified peptide (EP_3 eLP_2)

All NMR experiments were carried out on a Bruker Avance 600 MHz NMR spectrometer with a 5 mm Quadra-resonance cryo-probe at 293 K. Water peak was suppressed by the Excitation Sculpting method (Callihan et al., 1996). 2D NOESY (300ms mixing time), TOCSY and DQF-COSY for the above samples were recorded. Thereafter, 2.5 µl, 5 µl, 10 µl, 20 µl and 40 µl of PGE_2 in Ethanol-d_6 solution (1 mg/100 µl) was added into the sample and the 1D proton spectra were recorded. 2D NOESY (200ms mixing time) and TOCSY spectra were then recorded for the final mixture of EP_3 elp_2 and PGE_2. All 1D spectra contained 8k data points. NOESY and TOCSY spectra contained 2048 x 512 data points, and DQF-COSY spectra contained 4096 x 512 data points. NOESY was recorded with 300 ms mixing time. For the experiments of the peptide in the presence of ligand, NOESY was recorded with 150 ms mixing time. The TOCSY spectra were carried out with MLEV-17 spin-lock pulse sequence with a total mixing time of 70 ms. Quadrature detection was achieved in the F1 (Frequency one) by the States-TPPI method (Marion et al., 1989). The NMR data were processed using Felix 2000 (Accelrys, San Diego, CA). Shifted sine-bell window functions of 0° (for DQF-COSY), 70° (for TOCSY) or 90° (for NOESY) were used in both dimensions. Chemical shift was referenced to the internal standard DSS (contained in the D_2O) (Marion et al., 1989, Ruan et al., 2001)(Figure 12,13 & 14).

3.6. Site-directed Mutagenesis of residues identified by NMR in EP_3 eLP_2

pAcSG-EP_3 wild-type cDNA was first subcloned into *Eco*RI/*Xba*I sites of the pcDNA3.1 (+) expression vector. The EP_3 receptor mutants were then constructed using standard PCR. The plasmids were then prepared using Midiprep kit (Qiagen) for the transfection into HEK293 cells for expression (Ruan et al., 2003).

3.7. Expression of EP_3 Receptor Wild-type and Mutants in HEK293 Cells

HEK293 cells, placed on 10-cm dishes at a density of 2.0×10^6, were cultured overnight, at 37 °C in a humidified 5% CO_2 atmosphere in DMEM containing 10% fetal bovine serum (FBS) , antibiotics, and antimycotics. Then, the medium was replaced with DMEM+FBS without antibiotic and antimycotic. HEK293 cells were transfected with purified cDNA of pcDNA3.1 (+)/EP_3 wildtype or mutants with Lipofectamine. Twelve hours later, the medium was replaced with DMEM + 10% FBS + antibiotics and antimycotics. Approximately 48 hrs after transfection, the cells were subcultured and incubated with G418 (selection antibiotic) for six weeks to generate four separate stable cell lines. Western blot was performed to evaluate the protein expression (Figure 15A).

3.8. Ligand Binding Assay of wild type and EP_3 mutants

Ligand binding assays for the wild type and mutant EP_3 receptor were performed on whole cells in 48-well culture plates with 0.0355 nM and 1.1185 nM [^{3}H]PGE_2 (3,000 and 30,000 cpm respectively, 30 Ci/mol,) in the presence and absence of 5 μM of

unlabeled (cold) PGE_2 in the 0.1-mL reaction volume of DMEM at room temperature for 60 min. The reaction was terminated by adding 1 mL of ice-cold washing buffer (25 mM Tris-HCl, pH 7.4) and the wells were washed. The ligand-bound cells were dissolved in 0.5 N NaOH, which was later neutralized with glacial acetic acid. The radioactivity was counted using a micro beta TRILUX 1450 counter. The procedure was modified from the following reference (D'Angelo et al., 1996) (Figure 15 B &C).

3.9. Calcium signaling assay of wild type and the mutants S211L, R214L and N217L using PGE_1 and PGE_2

The calcium assays were performed on the stable cell lines of the wild type and the mutants S211L, R214L and N217L using PGE_1 and PGE_2 using Fluo8-AM dye. The cells were cultured in 6-well plates for the Cytofluor plate reader, and incubated with Fluo8-AM dye dissolved in Modified Hank's buffered salt solution (HBSS, without Ca and Mg), containing 10 mM HEPES, pH 7.6, and 0.1% bovine serum albumin (HBSSHB buffer) for a total of 20 minutes. The cells were then washed with wash buffer containing HBSSHB with probenecid acid (2.5 mM) and pluronic F-68 (0.1%) and incubated additionally for 10 minutes. Then 10 nM concentrations of both PGE_2 and PGE_1 were tested for a Ca^{2+} signal in a reaction volume of 1 mL wash buffer (Figure 16). The cells were then suspended in the wash buffer and counted using a hemocytometer (neubauers chamber). The Ca^{2+} signal was then normalized with respect to the number of cells.

High throughput mutagenesis

3.10. High throughput mutagenesis of EP_1 receptor using PCR

Due to the differences found in the calcium signaling assay of EP1 receptor with PGE_1 and PGE2 we decided to chose the EP1 receptor extra cellular loops for high throughput mutagenesis experiment. Twenty four residues of the extra cellular loop one and two of the EP_1 receptor were point mutated using conventional PCR (Figure 17A). The mutations were contained in both of the primers (forward and reverse) which were designed using primerX software. The primers are phosphorylated so that the PCR product can be ligated into a circle and used to transform cells. The primers were designed such that the *annealing* portion had a T_m ~60-63º. The primers were phosphorylated using the polynucleotide kinase enzyme PNK as mentioned in the kit. Thereafter the reaction was heated at 65 °C for 20 minutes to kill the PNK. The primers were used with the wild type EP_1 receptor pcDNA as the template. The template was digested in the PCR reaction mixture by adding 1 µL of DpnI, mixed, and incubating it for at least 60 minutes at 37 °C. The reaction mixture of linear EP_1 mutant DNA was incubated overnight at room temperature with ligase (*e.g.* 9° North and Taq) enzyme to join the phosphorylated end and form a circular DNA (Figure 17B). Agarose gel (1%) was used to detect the amplified mutant EP_1 receptor bands (Figure 18B).

3.11. Generation of 24 EP_1 receptor mutation stable cell lines in HEK293 cells for western blot, radioligand binding and calcium assay

HEK293 cells were transfected with 16 μg of ligated PCR product of EP_1 receptor with 40 μL of Lipofectamine 2000 (Invitrogen) as mentioned previously. Twelve hours later, the medium was replaced with DMEM + 10% FBS + antibiotics and antimycotics. Approximately 48 hrs after transfection, the cells were subcultured and incubated with G418 (selection antibiotic) for six weeks to generate twenty four separate stable cell lines. Western blot (Figure 18A) and [^{3}H]PGE_2 ligand binding assays (Figure 19 A&B) were performed as mentioned previously on all the twenty four EP_1 mutant stable cell lines. Calcium signaling assays were also performed on all the stable cell lines. The details of the calcium signaling assay are mentioned previously (Figure 20).

EP Receptor Binding and Signaling Studies

3.12. EP receptor pcDNA

A pAcSG-EP cDNA cloned by our laboratory was first subcloned into EcoRI/XhoI sites of pcDNA3.1 (−) expression vector to generate the plasmid of pcDNA:humanEP. The pcDNA vector has a Cytomegalovirus (CMV) promoter and geneticin (G418) as the selection antibiotic. All four wild type EP receptor plasmids were amplified using Qiagen miniprep and maxiprep kits.

3.13. Generation of HEK293 Cell lines expressing Recombinant EP Receptors

HEK293 cells were transfected with 16 µg of purified cDNA of pcDNA: hEP receptors (EP_1, EP_2, EP_3 and EP_4) and 40 µL of Lipofectamine 2000 (Invitrogen) as mentioned previously. Twelve hours later, the medium was replaced with DMEM + 10% FBS + antibiotics and antimycotics. Approximately 48 hrs after transfection, the cells were subcultured and incubated with G418 (selection antibiotic) for six weeks to generate four separate stable cell line.

3.14. Western Blot analysis and confocal microscopy

Transfected HEK293 cells were scraped from 10-cm plates into ice-cold PBS buffer, pH 7.4, and collected by centrifugation. After washing three times, the pellet was resuspended in a small volume of the same buffer. Protein estimation was performed using fluorescence spectroscopy. Each protein sample (15 µg) was separated by 10% polyacrylamide gel electrophoresis under denaturing conditions and then transferred to a nitrocellulose membrane. Bands for the EP receptors were recognized by the individual EP receptor polyclonal antibodies and visualized with horseradish peroxidase-tagged secondary antibody. Since the antibody was polyclonal, and detected multiple bands we chose another non-specific band at 35 kDa (EP_1), 40 kDa (EP_2), 150 kDa (EP_3) and 40 kDa (EP_4) as a loading control which was not our band of interest (Figure 21A).

Confocal microscopy was also performed to confirm the surface receptor expression in the EP receptor stable cell lines (Figure 21D).

3.15. Ligand binding assay on the EP receptors as stable cell lines

Ligand binding assays for the EP receptors over expressed in the HEK293 cells as stable cell lines were performed in 48-well plates. The stable cell lines grown in 10-cm plates were suspended in phosphate buffered saline and the cell count per microliter was performed using hemocytometer (neubauers chamber). Equal amount of cells were pipetted and subcultured in 48-well plates for the [^{3}H]PGE_2 radioligand binding. For the saturation kinetics (to calculate the Kd) on the EP receptors (Figure 22(I)), the wells were incubated for one hour at room temperature with increasing amounts of [^{3}H]PGE_2 in a reaction volume of 100 µl DMEM medium. The reactions were terminated by washing the wells three times with cold PBS. The cells were then solubilized in 0.5N NaOH and neutralized by glacial acetic acid. The solubilized cells' [^{3}H]PGE_2 count was then read using a microbeta trilux counter. A set of three experiments were performed. [^{3}H]PGE_2 binding on HEK293 cells was also evaluated for non-specific binding (Figure 22(I)). For the calculation of IC50, [^{3}H]PGE_2 was displaced with increasing log concentrations of cold PGE_2 and cold PGE_1 and the counts measured accordingly (Figure 22(II)). The [^{3}H]PGE_2 binding was also analyzed using various antagonists to the EP receptors. We used three antagonists, namely SC19220 (EP_1 selective antagonist, 10 µM), AH6809

(non-selective EP_1, EP_2, EP_3 antagonist, 20 µM), and GW627368X (EP_4 selective antagonist, 100 nM) (Figure 25A).

3.16. cAMP Assay on the EP receptors as stable cell lines

The EP receptors in HEK293 cell lines were analyzed for signal transduction capability mediated by Gs coupling using a cAMP assay according to the manufacturer's instructions (Amersham Biosciences). The stable cell lines (placed in 96-well plates) were cultured overnight, at 37 °C in a humidified 5% CO_2 atmosphere in DMEM+ 10% FBS + antibiotics and antimycotics. The cells were then incubated with 100 pM and 10 nM PGE_2 and PGE_1, respectively for 10 min at 37 °C in the culture medium. Afterward, the medium was removed and the cells were lysed. The intracellular cAMP produced by the individual EP receptors was quantified in the 96-well microplates by Enzyme Immunoassay (EIA) using a cAMP Biotrak EIA System. A set of three experiments were performed. The cyclic AMP in HEK293 cells (as controls) was compared with that of the EP receptors stimulated by PGE_1 and PGE_2 (Figure 26).

3.17. Calcium assay on the EP receptors as stable cell lines

The calcium assays were performed on the HEK293 EP receptor stable cell lines using Fluo8-AM dye. The cells were cultured in 6-well plates for the Cytofluor plate reader, and in 12-well glass bottom plates for the Nikon Ti-S eclipse microscope (40x

objective) (Figure 23) and incubated with Fluo8-AM dye dissolved in Modified Hank's buffered salt solution (HBSS, without Ca and Mg), containing 10 mM HEPES, pH 7.6, and 0.1% bovine serum albumin (HBSSHB buffer) for a total of 20 minutes. The cells were then washed with wash buffer containing HBSSHB with probenecid acid (2.5 mM) and pluronic F-68 (0.1%) and incubated additionally for 10 minutes. Then 100 pM and 10 nM concentrations of both PGE_2 and PGE_1 were tested for a Ca^{2+} signal in a reaction volume of 1 mL wash buffer (Figure 23 & 24). The cells were then suspended in the wash buffer and counted using a hemocytometer (neubauers chamber). The Ca^{2+} signal was then normalized with respect to the number of cells. The Ca^{2+} signal was also analyzed using various antagonists as mentioned above to the EP receptors (Figure 25B)).

3.18. Determination of leukotrine C4/D4/E4 in the EP_1 stable cell line using ELISA

Quantification of leukotrine C4/D4/E4 in the cultured cells stimulated with PGE_1 and PGE_2 was detected using an ELISA Kit. Briefly, the EP_1 stable cell line grown in 10-cm culture plates were washed three times with PBS and stimulated with 100 pM PGE_1 and PGE_2 separately for 20 minutes in DMEM medium. The cell culture media and cell lysate was collected and applied to a C18 cartridge. After washing with water, the bound metabolites in the cartridge were eluted with acetone, dried by nitrogen gas, and then dissolved in extraction buffer. The experiment (n=3) was performed according to the manufacturer's instructions (Figure 27 A&B).

3.19. Determination of the Lipoxin B4 peak in the PGE_1 stimulated EP_1 stable cell line using LC/MS

Quantification of Lipoxin B4 peak in the EP_1 stable cell line was detected by LC/MS following the reported methods (Yang et al., 2002, Nithipatikom et al., 2003). Briefly, the EP_1 stable cell line was incubated with 100 pM PGE_1 and PGE_2 and the serum free cell culture media was collected and applied to a C18 cartridge. After washing with water, the AA metabolites that had bound to the cartridge were eluted with acetone, dried by nitrogen gas, and then dissolved in buffer A (30% acetonitrile and 0.1% acetic acid). The sample was injected into the Waters Micromass LC/MS/MS system by an auto-sampler. The metabolites are first separated by the RP-HPLC C18 column and then automatically injected into the mass detector equipped with an ESI source in a negative mode. Synthetic 5(S), 14(R) Lipoxin B4 standards were obtained from Cayman Chemical Company (Ann Arbor, MI), and were used as standards to calibrate the LC/MS system, identify the corresponding prostanoids, and normalize the detection limits and sensitivities (Figure 28).

Establishing a tumor model

3.20. Engineering cDNA plasmids encoding the hybrid enzyme COX-2-10aa-mPGES-1 sequences

The pcDNA 3.1 vector containing a cytomegalovirus early promoter was cloned with cDNAs of the COX-2 and mPGES-1 using a PCR (polymerase chain reaction) cloning

approach. The sequences were confirmed by DNA sequencing and endonuclease digestion analyses. The COX-2 and the mPGES-1 were linked through the 10 amino acid (aa) sequence on the pcDNA 3.1(+) vector (Ruan et al., 2009).

3.21. Expression of the hybrid enzyme synthases in HEK293 cells

The recombinant pcDNA 3.1 vector containing COX-2-10aa-mPGES-1 synthases were expressed in HEK293 cells as described (Deng et al., 2002, 2003; Ruan et al., 2005). The HEK293 cells were grown and transfected with the cDNA of the recombinant synthases (COX-2-10aa-mPGES-1) by the Lipofectamine 2000 method (Hatae et al., 2002), following the manufacturer's instructions (Invitrogen). The stable cell line was created after 4 weeks of using Geneticin (G418) as the selection antibiotic. The stable cell line was harvested for further enzyme assays and a Western blot analysis and immunostaining was performed to identify the stable expression. Similarly, a stable cell line co-expressing COX-2 and mPGES-1 was also generated and evaluated using western blot and immunostaining (Figure 31 & 32).

3.22. Cell culture

HEK293 cells from ATCC were cultured in a 10-cm cell culture dish with high glucose DMEM containing 10% fetal bovine serum and 1% antibiotic and antimycotic acid, and were grown at 37 °C in a humidified 5% CO_2 incubator.

3.23. Western blot analysis of hybrid enzyme expression

Both HEK293 cells transfected and untransfected were washed with ice-cold PBS (0.01 M phosphate buffer, pH 7.4, containing 0.15 M NaCl), and collected by centrifugation. The pellets were washed three times and re-suspended in a small volume of the same buffer and stored in -80°C, until further assays were performed. The whole cell proteins were extracted by 10% SDS, separated by 8-16% (w/v)-PAGE under denaturing conditions, and then transferred to a nitrocellulose membrane. COX-2 and mPGES-1 primary antibodies were used to visualize the bands with horseradish peroxidase-conjugated secondary antibody (Lin *et al., 2000*). Similarly COX-2 and mPGES-1 co-transfected HEK293 cells were also assessed by western blot analysis for protein expression (Figure 31 & 32).

3.24. Determination of Enzyme activity for COX-2-10aa-mPGES-1 using the High Performance Liquid Chromatography (HPLC) method

To determine the activities of the synthases that converted AA into PGE_2 through the tri-catalytic functions, different concentrations of [^{14}C]AA were added to the stable cell lines in a total reaction volume of 0.225 mL (25µL cells + 200µL 2.5mM glutathione in PBS). After an incubation for 0.5 – 5 minutes the reaction was stopped by adding 0.2 mL 0.1% TFA (trifluoroacetic acid) and 0.2 mL 2mM $SnCl_2$ (Ruan et al., 2009). The

mixture was briefly vortexed for 1 min to ensure termination of the reaction. After centrifugation (6,000 rpm, 5 minutes), the supernatant was passed through a C18 octadecyl column (Honeywell Burdick & Jackson) and eluted with 0.5 mL acetone, which was then evaporated under a gentle stream of air. Buffer A was used to re-dissolve the protein and load the sample onto an HPLC C18 column (Varian Microsorb-MV 100-5, 4.6 × 250 mm) using the solvent A with a gradient from 35 to 100% acetonitrile for 45 min at a flow-rate of 1.0 mL/min. The metabolized [^{14}C]AA into [^{14}C]PGE_2 as the end-product profile was monitored directly by a flow scintillation analyzer (Packard 150TR) (Figure 33).

3.25. PGE_2 level determination in tumor containing nu/nu mice serum using enzyme immunoassay (EIA)

The BALB/c nu/nu mice with 1 month old tumors growing on their flanks were sacrificed by cervical dislocation and the blood collected from the heart. The blood was centrifuged and the serum collected for evaluation of PGE_2 levels. Supernatant of the blood (serum) was diluted 100 times using PBS containing 0.1% bovine serum albumin and then used for determination of the end-product, PGE_2, using an EIA kit following the manufacturer's instructions (Cayman Chemical Co) (Figure 35B).

3.26. PGE_2 level determination in serum of BALB/c/nu/nu mice with tumors using LC/MS/MS and ELISA

The serum collected from BALB/c nu/nu mice as described above was passed through the C18-Sephadex column and eluted with acetone in a glass tube. The acetone was evaporated and the solute was dissolved in 0.25mL buffer A. Quantification of PGE_2 was detected by LC/MS/MS following the reported methods (Takiguchi et al., 1999). The sample was directly injected into the Waters Micromass LC/MS/MS system by an auto-sampler. The synthetic PGE_2, obtained from Cayman Chemical Co., was used as a standard to calibrate the LC/MS/MS system, identify the corresponding prostanoid and normalize the detection limits and sensitivities. The serum was also used to perform ELISA using anti PGE_2 antibody (Figure 35A).

3.27. Immunofluorescence staining of stable cell lines

The stable cell line and the non-transfected cell controls were grown on a cover glass and washed with PBS and then incubated with 3.7% formaldehyde for 10 minutes. They were then blocked for 20 minutes before being incubated with 1% saponin for 20 minutes. Then the primary antibody was added (10 μg/mL of affinity-purified anti-human COX-2 or mPGES-1 antibody) in the presence of 0.25% saponin and 10% goat serum for one hour. The cells were incubated for another hour with the secondary antibodies after washing with PBS (Deng *et al.,* 2002; Lin *et al.,* 2000). Cells stained with

the FITC- or Rhodamine-labeled antibody were viewed under the Zeiss Axioplan 2 epifluorescence microscope (Figure 32).

3.28. Subcutaneous tumors on BALB/c nu/nu mice with cotransfected and COX-2-10aa-mPGES-1 in HEK293 cells

The COX-2, mPGES-1 co-transfected stable cell line, COX-2-10aa-mPGES-1 stable cell line and HEK293 cells as controls were harvested in PBS and counted using a neubauers hemocytometer chamber. Approximately 50,000 cells containing COX-2-10aa-mPGES-1 and COX-2, mPGES-1 co-transfection were subcutaneously injected separately on the right flank of eight 4-week old BALB/c nu/nu mice using a 23 bore needle (Figure 34).

3.29. Subcutaneous peripheral EP receptor tumors on BALB/c nu/nu mice with COX-2-10aa-mPGES-1 in HEK293 cells

EP receptor stable cell line (20 total injections for each group) was injected peripherally around the central hybrid enzyme tumor producing high amount of PGE_2 levels. The EP stable cell lines were monitored for growth around the central PGE_2 producing tumor. The tumor occurrence for each of the EP stable cell line was noted for evaluation using the fisher's exact test (Fisher, 1922) (Figure 36 & 37).

3.30. Primary culture of tumors grown on BALB/c nu/nu mice

The mice were sacrificed by cervical dislocation and the tumors generated were harvested in oxygenated DMEM containing FBS and AA in a 10-cm cell culture plate. The tumors (COX-2-10aa-mPGES-1, COX-2, mPGES-1 co-transfection and EP_1) were cut into fine pieces using a regular blade and the tumor debris manually removed using a forceps. The cells detached from the tumor and suspended in the culture medium were cultured in a new 10-cm plate with the same culture medium. After the primary culture cells began to attach and multiply in the plate, G418 was added for cell selection to generate a stable cell lines from the primary culture. Thus stable cell lines containing COX-2-10aa-mPGES-1, COX-2, mPGES-1 co-transfection and EP_1 receptor were re-established from the tumor primary culture. The stable cell lines were confirmed by western blot and immunostaining (Figure 31,32 & 38).

4. RESULTS

4.1. Homology Model and Peptide design

A peptide mimicking human EP receptor eLP_2 (residues 189-227) with homocysteine added at both ends of the loop was synthesized. The peptide was cyclised by formation of a disulfide bond between the homocysteine residues. A model of human EP_3 receptor with seven TM domains and extracellular loops was created by homology modeling using the recently crystallized beta2 adrenergic receptor as the template for the transmembrane domains. The eLP_2 region is indicated by a circle. The distance between the transmembrane helices is between 12-14 angstroms which is similar to the distance between the disulphide bonds formed by the homocysteine residues in the peptide (Figure 8).

4.2. Sequence alignment of the eLP_2 regions from the eight human prostanoid receptors

Sequence alignment of the identical residues among the eLP_2 regions was performed. The identical residues, QW-PGTWCF, in the eLP_2 regions are centrally located within the eLP_2. The identified key residues, S211 and R214, are not conserved in other eLP_2's. This indicates that these residues of EP_3 eLP_2 could be involved in specific ligand recognition (Figure 9) (Chillar et al., 2008).

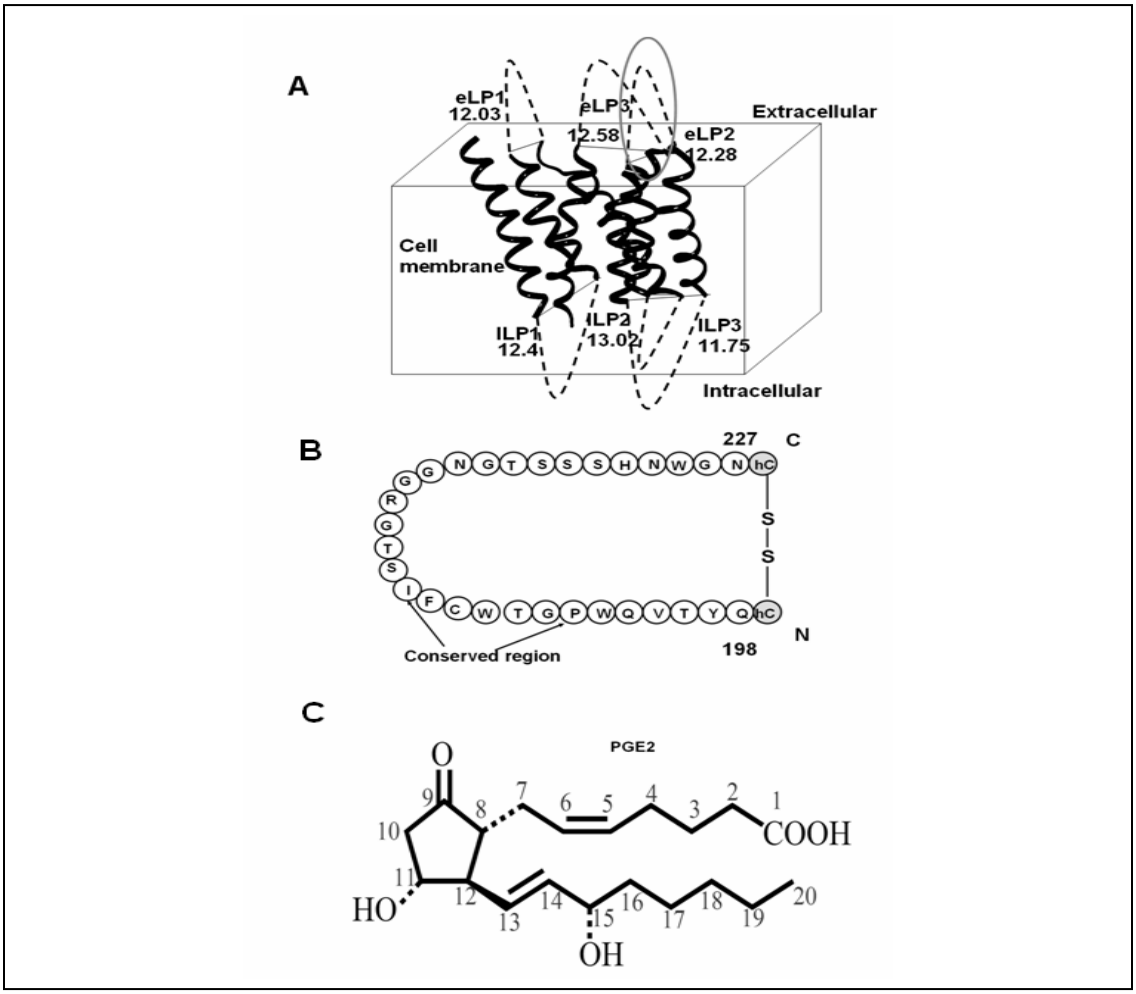

Figure 8: (A) The seven transmembrane domains (TM1–TM7) model of the human EP_3 receptor created by homology modeling based on the Xray structure of β2 adrenergic receptor. The distance in angstroms (Å) between the termini of the fourth (TM4) and fifth (TM5) transmembrane domains and others was shown. The synthesized peptide, EP_3eLP2, is marked with a circle. (B) The amino acid sequence of the synthesized eLP_2 is shown in the constrained form, which had a connection between the N- and C-termini by a disulfide bond using additional homocysteine residues to give a separation of about 12Å as indicated in the model (A). (C) The chemical structure of PGE_2.

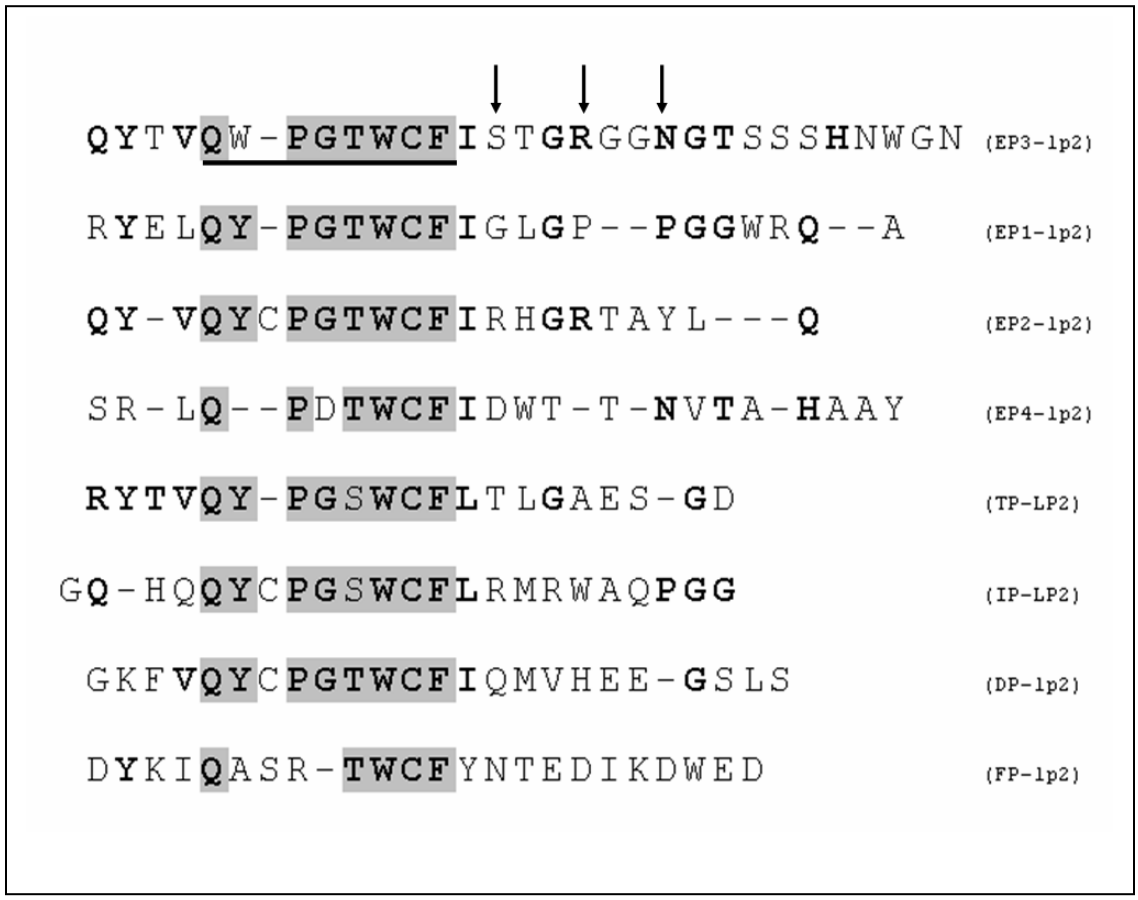

Figure 9: Sequence alignment of the eLP_2 of different prostanoid receptors. The highlighted residues are conserved among all the receptors. The conserved residues in EP_3 are underlined and the residues for mutation identified by NMR are indicated by arrows.

4.3. Characterization of the interaction between PGE_2 and the constrained and crude EP_3 eLP_2 segment using fluorescence spectroscopy and radioligand binding

The intrinsic fluorescence signal generated from Trp residues is sensitive to the conformational change of the constrained peptide induced by the interaction with its ligand. The distance between the centers of the TM4 and TM5 connecting the eLP_2 is

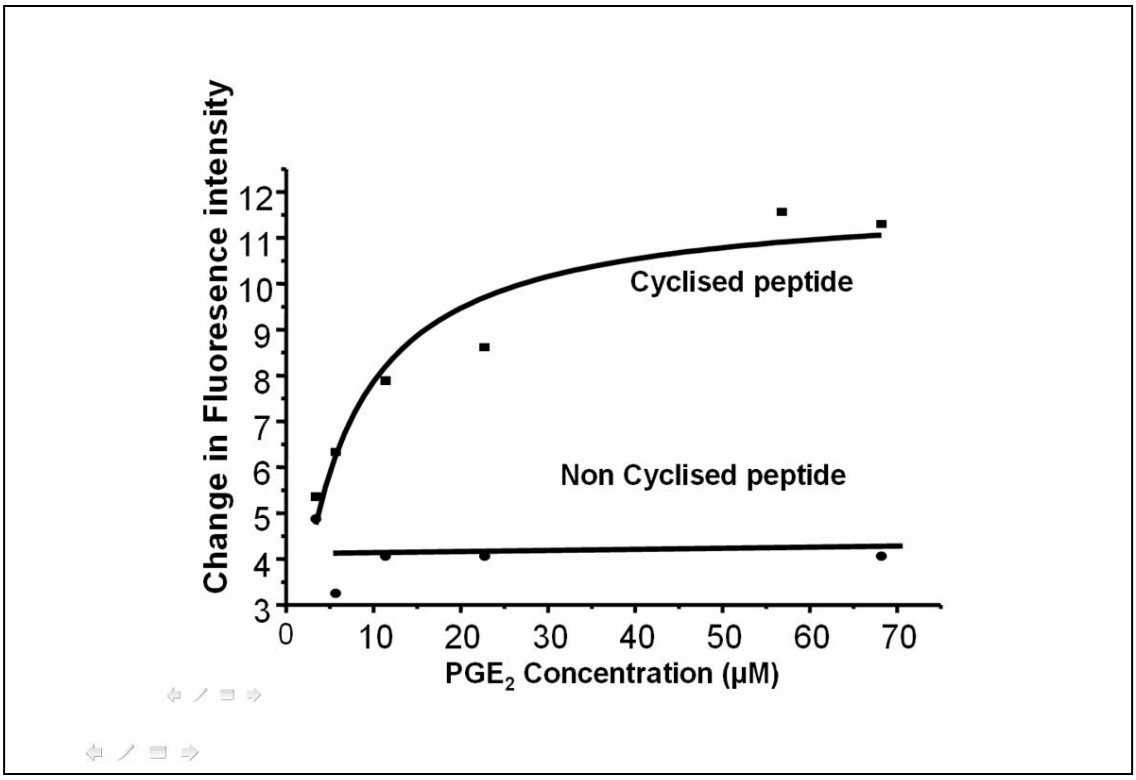

Figure 10: Fluorescence spectroscopic analysis for the interaction of the receptor ligand with the synthetic peptide, corresponding to the eLP_2 of the EP_3 receptor. The fluorescence spectra were recorded as described under ''methods.'' The fluorescence enhancement of the synthetic cyclised peptide (0.1 mg/ml) by the addition of its ligand (3.4– 68.1µM) was plotted. The increase in the fluorescence intensity of the peptide was calculated by subtracting the fluorescence intensity obtained from the peptide in the absence of the ligand. The fluorescence changes of the non cyclised or crude EP_3 eLP_2 peptide (0.1 mg/ml) with addition of PGE_2 (3.4– 68.1µM) is also plotted.

12.28Å, based on the human EP_3 receptor model generated by molecular modeling using the β_2 adrenergic receptor as a template (Figure 8A). The cyclised peptide (Figure 8B), with PGE_2 was tested by fluorescence spectroscopy (Figure 10). The fluorescence intensity of the constrained EP_3 eLP_2 peptide increased by 11-14% (Kd -5.12) with PGE_2 in a concentration-dependent fashion, which started at 3.4 µM and became saturated at

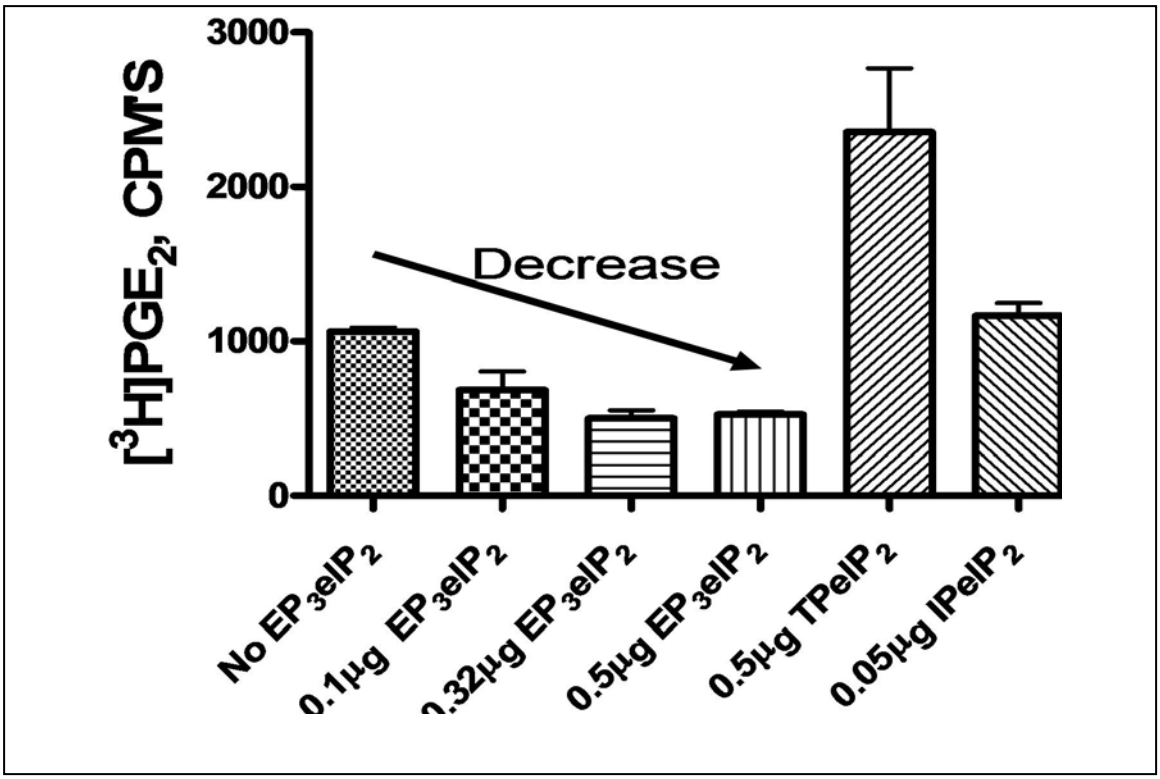

Figure 11: Concentration dependant decrease in $[^3H]PGE_2$ binding in presence of peptide EP_3eLP_2. The increasing concentration of the peptide EP_3elp2 showed a decreased binding with the EP_3 receptor. This indicated that the synthetic peptide was functionally active and was binding to the radioligand $[^3H]PGE_2$. The thromboxane A_2 receptor (TP) and prostacyclin receptor (IP) eLP_2's were used as controls. The TP showed a very high binding due to large number of hydrophobic residues in TP eLP_2.

68.1 µM of the ligand (Figure 10). However, non-significant fluorescence changes (4%) were induced upon the addition of PGE_2 to the crude EP_3 eLP_2. There was a concentration dependent decrease in $[^3H]PGE_2$ binding with increasing concentrations of EP_3 eLP_2 peptide (Figure 11). These results indicate that the constrained EP_3 eLP_2 peptide is able to adopt an active conformation, which mimics the eLP_2 of the EP_3 receptor.

4.4. Characterization of the interaction between PGE_2 and the EP_3 eLP_2 segment using 2D proton NMR spectroscopy

To further identify which proton in PGE_2 contacts with the EP_3 eLP_2 fragment, 2D proton NMR spectroscopy was used. NOESY, TOCSY of PGE_2 in the absence and presence of the constrained EP_3 eLP_2 peptide were recorded in H_2O with 10% D_2O. The binding of PGE_2 to the peptide was supported by the changes of the proton cross-peaks, from the negative phase (green peaks, fast tumbling) in free PGE_2 (Figure 12A) to the positive phase (blue peaks, slow tumbling) in PGE_2 with the EP_3 eLP_2 peptide (Figure 12B). This is a strong indication of the transition of PGE_2 from free to bound status. By analysis, more cross-peaks appeared in the NOESY spectrum of PGE_2 with the eLP_2 peptide which clearly indicates that a stable conformation of PGE_2 was induced by the peptide.

4.5. Identification of residues for point mutation

Recently, the residues for ligand recognition in the eLP_2 region of human TP was assessed by So et al., 2003 which provided fundamental information suggesting that eLP_2's are involved in specific ligand recognition. On further analysis of the cross peaks in the NOESY spectra of the EP_3 eLP_2 and PGE_2 mixture, intermolecular cross peaks were identified for two residues (serine 211 and arginine 214). These cross peaks indicated a

close contact between these two residues and PGE_2. This suggests that these two residues will also interact with PGE_2 in the entire EP_3 receptor. The Figure 13 &14 shows the

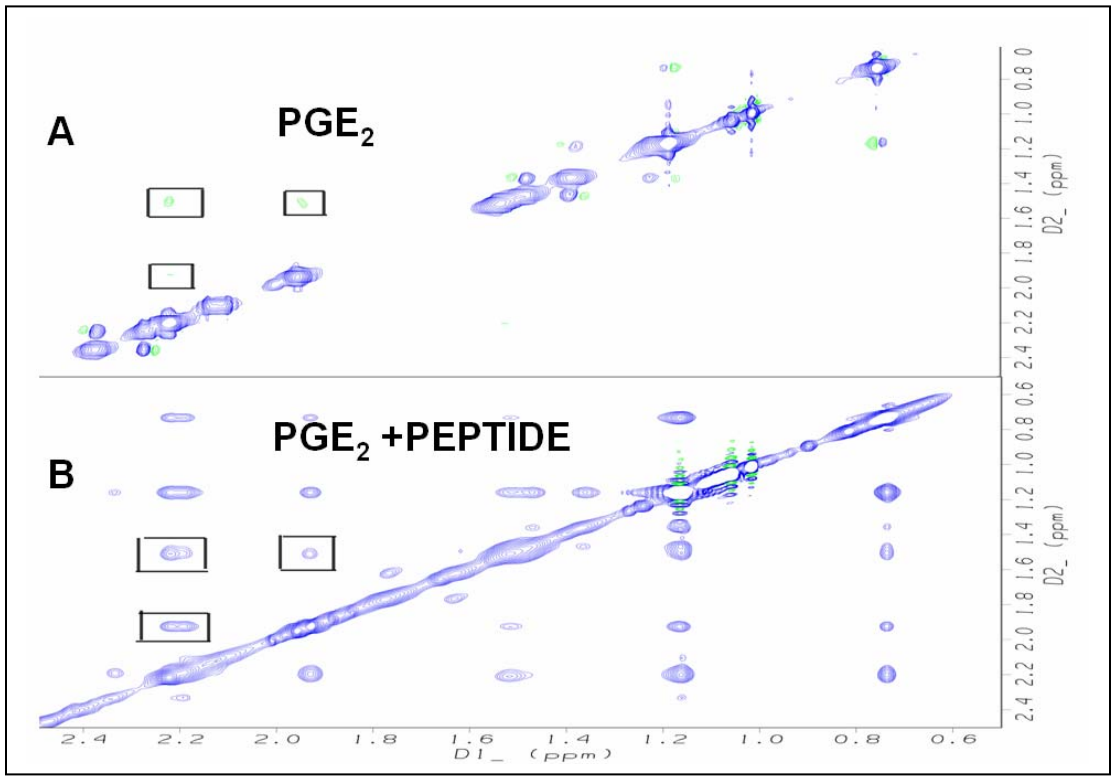

Figure 12: NOESY spectra of PGE_2 without (A) and with (B) the presence of the EP_3 eLP_2 peptide. The cross-peaks in (A) contained the negative (green) phases (fast tumbling), compared to the diagonal, whereas the cross-peaks in (B) contained mostly the positive phase (blue phases), (slow tumbling). The peaks appearing from in both spectra are labeled with a rectangle. (A) Peaks generated by PGE_2. (B) Peaks indicate extra intra-molecule NOEs of PGE2 when interacted with EP_3 eLP_2 peptide which represents their interaction.

intermolecular NOE cross peaks identified. The beta proton of serine 211 was shown to contact with H7 of PGE_2, and the δ guanidine hydrogen of residue Arg214, was shown to

come in contact with protons, H2, H4, and H13/14 of PGE_2 in solution. Residue asparagine (N217) was chosen as an internal control due to its similarity in size and hydrophilicity. All three residues identified were mutated to leucine (Norclone biotech laboratories) which is more hydrophobic in nature.

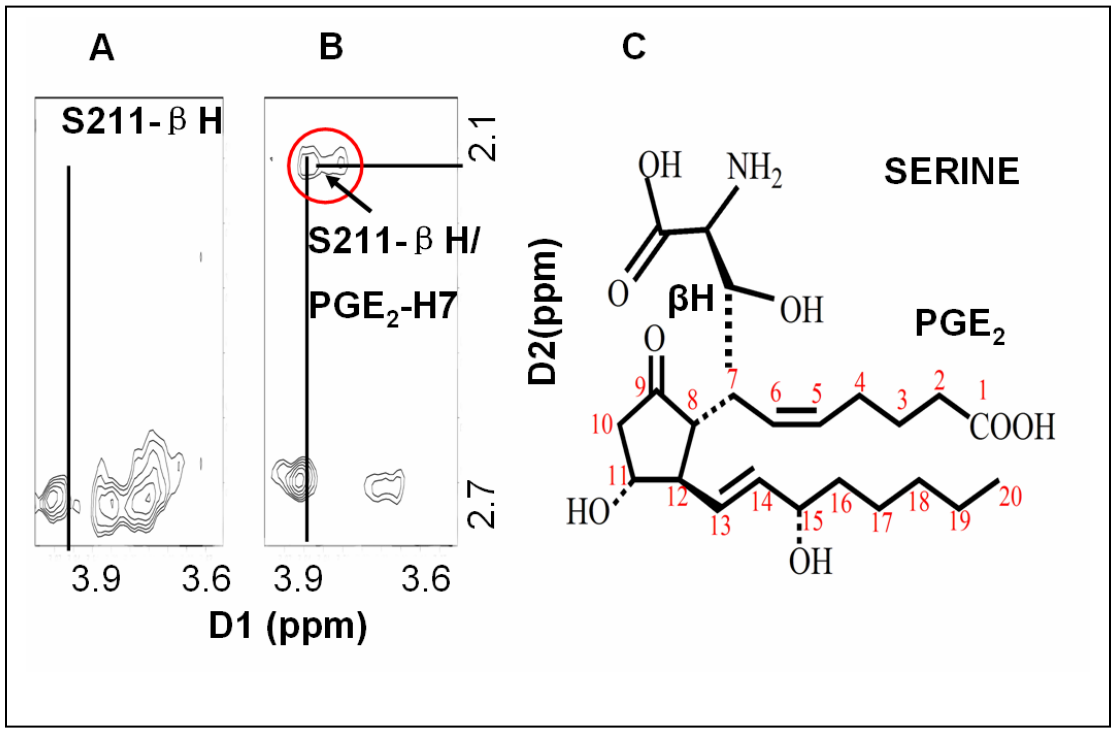

Figure 13: Residue identification from NOESY spectrum of EP_3 eLP_2 with and without PGE_2. (*1*) Peaks for serine 211 of eLP_2 peptide only. (2) Cross peaks of peptide with PGE_2 for residue serine 211 β proton (dimension 1) in contact with proton 7 of PGE_2 (dimension 2) (*3*), Chemical structure representation of serine 211 in contact with PGE_2.

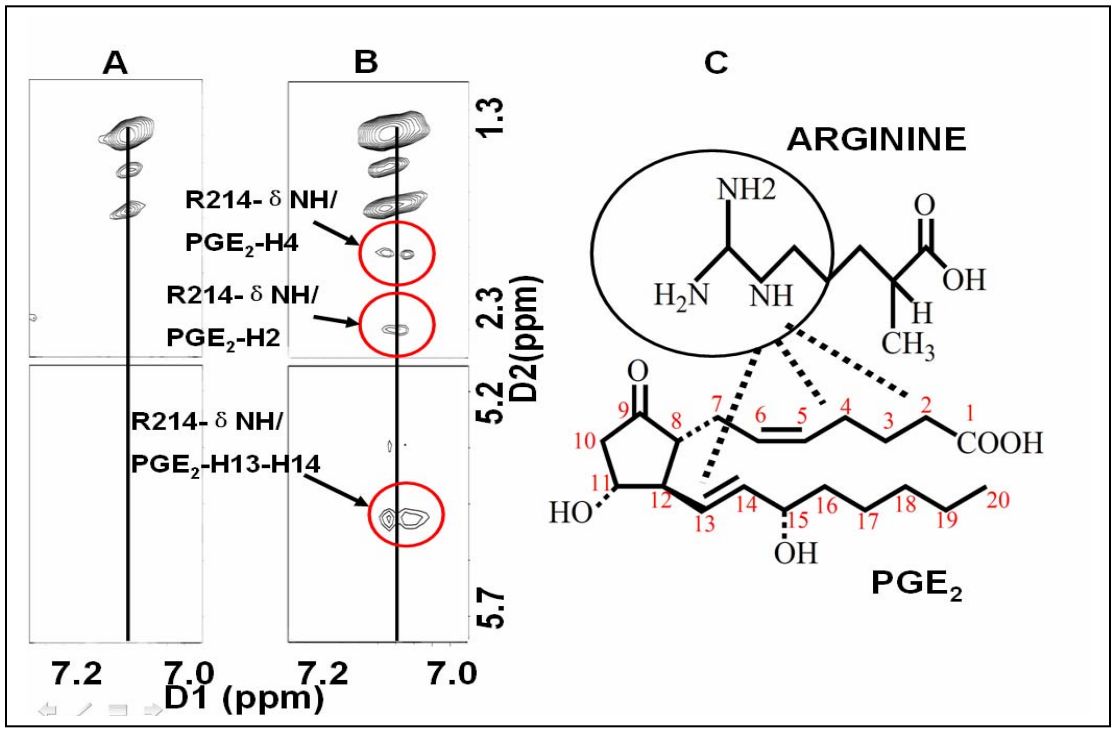

Figure 14: Residue identification from NOESY spectrum of EP_3 eLP_2 with and without PGE_2. (*1*) Peaks for arginine 214 of eLP_2 peptide only.(2)Cross peaks for residue arginine 214 guanidine protons(dimension 1) in contact with proton 2, 4 and 13 /14 of PGE_2 (dimension 2).(D) Chemical structure representation of arginine 214 in contact with PGE_2.

4.6. Radioligand binding of EP_3 wild type versus mutants

The cells expressing recombinant EP_3, were incubated with [^{3}H]PGE_2 with and without unlabelled PGE_2 (Cold PGE_2). The mutants S211L and R214L showed significantly reduced binding when compared to the EP_3 wild type. The mutant N217 which served as our internal control showed binding similar to the wild type. Cold PGE_2 inhibited the

[^{3}H]PGE_2 binding which was similar to that of HEK293 only. The results are presented as the mean ± SD from three assays (n = 3) in (Figure 15). On comparing the [^{3}H]PGE_2

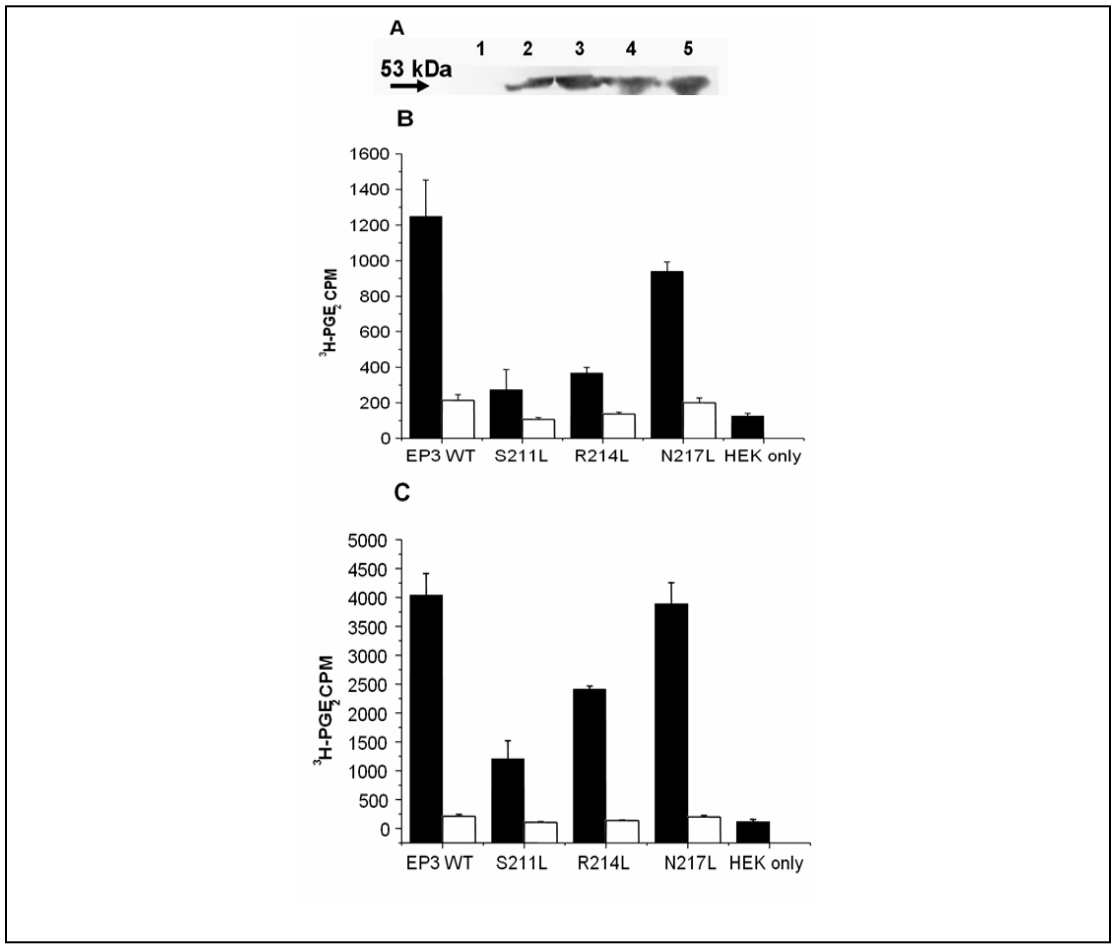

Figure 15. (A) Western blot of the transfected wild-type and mutant EP3 receptors on HEK cells showing good protein expression. (1)HEK only, (2) wild type EP3 (3) Mutant S211L, (4) Mutant R214L,(5) Mutant N217L. (B), Histograms showing total binding and nonspecific binding for the EP3 wild type and mutants, showing a significant decrease in binding for the mutants with low [3H] PGE2 counts (0.03555nM, 9000 cpm's) in the reaction volume (100µL).(C) Shows an increase in binding for the mutants at higher counts (0.1185nM, 30,000 cpm's) but it is still less than the wild type and the internal control mutant N217L. Thus both the mutants S211L and R214L show significantly decreased binding when compared to wild type and the internal control mutant N217L. Binding to HEK only was comparable to the nonspecific binding in the presence of Cold PGE2 (5µM). The results are presented as the mean ± SD and are representative data from three assays (n = 3).

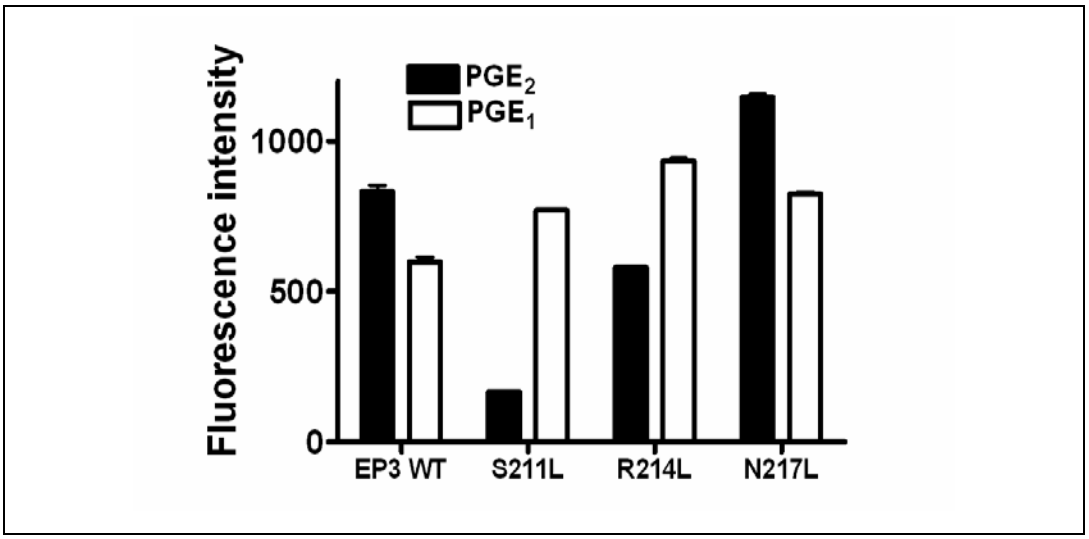

Figure 16: Calcium signaling assay of wild type and the mutants S211L, R214L and N217L using PGE_1 and PGE_2. 10nM PGE_1 and PGE_2 was tested for a calcium signal. Mutant S211L was able to differentiate between the two ligands as it showed a normal calcium signal with PGE_1 and reduced signal with PGE_2. Cells were grown in 6 well plates and incubated with Fluo8 AM dye as mentioned in the procedure. The calcium signal was detected one well at a time using multi well cytoflour plate reader.

binding at low concentration (0.03555 nM, 9000 cpm) and high concentrations (0.1185 nM, 30000 cpm) it was observed that there was an increase in $[^3H]PGE_2$ binding to the mutants, yet it was still significantly less as compared to wild type and internal controls (Figure 15 B&C). This signifies that a single point mutation can significantly alter the receptor binding and that the binding is not restored even with high concentration.

4.7. Calcium signal of EP_3 wild type versus mutants

HEK293 cells expressing recombinant EP_3 and mutant receptors were grown in 6-well plates and the Ca^{2+} signal as fluorescence intensity, for PGE_1 (10 nM) and PGE_2 (10

nM) was detected using Fluo8-AM dye. PGE_1 showed a higher Ca^{2+} signal with mutant S211L receptor as compared to PGE_2. Thus the calcium signal difference between PGE_1 and PGE_2 suggested that the mutant specifically inhibited PGE_2 activity and not PGE_1 (Figure 16).

High throughput mutagenesis

4.8. Establishing twenty four stable cell lines expressing EP_1 mutant receptors from PCR product direct transfection

Twenty four stable cell lines in HEK293 cells expressing mutant EP_1 receptors were generated using PCR product direct transfection using lipofectamine as mentioned before. The residues indicated in Figure 17A were mutated using the method shown in Figure 17B. The PCR amplification band is shown in Figure 18B. Western blot analysis was performed (primary Ab: Rabbit anti EP, secondary Ab: Goat anti-rabbit HRP) to evaluate the receptor protein expression, and revealed a good mutant EP_1 protein expression with GAPDH as loading controls (Figure 18A).

4.9. Radioligand binding of EP_1 wild type versus twenty-four EP_1 mutants generated by high throughput mutagenesis

The stable cell lines expressing twenty-four EP_1 mutants in HEK293 cells (produced by direct transfection of PCR products) were incubated with $[^3H]PGE_2$ (0.03555 nM, 9000 cpm) with and without unlabelled PGE_2 (Cold PGE_2). The mutants

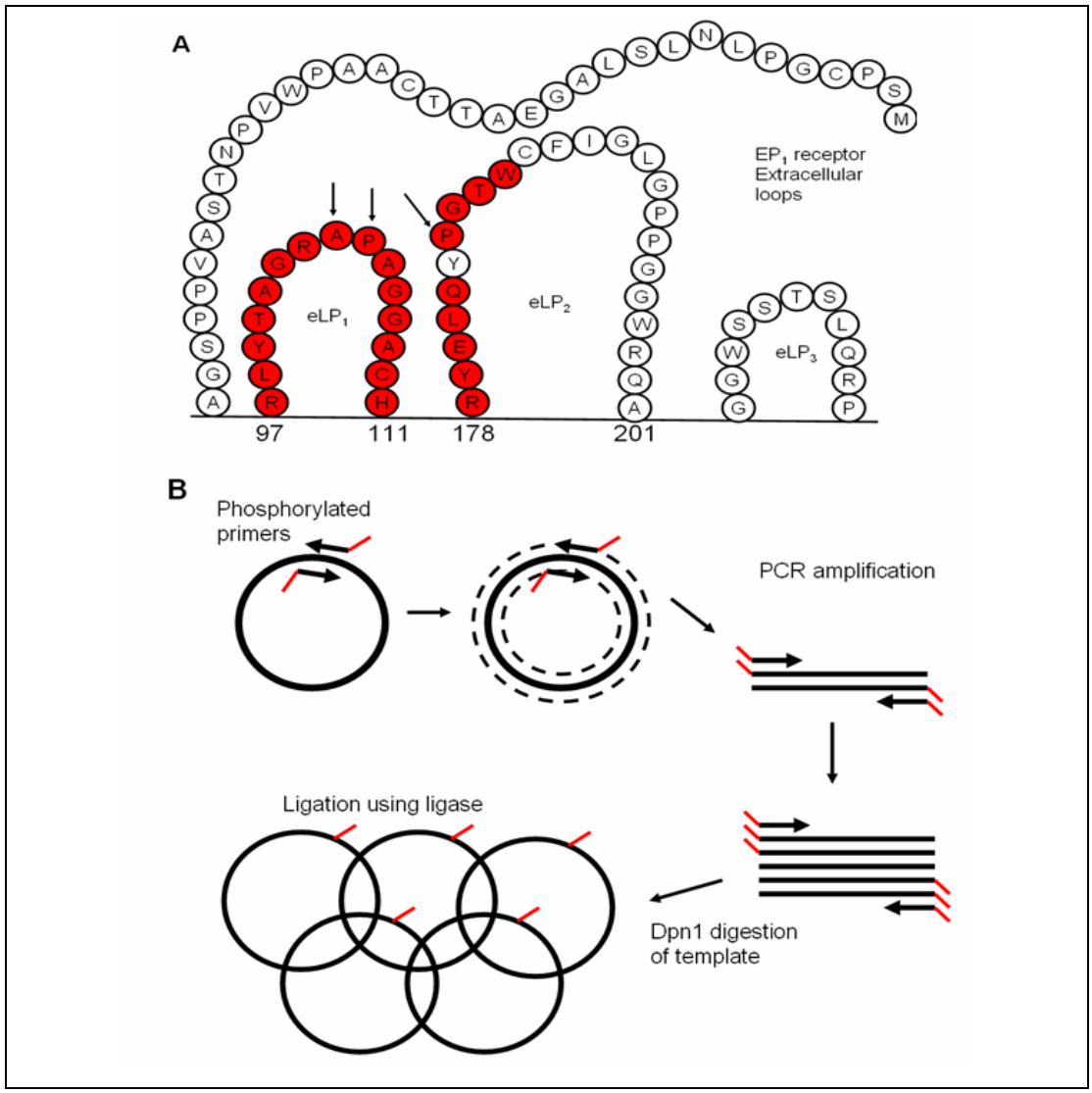

Figure 17: (A) The amino acid sequence of the extra cellular loops of the EP_1 receptor. The residues in red indicate the region of the residues chosen for mutation to alanine. Alanine was however mutated to glycine. Residue 183 was not mutated as the sample was lost to experimental spilling. The arrows indicate the residues identified which showed reduced binding to $[^3H]PGE_2$ after direct transfection of PCR product into HEK293 cells as a stable cell line. (B) Principle applied for point mutation using PCR. The phosphorylated primers were used for generating point mutations in the wild type EP_1 pcDNA template. The amplified linear strands produced were incubated with Dpn-1 for digesting the template. These linear strands were treated with T4 DNA ligase to ligate the phosphorylated ends. The circular DNA thus generated was used for direct transfection into HEK293 cells to generate stable cell lines.

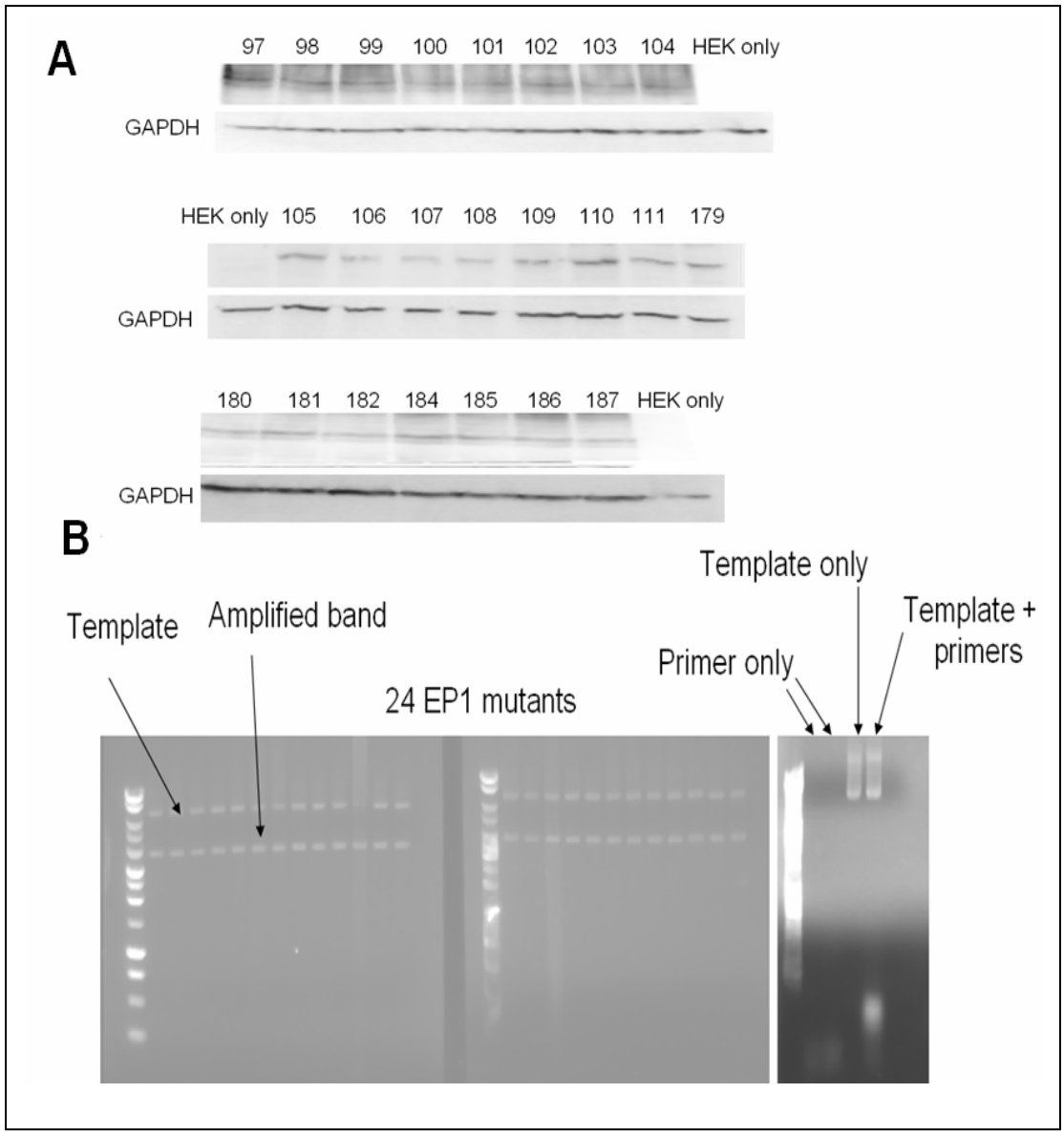

Figure 18. (A) Western blot of the 24 EP_1 receptor mutants expressed in HEK293 cells. The 24 EP_1 mutant stable cell lines (15µg protein) were run through a 8-16% SDS Page gel. The EP_1 bands were detected at 42 kDa for all the stable cell lines with their respective GAPDH controls. (B) Agarose gel (1%) of the mutated PCR product. Ethidium bromide illumination of the amplified PCR product of the mutated EP_1 receptor used for direct transfection into the HEK293 cells is at 4000kb. The template is visible at 8000kb. The lanes showing primer only, template only and template plus primers is marked with arrows.

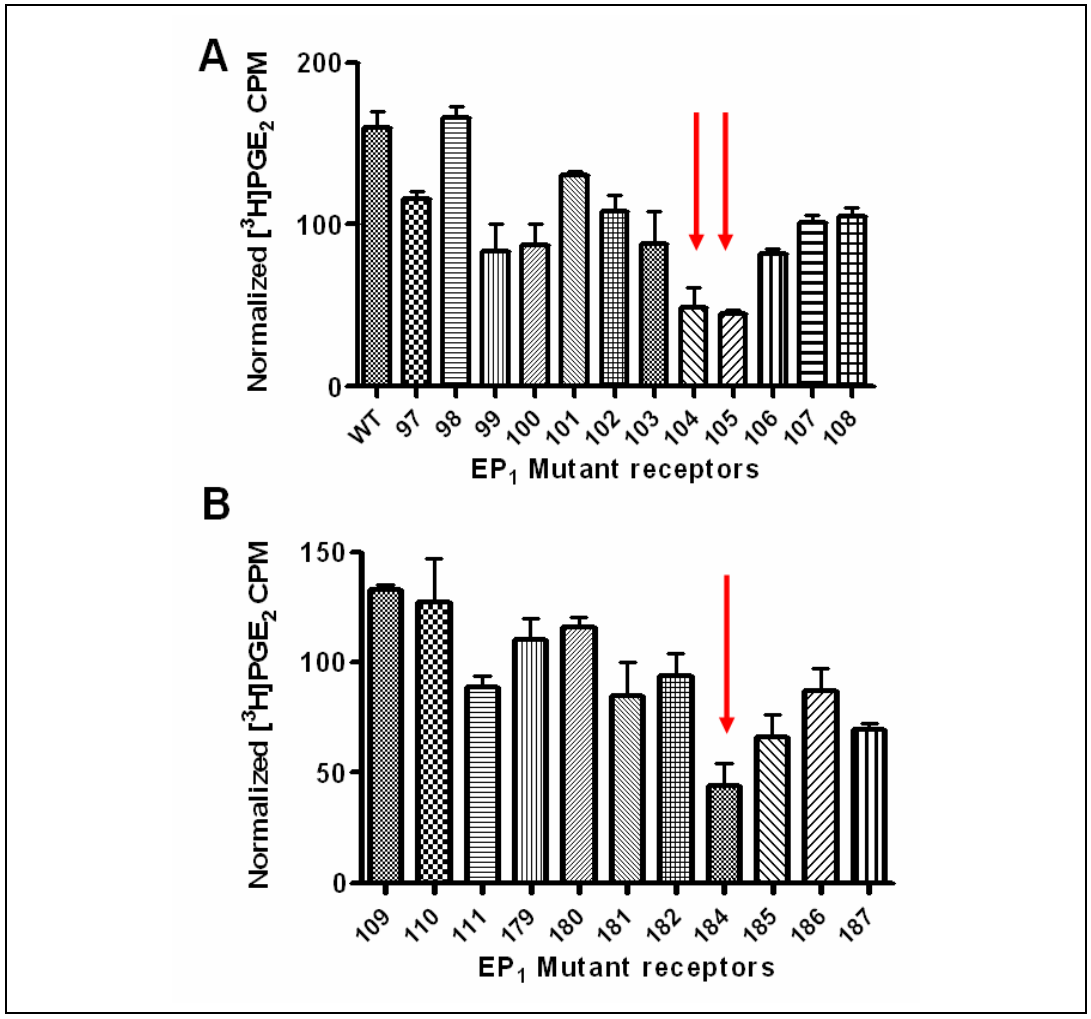

Figure 19: Radioligand [^{3}H]PGE$_2$ binding to the EP$_1$ mutant receptors as stable cell lines. (A) The histograms represent the normalized [^{3}H]PGE$_2$ binding on the wild type EP$_1$ receptor and the 12 EP$_1$ mutants of the extra cellular loop one and two, as a stable cell line. (B) The histograms represent the normalized [^{3}H]PGE$_2$ binding on the remaining 12 EP$_1$ mutants of the extra cellular loop one and two, as a stable cell line. The red arrows represent the mutants showing reduced [^{3}H]PGE$_2$ binding. The experiments were performed in 24 well plates with 1.1185nM [^{3}H]PGE$_2$ per well in a reaction volume of 200µL as mentioned in procedure with n=3 experiments..

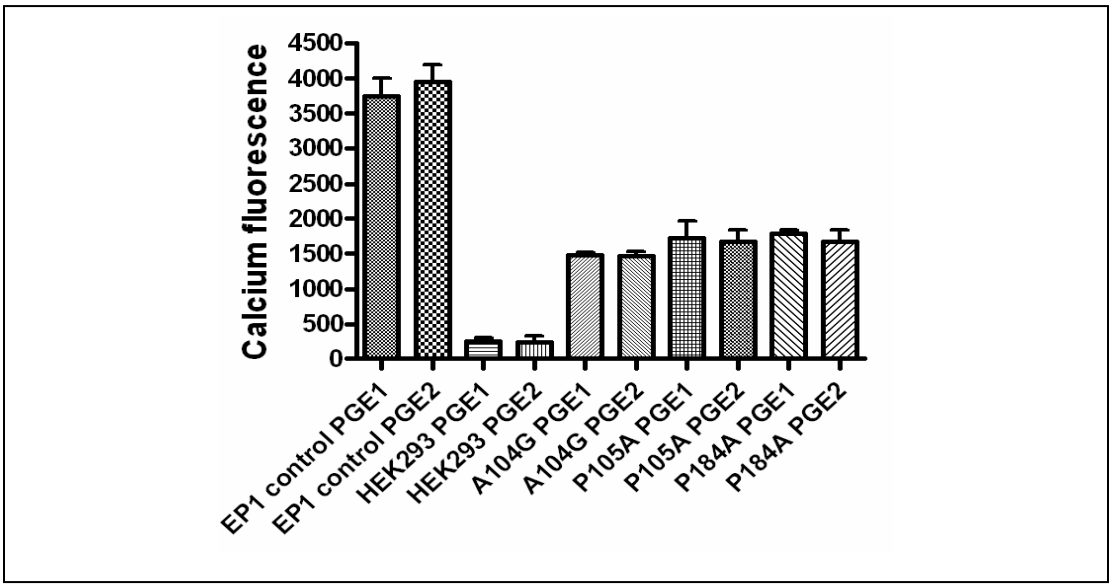

Figure 20: Calcium assay of the wild type EP_1 receptor, HEK293 alone and the three mutants identified by radioligand binding. The significantly decreased calcium signal for the mutants was elicited by 10nM PGE_1 and PGE_2 but was not able to differenciate between the two ligands. The remaining 21 mutants showed a normal calcium signal comparable to the wild type. The calcium assay was performed by culturing the cells in glass bottom plates, incubating with fluo8AM dye and using the Nikon Ti-S eclipse microscope (40x objective) with n=3 experiments.

A104G, P105A and P184A showed significantly reduced binding when compared to the EP_1 wild type. The results are presented as the mean ± SD from three assays (n = 3) in (Figure 19 A&B).

4.10. Calcium signal of EP_1 wild type versus three mutants

HEK293 cells expressing recombinant EP_1 and mutants A104G, P105A and P184A receptors were grown in glass bottom plates and the Ca^{2+} signal as fluorescence

intensity, for PGE_1 (10 nM) and PGE_2 (10 nM) was detected using Fluo8-AM dye. All three mutants showed a lower Ca^{2+} signal with PGE_1 and PGE_2. Thus the calcium signal was not able to differentiate between the two ligands, PGE_1 and PGE_2 (Figure 20).

EP receptors binding and signaling studies

4.11. Establishing four stable cell lines expressing EP_1, EP_2, EP_3, & EP_4 receptors

Due to the co-expression of EP receptors in various tissues, organs and cancer cell lines (Artur et al., 1996; Sugimoto et al., 1992; Honda et al., 1993; Watabe et al., 1993; Katsuyama et al., 1995) it becomes difficult to assess the importance of the individual EP receptors. Therefore to study the EP receptors individually we generated four stable cell lines in HEK293 cells. There was no noticable difference in growth rate between the individual cell lines. Western blot analysis was performed (primary Ab: Rabbit anti EP, secondary Ab: Goat anti-rabbit HRP) to evaluate the receptor protein expression, and revealed that the EP_1 and EP_4 expression was lower when compared to EP_3 and EP_2 (Figure 21A). Since the primary antibody detected multiple bands, we chose non-relevant bands at 35 kDa (for EP_1), 40 kDa (EP_2), 150 kDa (EP_3) and 40 kDa (EP_4) as loading controls. Confocal microscopy, however, showed a good surface expression of the EP receptors in these stable cell lines with their adjacent HEK293 controls (Figure 21D).

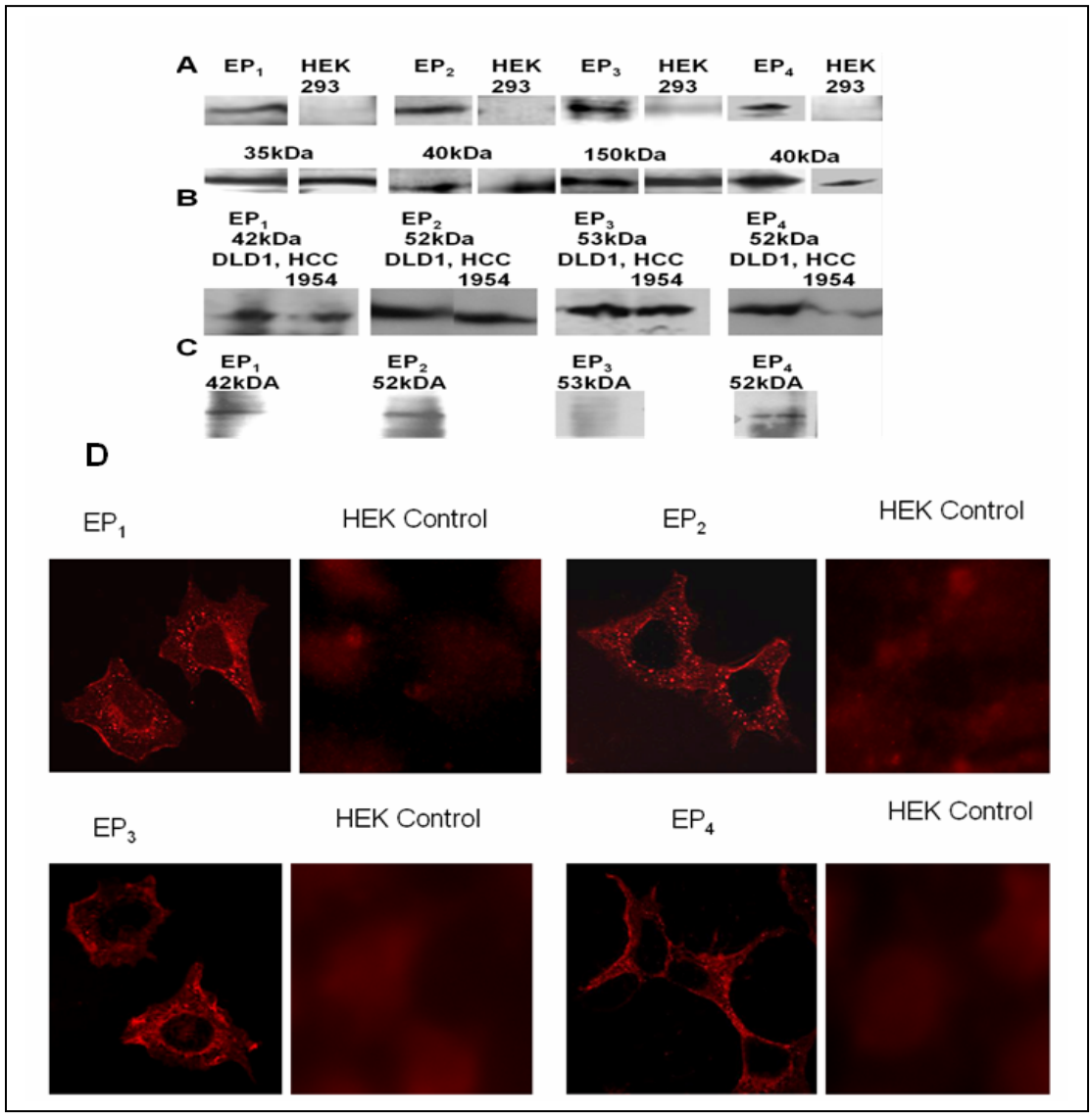

Figure 21: (A) Shows the western blot expression of the 4 EP receptor stable cell lines, and other bands at 35kDa (for EP1), 40kDa (EP2), 150kDa (EP3) and 40kDa (EP4) as loading controls due to the antibody detecting multiple nonspecific bands. (B) Shows the presence of EP receptors in two cancer cell lines DLD1 (colorectal adenocarcinoma) and HCC1954 (ductal carcinoma of the breast).(C) and in human embryonic stem cells.(D) Surface expression of EP receptors was detected by immunostaining on stable cell lines using confocal microscopy with their adjacent HEK293 controls using secondary antibody.

4.12. Expression of subtype EP receptors in cancer cell lines and stem cells

Western blot analysis of cancer cell lines (DLD1 or colorectal adenocarcinoma and HCC1954 or ductal carcinoma of the breast) was performed. Both the cancer cell lines showed expression of all the four EP receptors (Figure 21B). The human embryonic stem cells showed all EP receptors expression except EP_3 (Figure 21C).

4.13. Comparison of [^{3}H] PGE_2 binding to the four subtype EP receptor stable cell lines

HEK293 cells expressing recombinant EP receptors were incubated for 1hr with increasing concentration of [^{3}H]PGE_2 following the saturation kinetics. The Kd of [^{3}H]PGE_2 for the EP_1, EP_2, EP_3 & EP_4 receptors was 0.21 nM, 0.16 nM, 0.42 nM, and 0.15 nM respectively. The BMax thus calculated was EP_1 (1.48), EP_2 (2.05), EP_3 (28.3) and EP_4 (15.57). Thus PGE_2 showed higher affinity or preference for EP_2 and EP_4 receptors as compared to EP_1 and EP_3 (Figure 22(I) A&B). The IC50 thus calculated from [^{3}H]PGE_2 displacement experiments for cold PGE_1 and PGE_2 on the EP receptors is: EP_1 (PGE_1: 3 µM, PGE_2: 8 µM), EP_2, (PGE_1: 0.1 mM, PGE_2: 5 µM), EP_3 (PGE_1: 1 µM, PGE_2: 100 nM) and EP_4 (PGE_1: 1 µM, PGE_2: 100nM) (Figure 22(II) A,B,C & D).

4.14. Effect of [^{3}H] PGE_2 binding to the four subtype EP receptor using available antagonists

[^{3}H]PGE_2 (0.3 nM) was incubated with the antagonists, namely SC19220 (EP_1 selective antagonist, 10 µM), AH6809 (non-selective EP_1, EP_2, EP_3-III antagonist, 10 µM), and GW627368X (EP_4 selective antagonist, 100 nM). The antagonists showed minimal

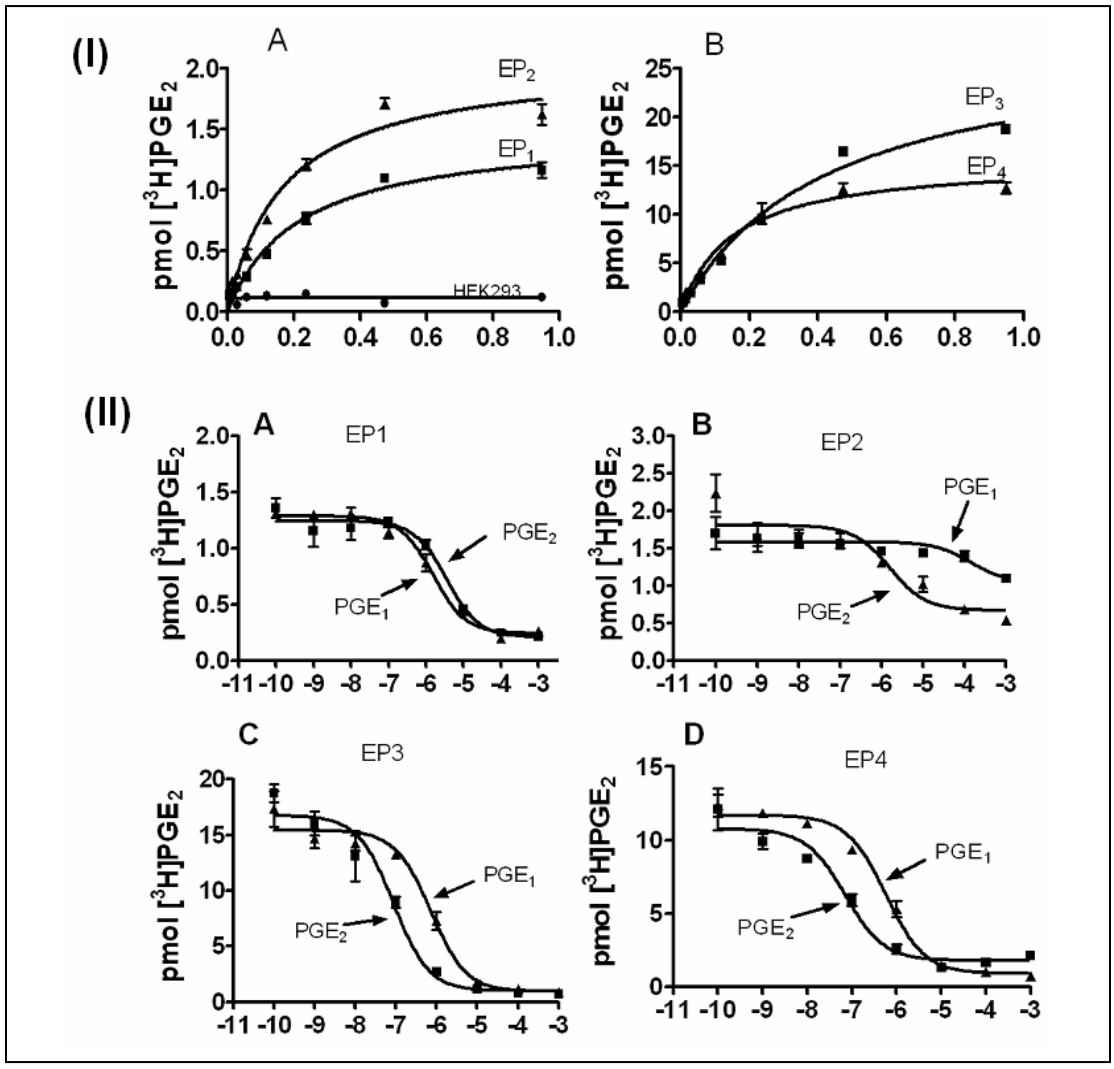

Figure 22: (I) (A) saturation kinetics of $[^3H]PGE_2$ in nM concentration binding to EP_1 and EP_2.(B) Binding to EP_3 and EP_4 as stable cell lines in whole cells. The Kd of $[^3H]PGE_2$ for the EP_1, EP_2, EP_3 & EP_4 receptors was 0.21 nM, 0.16 nM, 0.42 nM, and 0.15 nM respectively. The BMax thus calculated was EP_1 (1.48), EP_2 (2.05), EP_3 (28.3) and EP_4 (15.57). (II) Displacement kinetics of $[^3H]PGE_2$ using log concentrations of cold PGE_2 and PGE_1 on (A) EP_1, (B) EP_2 (C) EP_3 and (D) EP_4 recombinant receptors expressed in HEK293 cells for determination of IC50 values. The IC50 thus calculated is , EP_1 (PGE_1 3µM, PGE_2 8µM), EP_2, (PGE_1 0.1mM, PGE_2 5µM), EP_3 (PGE_1 1µM,PGE_2 100 nM) and EP_4 (PGE_1 1µM, PGE_2 100nM).

inhibition of [^{3}H]PGE_2 binding to EP_1, EP_4 and EP_2 receptors but no inhibition to EP_3 receptor (Figure 25).

4.15. Comparison of calcium signal of PGE_1 and PGE_2 on recombinant EP receptors expressed in HEK293 cells

HEK293 cells expressing recombinant EP receptors were grown in 6-well plates and the Ca^{2+} signal as fluorescence intensity, for PGE_1 (100 pM and 10 nM) and PGE_2 (100 pM and 10 nM) was detected using Fluo8-AM dye. PGE_1 showed a higher Ca^{2+} signal with EP_1 receptor as compared to PGE_2. There was a two-log concentration difference between PGE_2 and PGE_1 for generation of Ca^{2+} signal in EP_4 receptors. PGE_1 and PGE_2 generated the same intensity of Ca^{2+} signal for the EP_3 receptor whereas no significant Ca^{2+} signal was detected with EP_2 receptor (Figure 23).

4.16. Calcium signal confirmation using fluorescence microscopy

Single cell Ca^{2+} signal for the EP_1 receptor was evaluated using fluorescence microscopy with Fluo-8AM dye. The single cell Ca^{2+} signal as fluorescence intensity was plotted for both PGE_1 (100 pM and 10 nM) and PGE_2 (100 pM and 10 nM). PGE_1 was able to produce a significantly higher calcium signal at 100 pM concentration than PGE_2 as shown (Figure 24).

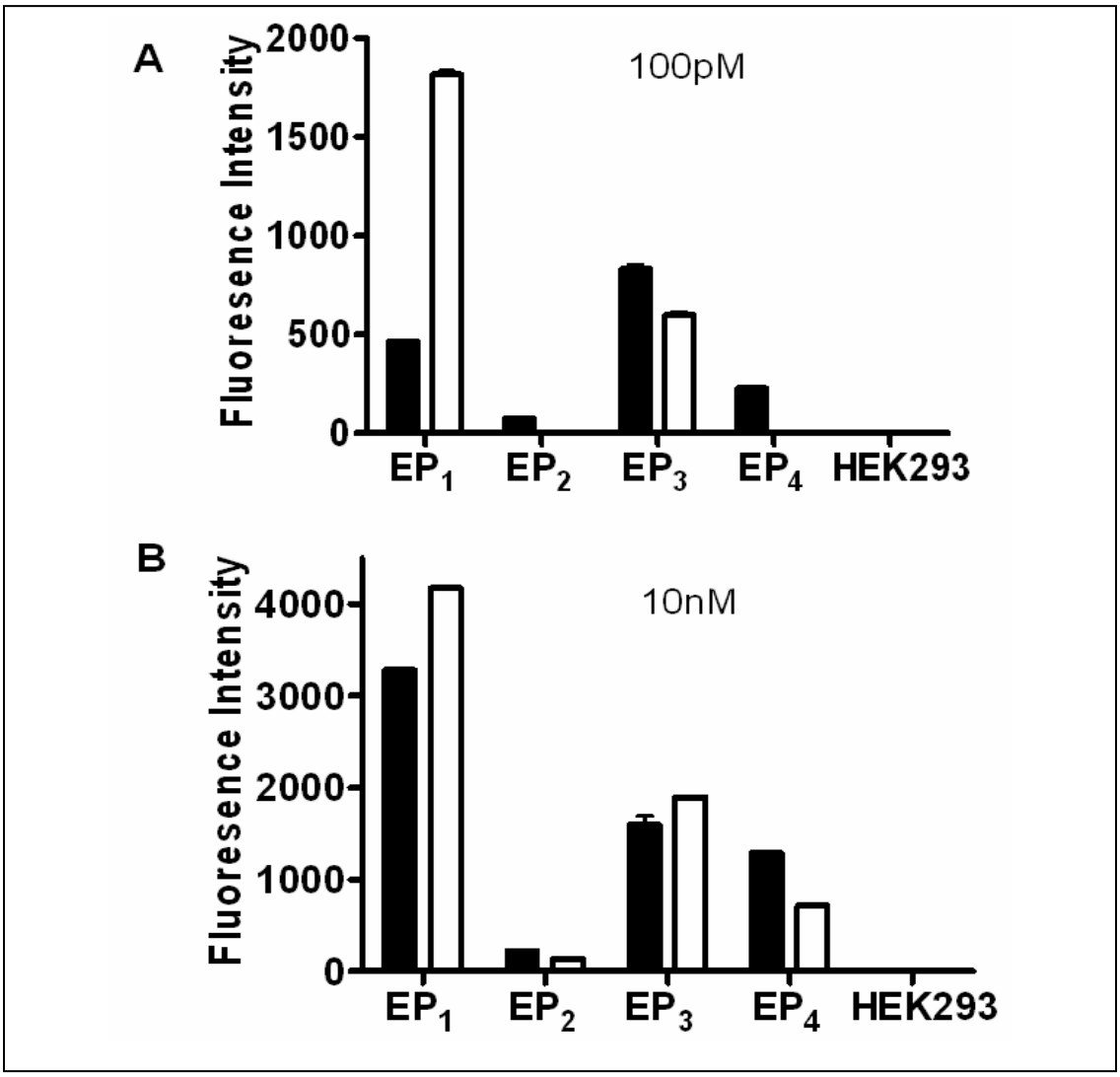

Figure 23: Calcium signaling assay of the EP receptor stable cell lines using PGE_1 and PGE_2. (A) Closed bars show the calcium signal as fluorescence intensity of 100pM PGE_2 and open bars for 100pM PGE_1. (B) Shows the calcium signal with 10nM PGE_2 (closed bars) and10nM PGE_1 (open bars). The EP_1 receptor was able to differentiate between the two ligands at 100pM concentration. PGE_1 showed a higher calcium signal than PGE_2 at 100pM concentration. The EP receptor stable cell lines were grown in 6 well plates, incubated with Fluo8AM dye and the calcium signal evaluated one well at a time using the multi well cytofluor plate reader with n=3 experiments.

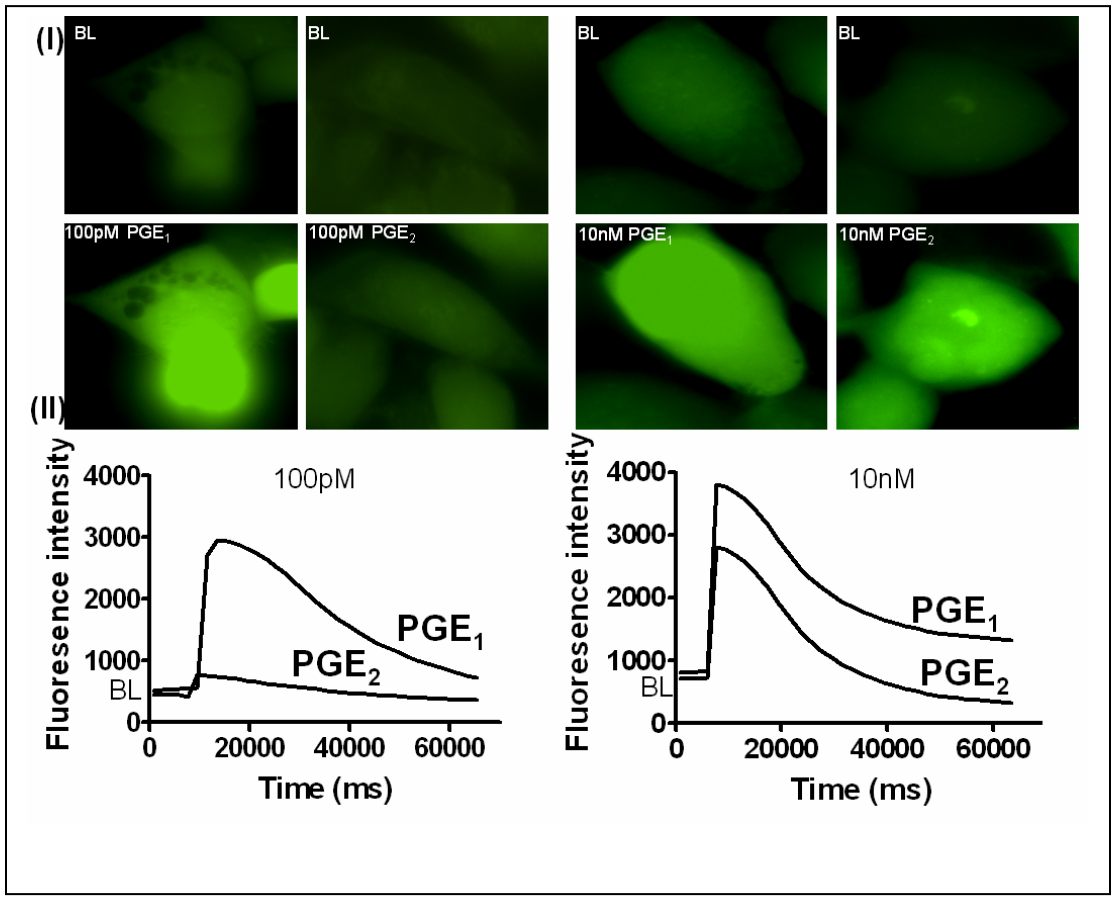

Figure 24: Shows single cell calcium signal for EP_1 receptors expressed in HEK293 cells as a stable cell line using 100pM and 10nM PGE_1 and PGE_2. (I) (BL) baseline calcium signal for HEK293 cells expressing EP1 receptors. The corresponding calcium signal is with 100pM PGE_1, 100pM PGE2, 10nM PGE_1 and 10nM PGE_2. (II) Single cell calcium signal as fluorescence intensity plot for (100pM) PGE_1 and PGE_2 on the left hand side and for 10nM PGE_1 and PGE_2 on the right hand side. The cells were grown in glass bottom plates, incubated with Fluo8AM dye and the calcium signal evaluated using Nikon Ti-S eclipse microscope.

4.17. Comparison of calcium signal of PGE_1 and PGE_2 in recombinant EP receptors expressed in HEK293 cells using available antagonists

The Ca^{2+} signal was analyzed using various antagonists to the EP receptors. The three antagonists, namely SC19220 (EP_1 selective antagonist, 10 µM), AH6809

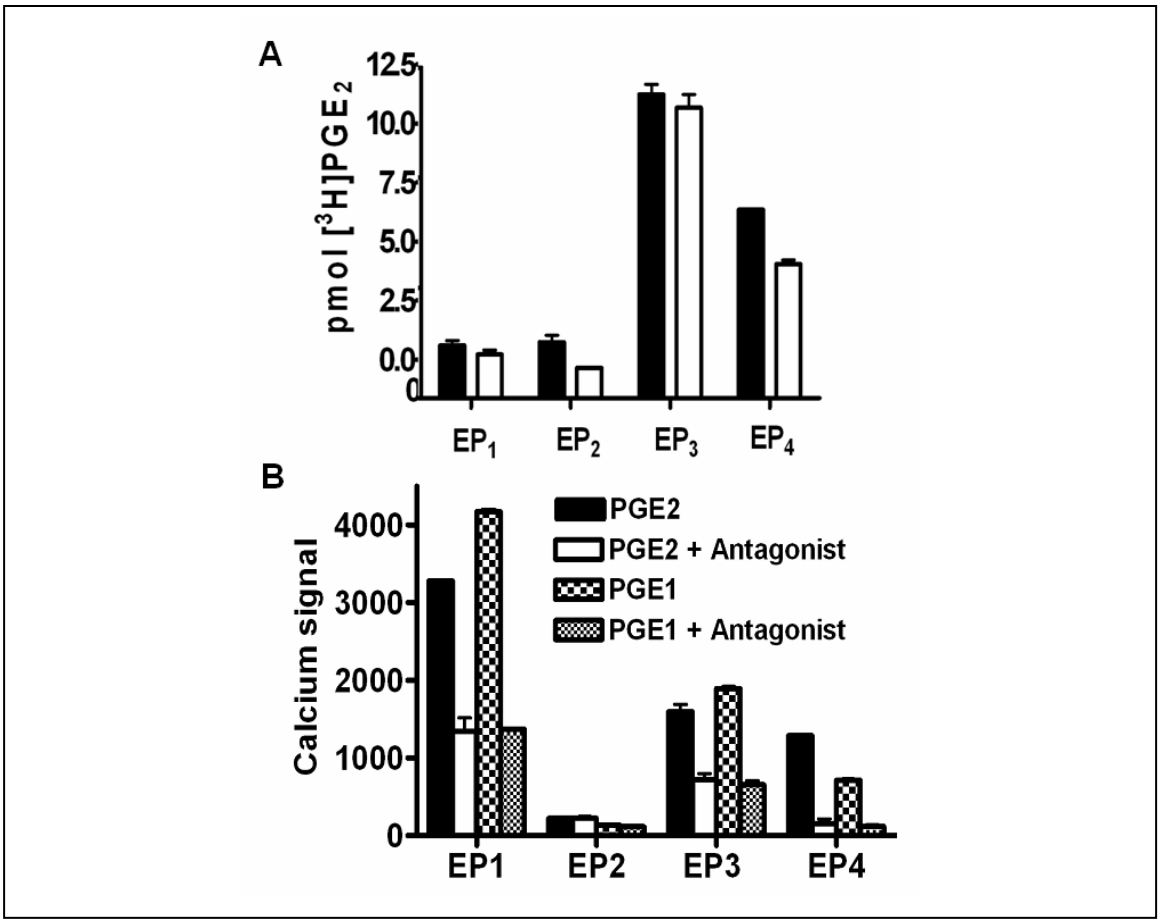

Figure 25: Radioligand binding ([^{3}H] PGE_2) and calcium signaling on EP receptor stable cell lines in presence of EP receptor antagonists as mentioned in procedure. (A) [^{3}H] PGE_2 binding in the presence of antagonists. (B) The calcium signal as fluorescence intensity using Fluo 8 AM dye for (10nM) PGE_2 and (10nM) PGE_1 on the EP receptors using the available antagonists. The three antagonists are SC19220 (EP_1 selective antagonist), AH6809 (nonselective EP_1, EP_2, EP_3-III antagonist), and GW627368X (EP_4 selective antagonist).

(nonselective EP_1, EP_2, EP_3-III antagonist, 20 µM), and GW627368X (EP_4 selective antagonist, 100 nM) were evaluated. They were able to partially inhibit the Ca^{2+} signal (Figure 25).

4.18. Comparison of cyclic AMP accumulation with PGE_1 and PGE_2 in recombinant EP receptors expressed in HEK293 cells

The 10-minute cyclic AMP accumulation upon stimulation of the EP receptors was quantified using the cAMP Biotrak Enzyme Immune Assay System. Both PGE_1 and PGE_2 (10 nM and 100pM) produced a moderate cAMP accumulation upon EP_1 receptor stimulation. The highest cAMP accumulation was seen through the EP_2 receptor whereas a comparable cAMP accumulation was seen for the EP_3 and EP_4 receptors. However, the cAMP accumulation was inconclusive in differentiating between the two ligands (Figure 26).

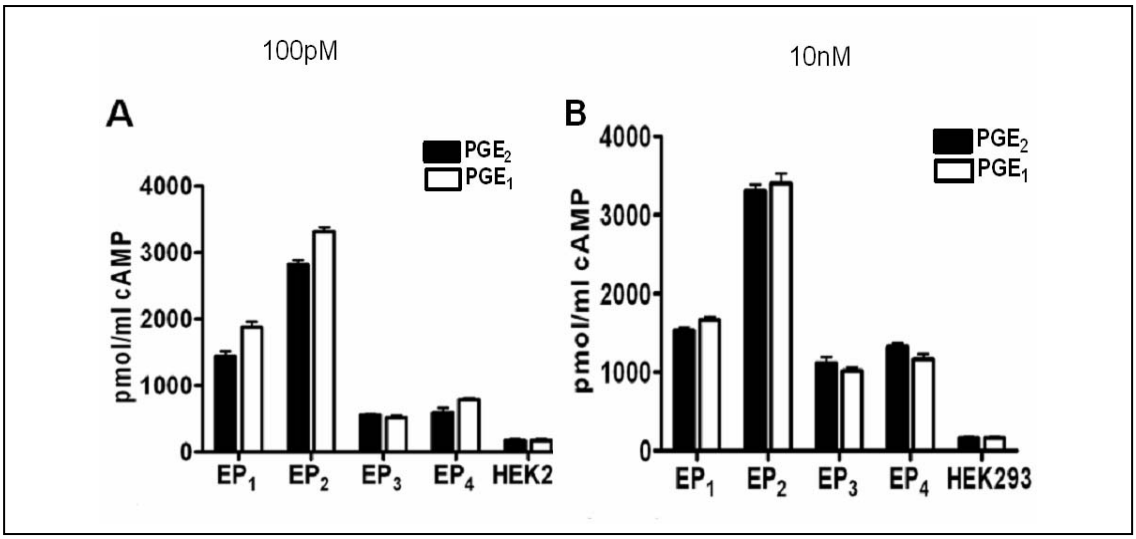

Figure 26. cAMP accumulation in EP stable cell lines treated with (A) 100pM, PGE_2 (closed bars) and 100pM, PGE_1(open bars) and (B) 10nM, PGE_2 (closed bars) and 10nM, PGE_1(open bars) on the EP receptor stable cell lines in HEK293 cells. EP_1 stable cell line was cultured in 10cm plates and incubated with PGE_1 and PGE_2. The treated cells were processed according to manufacturers instructions provided in the kit. The cells were processed in 5ml of the buffer provided in the cAMP Biotrak EIA System.

4.19. Comparison of leukotrine C4/D4/E4 levels with PGE_1 and PGE_2

LC/MS/MS analysis of supernatant from EP_1 stable cell line treated with PGE_1 and PGE_2 showed extra peaks resembling the molecular weights of many leukotrienes (Figure 27A) (Table 2). The leukotrine C4/D4/E4 levels in the EP_1 stable cell line were compared after stimulation with 100 pM PGE_1 and PGE_2. PGE_2 was able to stimulate higher levels of leukotrine C4/D4/E4 levels using the oxford biomedical research ELISA kit. The levels were 0.8 ng/mL with PGE_1 and 0.42 ng/mL with PGE_2. Control HEK293 cells also showed some amount of Leukotriene production (Figure 27B). PGE_2 is a known inflammatory molecule and we suggest that the increase in the Leukotrienes through the EP_1 receptor is the main differentiating feature between the two ligands.

4.20. Comparison of Lipoxin B4 peaks in EP_1 stable cell lines using LC/MS

The EP_1 stable cell line was incubated with 100 pM PGE_1 and PGE_2 for 20 minutes. The serum-free cell culture medium with the cell lysate was collected and passed through C18 column, eluted with acetone, dried and dissolved in solvent A. The metabolite of Lipoxin B4 called 20-hydroxy lipoxin B4 was detected with LC/MS at 21.441 minutes with MW 368.4633 g/mol. The standard 5(S), 14(R) Lipoxin B4 metabolite 20-hydroxy lipoxin B4 peak was also detected at 21.441 mins. Lipoxin B4 is a potent anti–inflammatory eicosanoid involved in phagocytic clearance of apoptotic leukocytes. We suggest that it could be lipoxin B4 which is involved in the anti-

inflammatory activity of PGE_1 through the EP_1 receptor (O'Sullivan, 2007, Parkinson, 2006) (Figure 27A, 28&29).

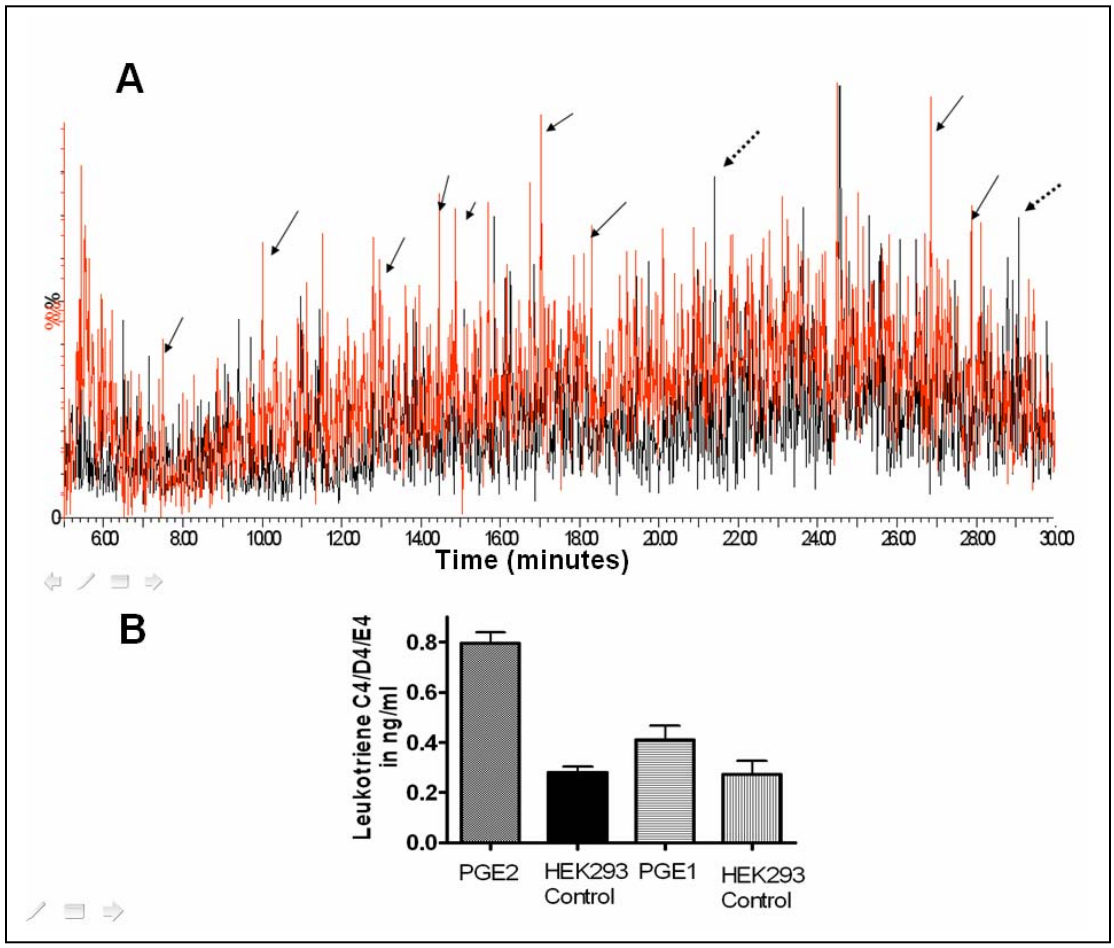

Figure 27: (A) Superimposed mass spectroscopic (LC/MS/MS) analysis of the supernatant of EP_1 stable cell line treated with 100pM PGE_1 and PGE_2. Cells were cultured in a 10cm plate and incubated with 100pM PGE_1 and PGE_2 for 20 mins. The supernantent was passed through C18 column and eluted with acetone. It was dried and dissolved in 100µL buffer A with 50 µL used for LC/MS/MS analysis. The dotted arrows indicate the extra peaks seen in the PGE_1 treated sample (similar MW of Lipoxin B4). The solid arrows indicate the extra peaks seen in the PGE_2 treated sample (similar MW of leukotrienes) Table 2.. (B) The leukotriene C4/D4/E4 detection assay of EP_1 stable cell line incubated with PGE_1 and PGE_2 using ELISA. EP_1 stable cell line in 10cm plates were incubated for in serum free DMEM medium with 100pm PGE_1 and PGE_2 with HEK293 controls. The medium with the cell lysate was passed through C18 column and the acetone eluted substance was evaluated using oxford biomedical research ELISA kit EA 39.

Table 2: Pubchem results for molecular weights similar to the extra peaks seen in LC/MS/MS of EP_1 receptor supernatant treated with PGE_1 and PGE_1 (Figure 27A).

PUTATIVE EXTRA PEAKS FOR PGE_2 TREATED SAMPLE	**MOLECULAR WEIGHTS**
lysine; L-lysine; lysine acid	**MW**: 146.187560 g/mol
L-Glutaminyl-peptide	**MW**: 203.195820 g/mol
T Cell modulatory peptide	**MW**: 233.264860 g/mol
Lysyl-serine; T Cell modulatory peptide	**MW**: 233.264860 g/mol
Gly-gly-his; Diglycyl-histidine	**MW**: 269.257200 g/mol
Phosphinic Peptide Inhibitor	**MW**: 271.249381 g/mol
PEPTIDE ANALOG; Pro-Gln-Ile-Thr-Leu-Trp	**MW**: 275.410720 g/mol
Gamma-glutamylcysteine; gamma-glutamyl cysteine peptide;	**MW**: 289.328080 g/mol
Cyclic peptide of azaserine	**MW**: 312.238880 g/mol
Peptide T analog; Thr-Thr-Thr	**MW**: 321.326920 g/mol
Tyrosyltyrosine; Tyr-tyr	**MW**: 344.361800 g/mol
Rgd peptide; RGD tripeptide; Arg-gly-asp	**MW**: 346.339680 g/mol
Arg-gly-asp; Rgd peptide	**MW**: 346.339680 g/mol
Rgd peptide; Bitiscetin; Bitistatin	**MW**: 346.339680 g/mol
Ibat cotransporter; ILBP; Sodium-bile acid cotransporter ...	**MW**: 376.877560 g/mol
Alpha-Bcp(1-7); Bag cell peptide (aplysia)	**MW**: 385.819340 g/mol
Bicyclic Smac peptide mimetic, 5	**MW**: 386.487900 g/mol
APGPR; Ala-pro-gly-pro-arg	**MW**: 496.560540 g/mol
Leukotriene D4; Leukotriene D; Leukotriene D	**MW**: 496.659900 g/mol
Epp peptide; Epidermal pentapeptide; Pglu-glu-asp-ser-glyoh ...	**MW**: 517.443980 g/mol
PKR Inhibitor; RNA-Dependent Protein Kinase Inhibitor	**MW**: 268.293820 g/mol
Acetylcarnitine; Acetyl carnitine	**MW**: 203.235580 g/mol
Complement 3a-hexapeptide;	**MW**: 414.453320 g/mol
Ubiquinone; Coenzyme Q; Ubiquinone Q2	**MW**: 318.407340 g/mo
Cryptochrome	**MW**: 584.870840 g/mol
Apoptosis Activator I	**MW**: 240.514220g/mol
Complement C3B	**MW**: 273.242600 g/mol
Death Activating Factor	**MW**: 305.324220 g/mol
leukotriene-A4; Leukotriene A4; Leukotriene A	**MW**: 317.442460 g/mol
Leukotriene A4; CID9818452	**MW**: 318.450400 g/mol
20-Hydroxyleukotriene E4; 20-OH-Leukotriene E4; 20-Hydroxy-leukotriene E4	**MW**: 455.607980 g/mol
14,15-Leukotriene D4	**MW**: 496.659900 g/mol
Leukotriene D-4 sulfone	**MW**: 528.658700 g/mol
Leukotriene F4;	**MW**: 568.722560 g/mol
Leukotriene C-3;	**MW**: 627.789760 g/mol
PUTATIVE EXTRA PEAKS FOR PGE_1 TREATED SAMPLE	
20-Hydroxylipoxin B4; 20-Hydroxy-lipoxin B4; 20-OH-Lxb4 ...	**MW**: 368.464480 g/mol
Peptide diphthamide	**MW**: 325.386700 g/mol

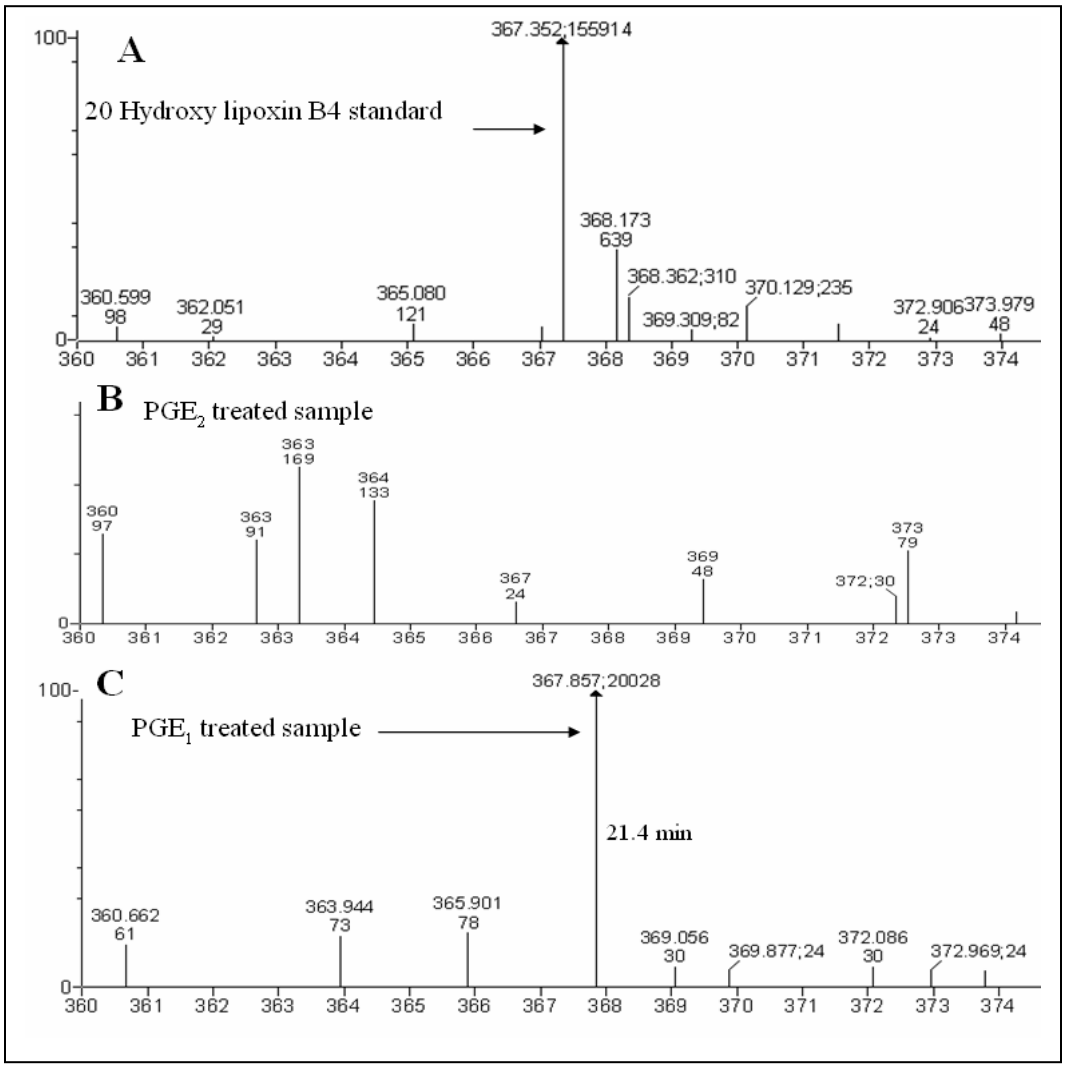

Figure 28: Determination of the Lipoxin B4 peak in the PGE_1 and PGE_2 stimulated EP_1 stable cell line using LC/MS/MS. The EP_1 stable cell line in a 10cm culture plate was incubated for 20 mins with 100pM PGE_1 and PGE_2. The serum free culture medium and the cell lysate was passed through C18 column, eluted with acetone, dissolved in buffer A and analyzed using LC/MS/MS (A) Shows the 20 hydroxy Lipoxin B4 standard peak at 21.4 minutes. (B) Shows the absence of the peak in the PGE_2 treated sample.(C) Shows the presence of the suspected Lipoxin B4 peak at 21.4 minutes in the PGE_1 treated EP_1 stable cell line.

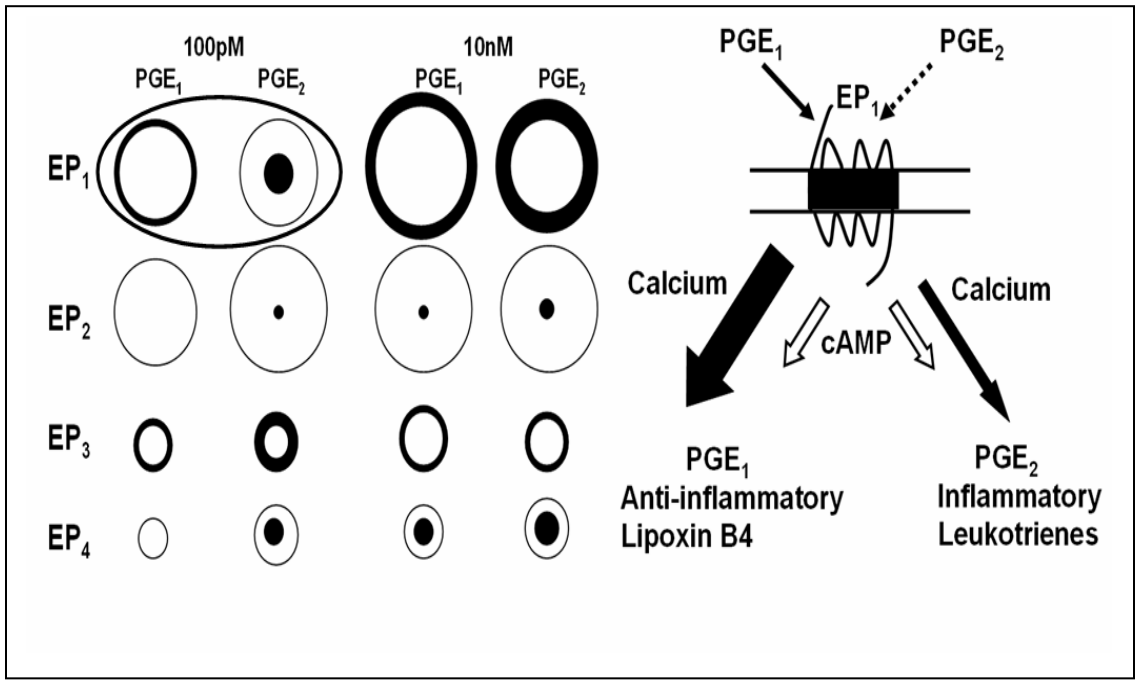

Figure 29: Schematic showing the comparison of calcium signal on all the four EP receptors (Left) Shows the combined Ca2+ (Black circle as fluorescence intensity) and cAMP (White circle as pmol/ml accumulation) signal for PGE_1 and PGE_2 (100pM and 10nM) superimposed on each other. The oval on EP1 receptor signal indicates the observed difference in calcium signal. (Right) A schematic showing that the higher calcium signal (closed arrow) with PGE_1 could relate to its anti-inflammatory property through Lipoxin B4 production. The inflammatory activity of PGE_2 could be attributed to the leukotriene sysnthesis.

4.21. The concept of mimicking Inducible COX-2 coupled to inducible mPGES-1 to overproduce PGE_2

Since various states of inflammation overexpress inducible COX-2 and inducible mPGES-1, the concept of coupling the two enzymes together should produce a state of chronic PGE_2 production. The COX group of enzymes produce PGH_2 which is the

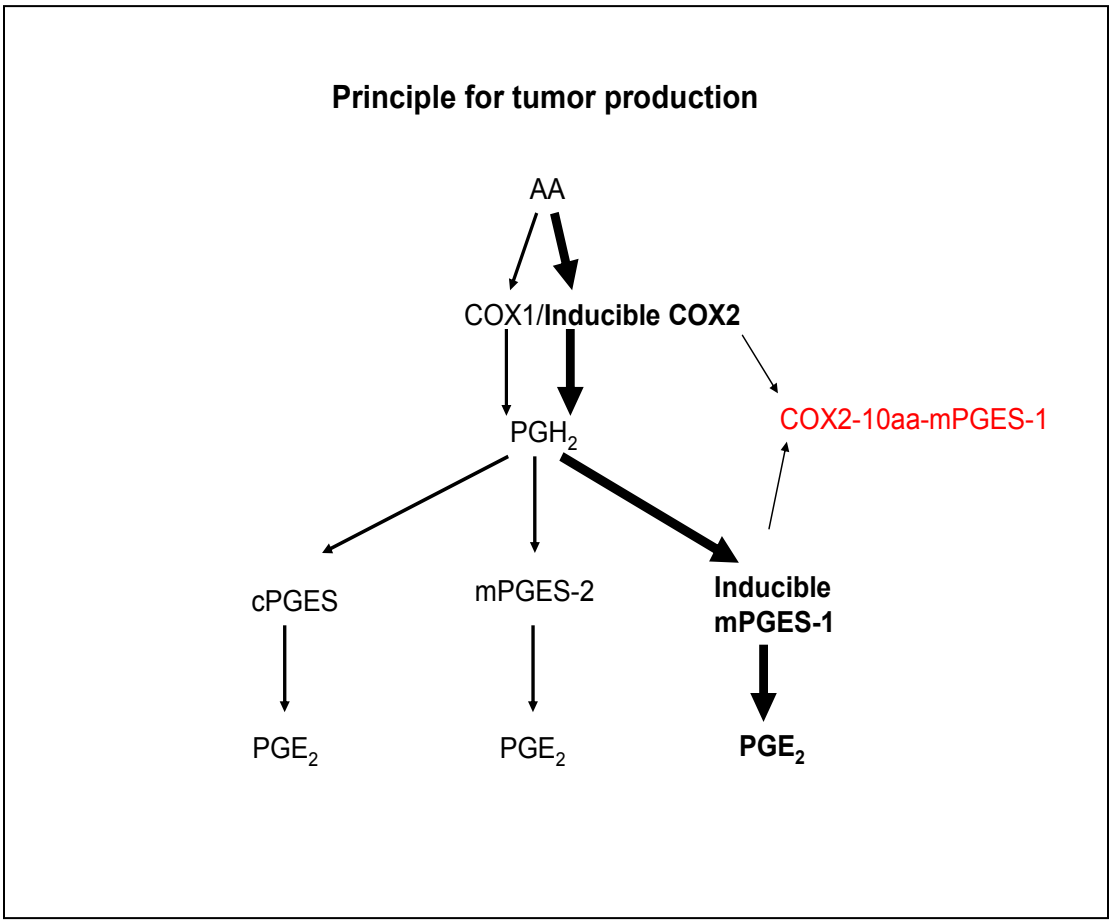

Figure 30: Schematic showing the principle used for tumor formation. The inducible COX-2 and inducible mPGES-1 were linked with a 10 amino acid linker to direct the substrates arachidonic acid and prostaglandin H2 towards excessive production of PGE_2 which induces tumor formation.

substrate for all three PGES enzymes namely, cPGES, mPGES-1 and mPGES-2. Of these three enzymes mPGES-1 is the one which is induced in inflammation. Also, when coupled with inducible COX-2 and overexpressed in cells, has been shown to over produce PGE_2 (figure 30).

4.22. Establishing a HEK293 cell line stably expressing COX-2-10aa-mPGES-1 and co-expressing COX-2 and mPGES-1 individually

A stable cell line expressing the hybrid enzyme and co-expressing COX-2 and mPGES-1 was generated by selecting with G418 antibiotic. The stable cell line was harvested for westernblot analysis and subcultured on glass slides for immunostaining. The western blot analysis showed a distinct band of hybrid enzyme COX-2-10aa-mPGES-1 expression at 91 kDa. The COX-2 band was seen at 72 kDa and mPGES-1 band was seen at 17 kDa. The stable cell line co-expressing COX-2 and mPGES-1 also showed bands at 72 kDa and 17 kDa respectively. The stable cell lines generated from primary culture of the tumor also showed a stable hybrid enzyme expression and co-expression of COX-2 and mPGES-1 (Figure 31). Immunostaining also confirmed the stable expression of both hybrid enzymes and co-expression of COX-2 and mPGES-1 on both the stable cell line and the primary culture (Figure 32).

4.23. Establishing the COX-2-10aa-mPGES-1 hybrid enzyme activity using HPLC method

Different concentrations of [^{14}C]AA were added to the stable cell line in a total reaction volume of 0.225 mL. After an incubation for 0.5 – 5 minutes the reaction was stopped by adding 0.2 mL 0.1% TFA and 0.2 mL 2mM $SnCl_2$. The [^{14}C]AA was metabolized by the hybrid enzyme into [^{14}C]PGE_2 as the product.

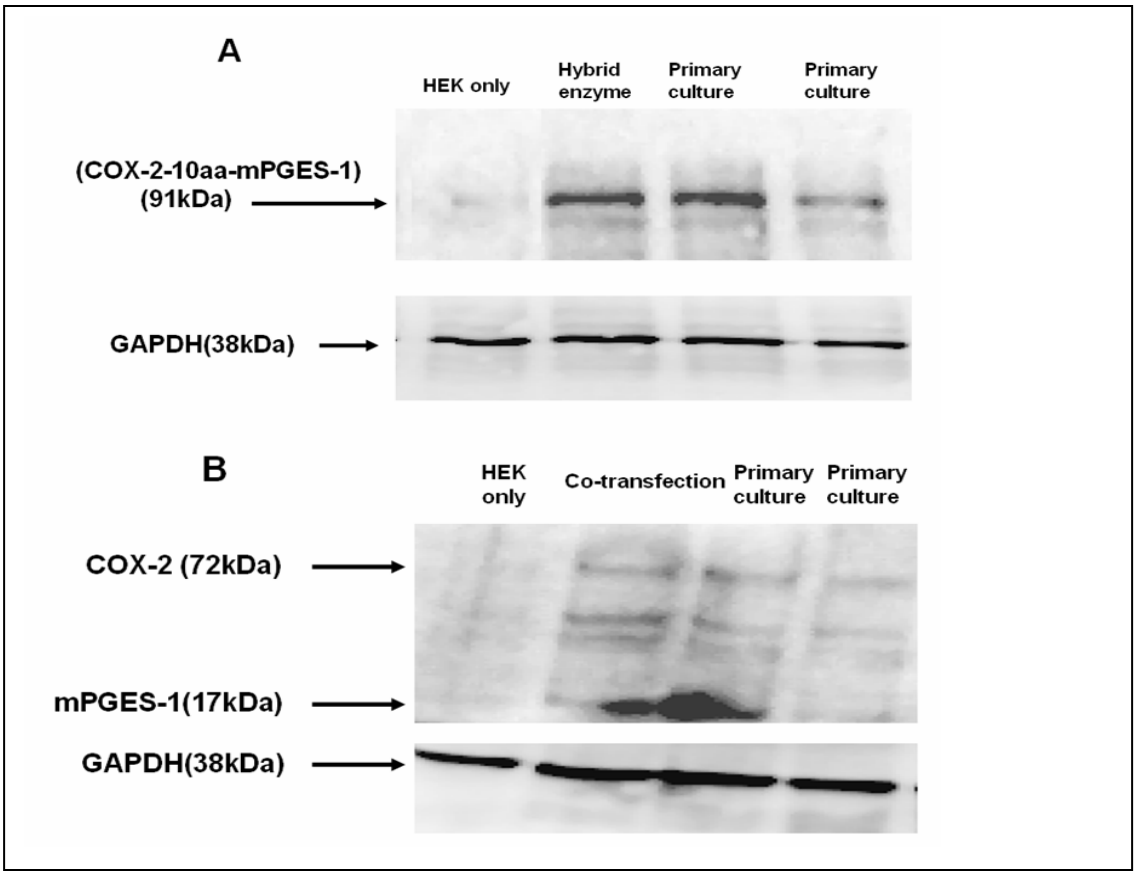

Figure 31: Western blot of COX-2-10aa-mPGES-1 stable cell line, co-transfection stable cell line and their primary culture along with HEK293 controls. 15µg of the whole cell protein was loaded in each well of the SDS page (8-16%) gel. (A) The COX-2-10aa-mPGES-1 hybrid enzyme band was detected at 91kDa for the stable cell line and the primary culture. The appropriate GAPDH loading control bands were detected at 38kDa. (B) The COX-2 and mPGES-1 enzyme band were detected at 72kDa and 17kDa respectively for the stable cell line and the primary culture. The appropriate GAPDH loading control bands were detected at 38kDa.

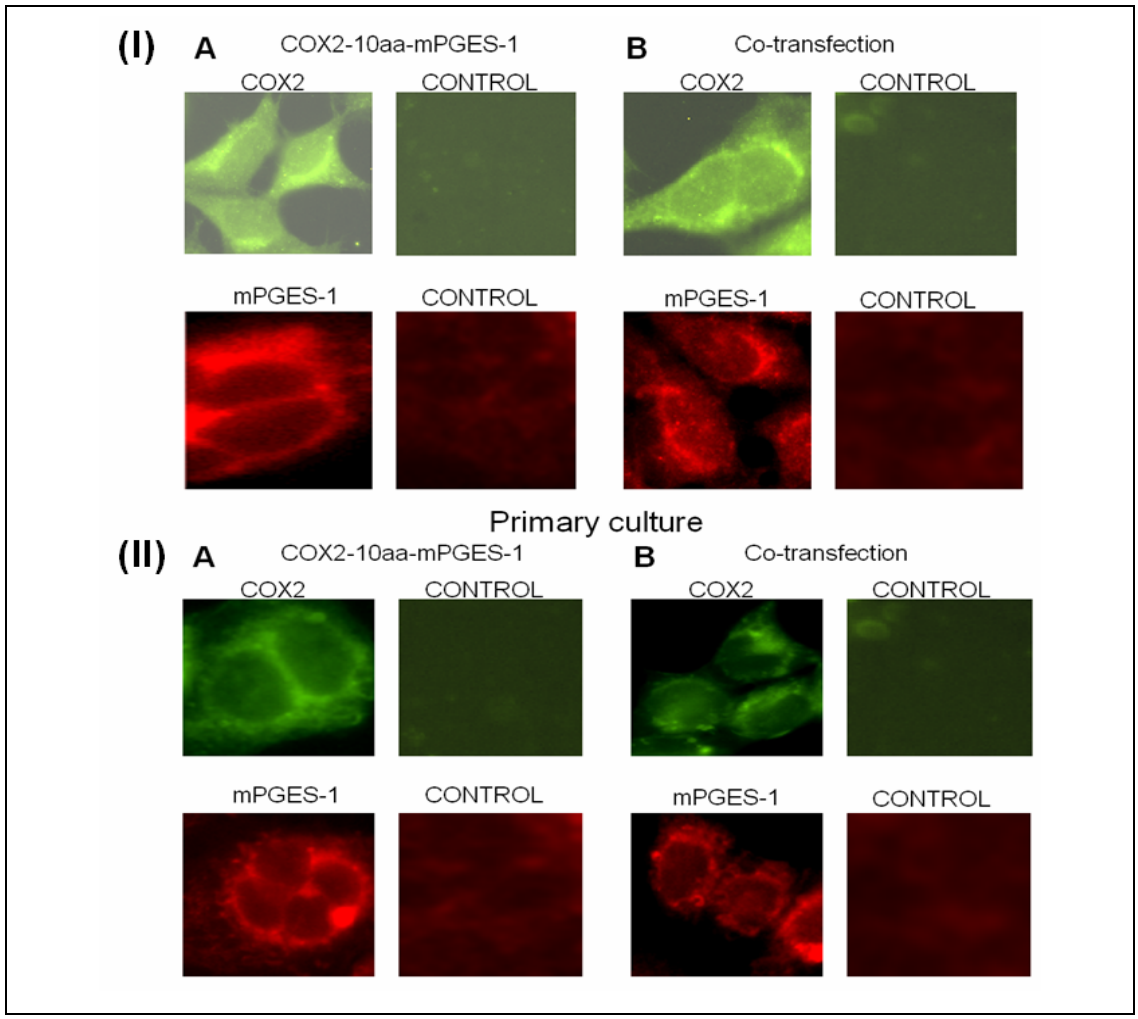

Figure 32: Immunostaining for COX-2 and mPGES-1 enzymes in the (I) (A) COX-2-10aa-mPGES-1 and (B) co transfection stable cell lines with their respective controls. (II) Immunostaining of the primary culture from the tumors, for COX-2 and mPGES-1 enzymes in the (A) COX-2-10aa-mPGES-1 and (B) co transfection stable cell lines with their respective controls. The stable cell line and primary culture were grown on cover slips, fixed with formalin, treated with 1% saponin as the cell permeant and analysed with appropriate primary and secondary antibody.

This [^{14}C]PGE_2 peak was detected at 14 minutes directly by a flow scintillation analyzer. The substrate [^{14}C]AA peak was detected at 35 minutes. The [^{14}C]PGE_2 peak was higher for the stable cell line expressing the hybrid enzyme when compared to the COX-2 and

mPGES-1 co-expression. HEK293 cell controls did not show any [^{14}C]PGE_2 peak (Ruan et al., 2009) (Figure 33).

4.24. The occurrence rate of the HEK293 cell cancer mass expressing the enzymes in the BALB/c nu/nu mice

The HEK293 cells expressing the hybrid enzyme COX-2-10aa-mPGES-1 was injected into the flank of 10 BALB/c nu/nu mice. The tumor occurrence rate was 100% whereas the occurence rate of tumors with the stable cell line co-expressing COX-2 and mPGES-1 was less than 50%. The Fisher's exact test analysis (Fisher, 1922) revealed that the tumor occurrence with the hybrid enzyme was statistically significant with $p<.05$. The tumor growth was faster with the HEK293 cells expressing the hybrid enzyme; it reached the maximum permissible limit (1.5 cm) according to the protocol in 20 days whereas it took 30 days for the co-expression stable cell line to reach the same limit (Figure 34).

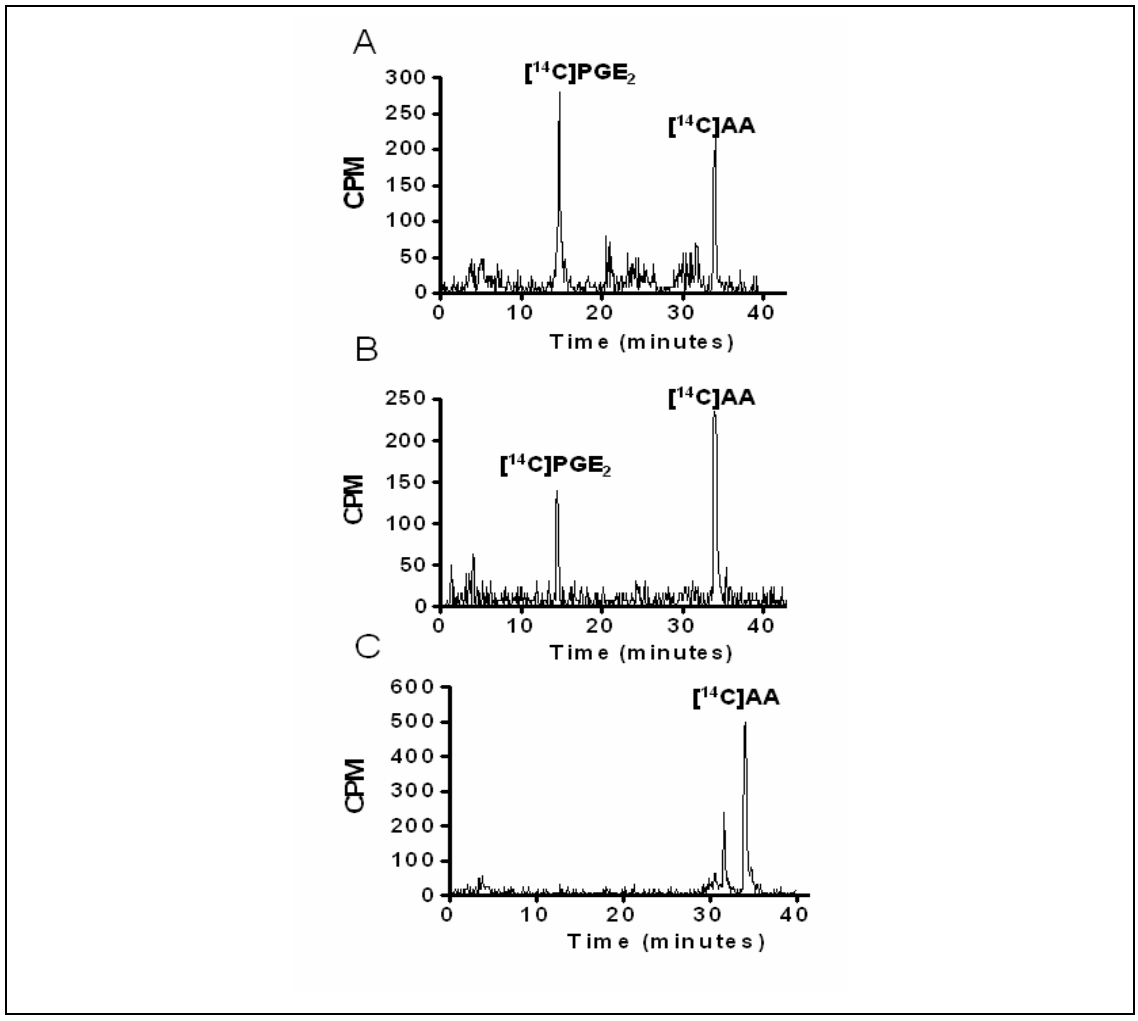

Figure 33: COX-2 and mPGES-1 enzyme activity assay using [^{14}C]AA and HPLC in (A) COX-2-10aa-mPGES-1 stable cell line (B) co transfection stable cell line and (C) HEK293 cells only. Approximately 150,000 cells of the stable cell lines were washed and used for each experiment. Different concentrations of [^{14}C]AA were added to the stable cell line in a total reaction volume of 0.225 mL. The [^{14}C]AA was metabolized by the hybrid enzyme into [^{14}C]PGE_2 as the end-product. This [^{14}C]PGE_2 peak was detected at 14 minutes directly by a flow scintillation analyzer. The substrate [^{14}C]AA peak was detected at 35 minutes. The hybrid enzyme with the linker was able to produce higher levels of PGE_2 in comparasion to co-transfection. This suggested that by linking the two enzymes it is possible to direct the PGH_2 produced from AA towards mPGES-1 to produce higher amounts of PGE_2.

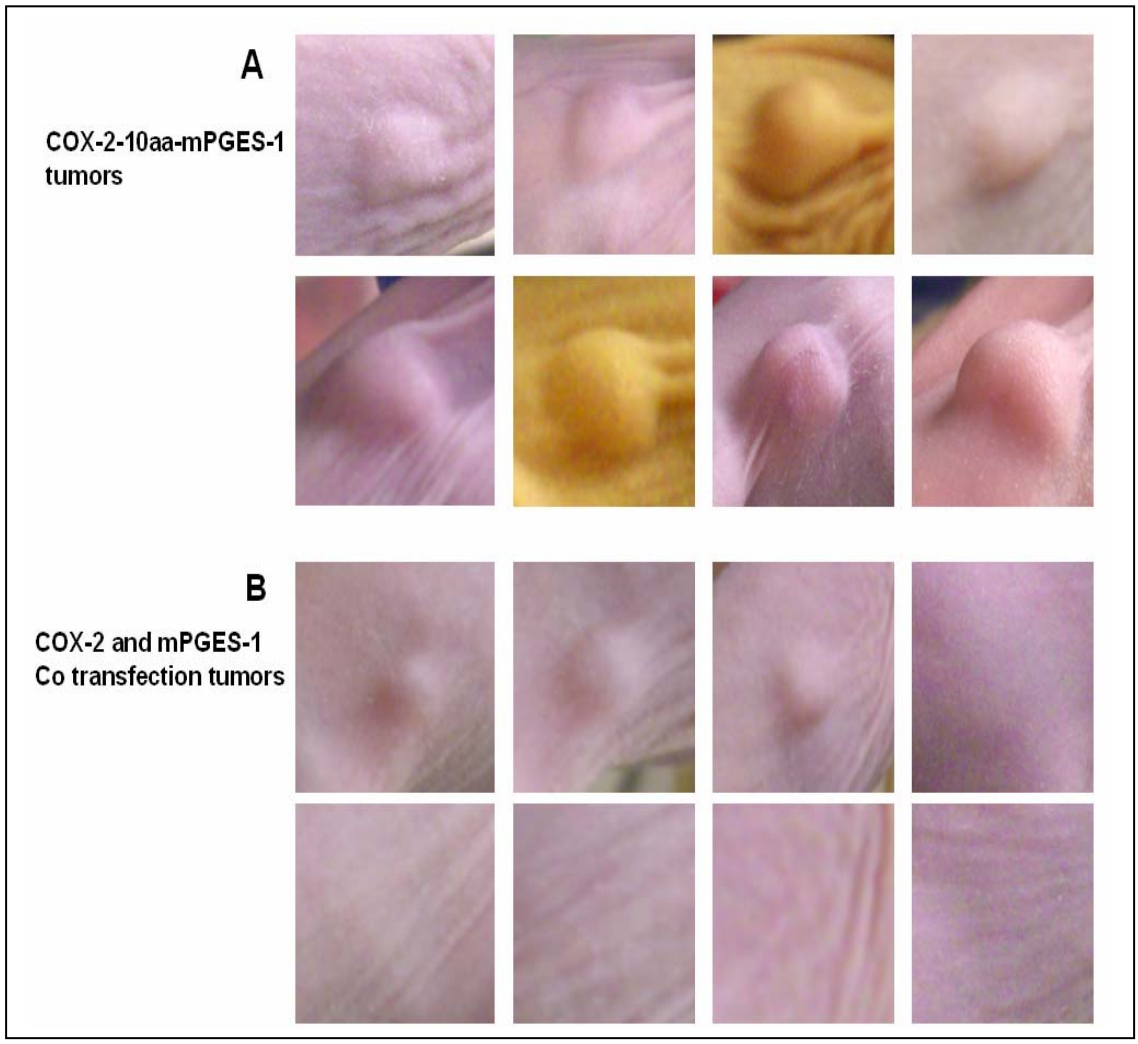

Figure 34: Subcutaneous tumors after 15 days on BALBc/nu/nu mice produced by injecting (A) COX-2-10aa-mPGES-1 stable cell line (B) co-transfection stable cell line. The stable cell lines were grown in 10cm plates. Approximately 50,000 cells were counted microscopically and injected subcutaneously on the right flank of 8 mice each. The hybrid enzyme producing higher amounts of PGE_2 was able to stimulate tumor growth at a faster rate with 100% occurance. The mice injected with the co-transfection stable cell line showed a less than 50% occurance of tumors with slower growth rate. The tumor was allowed to grow upto a maximally permissible limit of 1.5cm before the mice were sacrificed.

4.25. Evaluating the PGE_2 blood levels in BALB/c nu/nu mice using enzyme immunoassay (EIA kit)

The BALB/c nu/nu mice with tumors growing on their flanks were sacrificed by cervical dislocation and the blood collected from the heart. The serum was separated and collected for evaluation of PGE_2 levels using an EIA kit following the manufacturer's instructions. The results showed a significantly higher amount of PGE_2 levels in the mouse with tumors produced by the hybrid enzyme (COX-2-10aa-mPGES-1) when compared with the co-expressed enzymes and the HEK293 controls (Figure 35B).

4.26. Evaluating the PGE_2 blood levels in BALB/c nu/nu mice using LC/MS/MS

The blood from BALB/c nu/nu mice with tumors was collected by the tail cut method. The whole blood sample was prepared for the mass spectrometry analysis by passing it through the C18 sephadex column and eluting it with acetone as mentioned above. The mice with tumors showed a higher level of PGE_2 in the blood as compared to control mice (Figure 35A).

4.27. Evaluating the EP receptor peripheral tumor occurence around the central PGE_2-producing hybrid enzyme tumor

The four EP receptor peripheral tumors were counted for tumor occurrence. Eighteen EP_1 peripheral tumors out of 20 were detected in the EP_1 group whereas only

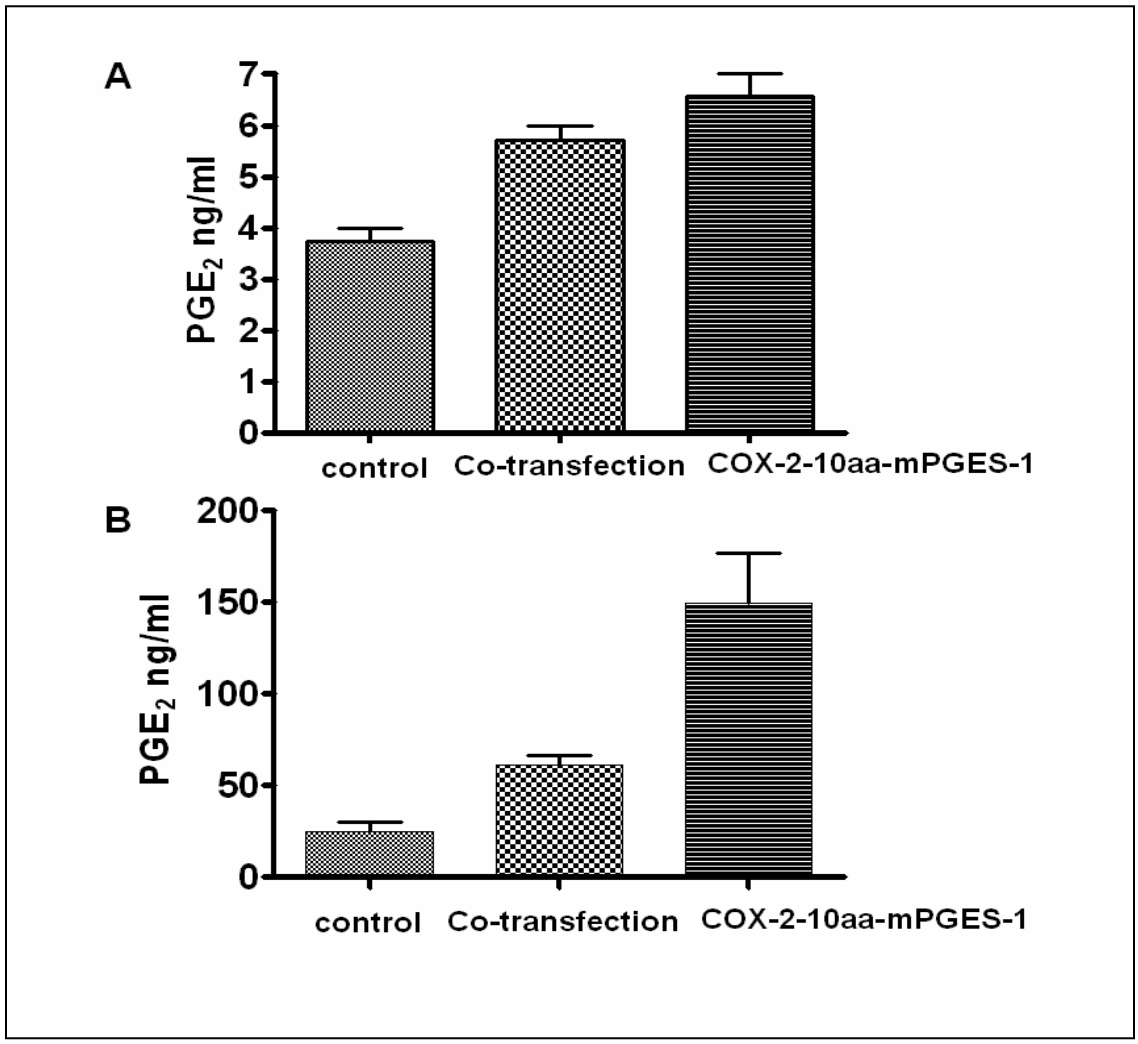

Figure 35: Serum PGE_2 levels in BALBc/nu/nu mice blood with tumors using (A) LC/MS/MS and (B) ELISA. The serum from the BALBc/nu/nu mice with tumors (COX-2-10aa-mPGES-1 tumor, co-transfection tumor and non tumor mice) was processed and analyzed for quantification by mass spectroscopy and ELISA (using anti PGE_2 antibody). The serum was passed through C18 column, eluted with acetone; dried and dissolved in 100µl buffer A for LC/MS/MS analysis. The blood PGE_2 level from mice with the hybrid enzyme tumors was significantly higher as compared to the co-transfection tumor mice. LC/MS/MS is not an ideal instrument for quantification therefore the PGE_2 levels detected were lower than those observed with ELISA.

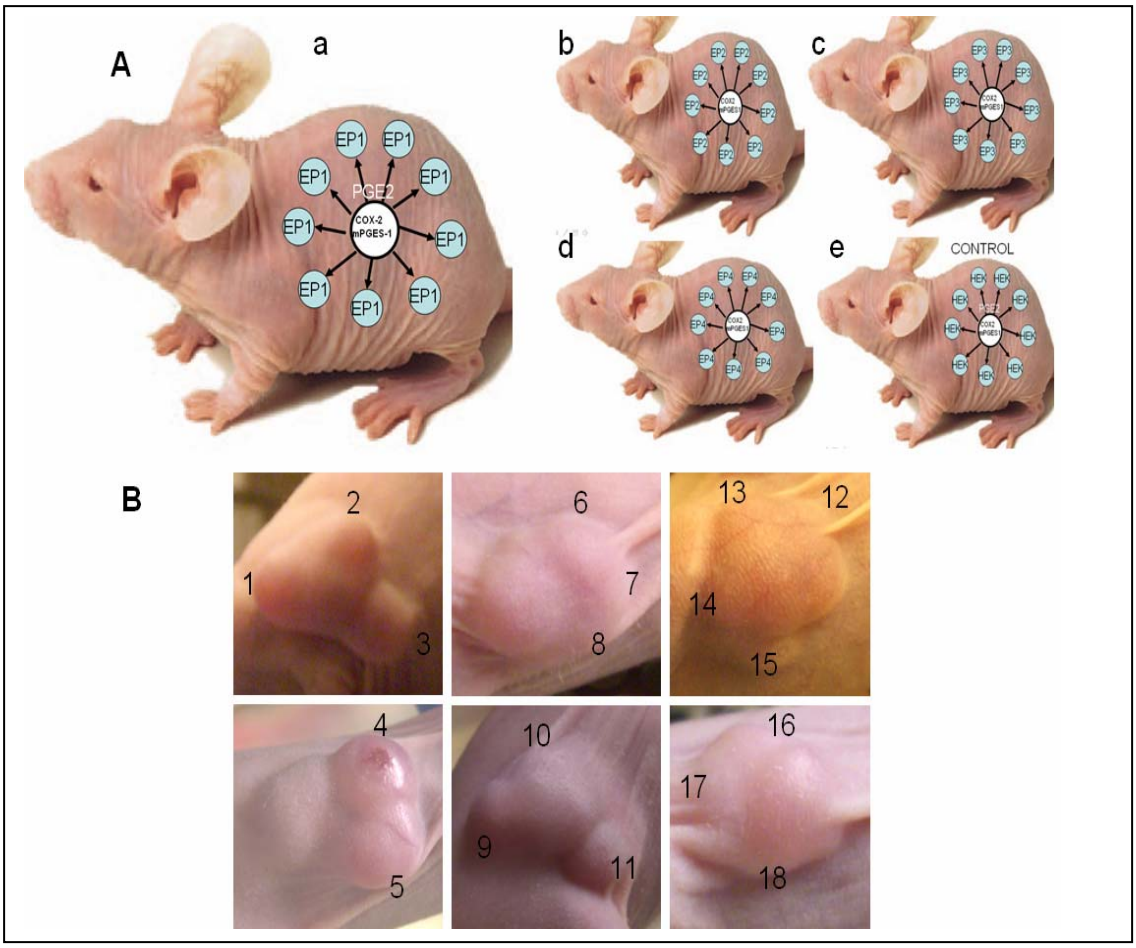

Figure 36; Novel tumor model producing excessive PGE_2 (A) The BALBc/nu/nu mice with the central COX-2-10aa-mPGES-1 tumor producing high levels of PGE_2. This PGE_2 is expected to diffuse in the surrounding and activate the peripherally injected EP receptors. (a) EP_1 receptors, (b) EP_2 receptors, (c) EP_3 receptors, (d) EP_4 receptors. (B) Subcutaneous peripheral EP_1 satellite tumors produced around the central COX-2-10aa-mPGES-1 tumor. The periphery of the day 15 central COX-2-10aa-mPGES-1 tumors was injected with approximately 50,000 cells of the EP stable cell lines as shown in (A). We suggest that the COX-2-10aa-mPGES-1 tumor was able to produce high amounts of PGE_2 which diffused into the surrounding to stimulate the EP_1 receptors and trigger tumor formation. The numbers indicate the tumors produced by EP_1 receptors in HEK293 cells. 18 out of the 20 injections in the periphery of the EP_1 stable cell line produced tumors. The occurance rate was evaluated using Fishers exact test with $p<.05$.

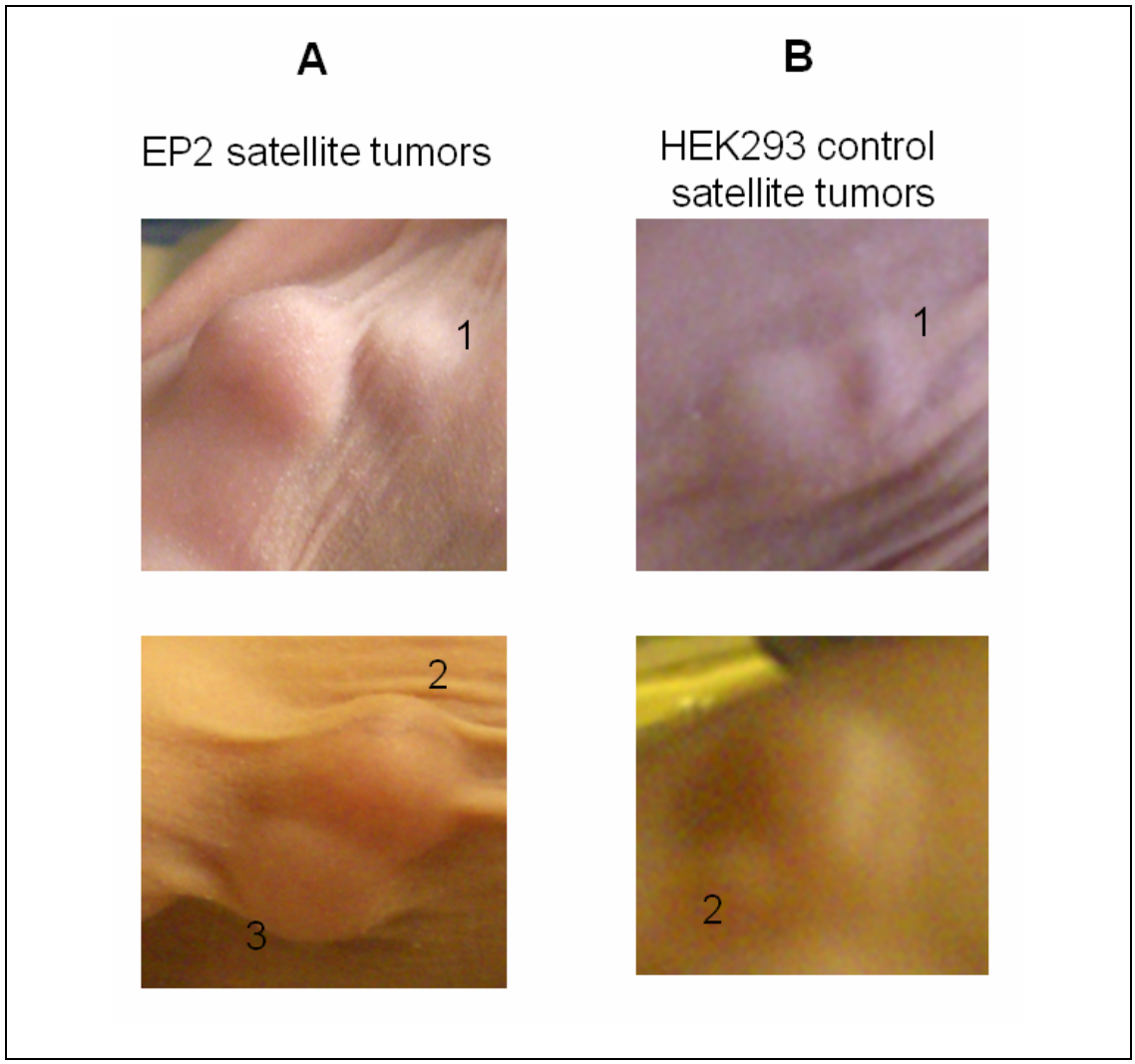

Figure 37:(A) Subcutaneous peripheral EP_2 satellite tumors produced around the central COX-2-10aa-mPGES-1 tumor. The periphery of the day 15 central COX-2-10aa-mPGES-1 tumors was injected with approximately 50,000 cells of the EP stable cell lines as shown in Figure 36A(b). We suggest that the COX-2-10aa-mPGES-1 tumor was able to produce high amounts of PGE_2 which diffused into the surrounding to stimulate the EP_2 receptors and trigger tumor formation. The numbers indicate the tumors produced by EP_2 receptors in HEK293 cells. (B) Similarly HEK293 alone peripheral tumors were injected as controls. We observed only two small nodules with the HEK293 cell alone. The satellite tumors are indicated by numbers. There were no noticeable satellite tumors for EP_3 and EP_4 stable cell lines.

three tumor occurrences were detected for EP_2 receptors. There was no tumor growth for the EP_3 and EP_4 receptor stable cell lines. The occurrence rate (18 tumors) was statistically significant for the EP_1 receptor using the fisher exact test with $P<0.05$ when compared to HEK293 and other receptors. Thus EP_1 and EP_2 receptors could be involved in cancer proliferation and could also prove to be potential drug targets for therapeutics (Figure 36&37).

4.28. Evaluating the primary cultures of tumor for enzyme and EP_1 receptor expression using western blot and immunostaining

The primary culture of the tumors (COX-2-10aa-mPGES-1, COX2 and mPGES-1 co-expression and EP_1 tumor) was established and the cells were selected again using G418. The stable cell lines thus generated were evaluated by western blot and immunostaining. The COX-2-10aa-mPGES-1 band was detected at 91 kDa for the tumor generated by the hybrid enzyme. The COX-2 band was detected at 72 kDa and the mPGES-1 band at 17kDa for the tumors produced by co-transfection. The EP_1 receptor protein band was detected at 42 kDa. All the primary cultures showed a good ammount of protein expression (Figure 38).

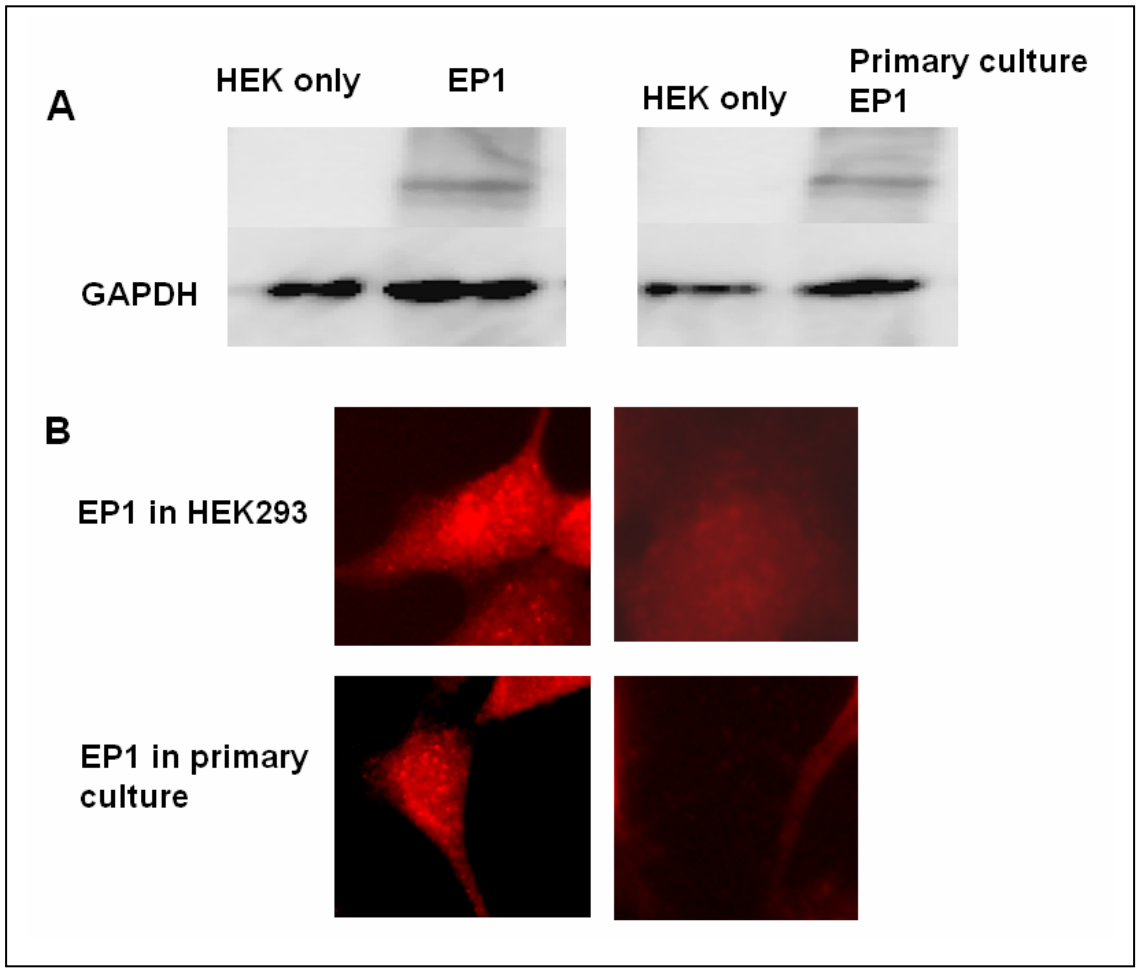

Figure 38: Western blot and immunostaining of EP_1 receptor stable cell line and its primary culture from tumor. (A) EP_1 receptor bands detected at 42kDa for stable cell line and primary culture with the HEK293 controls. (B) Immunostaining for EP_1 receptor stable cell line and primary culture with their appropriate controls. The western blot of the stable cell line and the primary culture stable cell line was performed using 15µg of whole cell protein.

5. DISCUSSION

5.1. NMR experiments with EP_3 eLP_2

Based on our molecular modeling studies, the TP receptor ligand, SQ29,548, must contact the extracellular domains of the receptor before binding to the residues on the third and seventh transmembrane domains. This means that the initial contact residues on the molecular surface are also specific. Also, the constrained eLP_2 peptide of the TP receptor changes its conformation upon the addition of the receptor antagonist (SQ29,548) (So et al., 2003, Moore et al., 1991). Studies have provided evidence to support the hypothesis of the second extracellular loop's involvement in ligand recognition (Funk et al., 1993, Chiang et al., 1996) and that point mutations of several cysteine residues at these loops reduce binding activity. Site-directed mutagenesis of seven conserved residues (198–205) clustered in the amino portion of the rabbit EP_3 eLP_2 has been performed and their ligand binding profiles assessed, in transfected HEK293 cells (Audoly and Breyer, 1997; D'Angelo et al., 1996; So et al., 2003). We chose the EP_3 receptor for its unique ability to couple to multiple G proteins such as the Gi subunits (adenylyl cyclase inhibition) and Gs subunit (cAMP stimulation) (Katoh et al., 1998; Tamma et al., 2003). We hypothesize that this selection of G proteins is likely to be ligand-dependent.

The residues identified by us for ligand recognition (S211 & R214) are chiefly located in the non-conserved region of the eLP_2 (Figure 9). This means that the conserved regions, though important for ligand recognition, may not be as important as the non-conserved region in defining the receptor's choice of signal transduction. The differences observed in the function of the receptors sharing a common ligand could in fact be due to the conformational changes brought about by these non-conserved residues which lead to the diversification of the signal transduction. The X-ray crystal structure for a majority of mammalian GPCRs is not yet available therefore the first step to identify the structural basis of the ligand-specific recognition of the extracellular parts is the understanding of the residues involved. We localized the residues within the eLP_2 region responsible for the ligand recognition, using two-dimensional NMR spectroscopy (Figure 12,13&14). The residues identified (S211 & R214) were further confirmed by the site-directed mutagenesis approach for the native EP_3 receptor. The radioligand ($[^3H]PGE_2$) binding further supports our hypothesis that the point mutation in the second extracellular loop of the receptors greatly decreases the binding (Figure 15). Our next step will be to use this data from the combination of the NMR experiments and mutagenesis to give detailed structural information about the interaction of the receptor and ligand, which cannot be achieved by other approaches such as general mutation approach, photoaffinity labeling, and site-specific antibody screening. This

approach can be used to characterize the ligand binding to other domains of the receptor as well.

The key factor in this study was to design a synthetic peptide with biological function. By using a constrained peptide, we successfully identified the ligand recognition site for the receptor (Figure 8). The identification of the residues in the EP_3 eLP_2 is the first step in solving the ligand-recognition pocket. We suspect that the ligand-recognition site might differ from the final ligand-binding site, as we have shown with the TP receptor. Though the ligand binding site located within the transmembrane domain is conserved, the initial docking residues of the prostanoid receptors are ligand specific (So et al., 2003). In conclusion, our proton-level information for identification of the EP_3 receptor ligand-recognition site on the extracellular domain will serve as a valuable tool to characterize the structure of the ligand-docking site and understand the variations in signaling outcomes. In addition, it will also provide reference information on specific recognition differences and predictions of ligand-docking sites for other prostanoid receptors.

5.2. High throughput mutagenesis

Our high throughput mutagenesis experiment showed that there is a potential for direct transfection of mutated PCR products of receptors to be incorporated into high throughput screening machines. We were able to generate 24 mutant EP_1

receptors in one experiment as stable cell lines. Conventionally each point mutation is studied separately but by our process the residues of an entire receptor or enzyme can be mutated in one experiment. This will reduce the cost of generating individual point mutations using transformation in E.Coli. Though further modifications will be required for it to be incorporated into high throughput screening, it still proves to be a promising strategy (Figure 17). We were able to identify three mutants in the EP_1 extracellular loop which showed reduced binding to PGE_2 and reduced signaling to both PGE_1 and PGE_2 (Figure 19&20).

5.3. EP receptors binding and signaling studies

The EP receptors are co-expressed in various organ systems (Artur et al., 1996; Sugimoto et al., 1992; Honda et al., 1993; Watabe et al., 1993; Katsuyama et al., 1995) and cancer cell lines (Figure 21 A,B&C); therefore we generated a stable cell line for each EP receptor to study them individually. We chose the two ligands PGE_1 and PGE_2 which act on all the four EP receptors but have been shown to have opposite action (Murota et al., 2008,; Sobota et al., 2008; Kawamura et al., 1997).

Our results show that PGE_1 and PGE_2 have different binding affinities for the EP receptors (Figure 22). However, the binding affinitiy does not have a direct positive correlation with the signaling intensity. The major difference between the two ligands was observed in the EP_1 receptor where despite the relatively weak affinity ($[^3H]PGE_2$ Kd

0.21 nM, IC50 PGE_1 3µM, PGE_2 8µM) there was a high Ca^{2+} and cAMP signal (Figure 23&26). However, here PGE_1 (100 pM) produced a significantly higher Ca^{2+} signal as compared to PGE_2 (Figure 23), which was also confirmed by fluorescence microscopy (Figure 24&29). This fact led us to postulate that the difference in the action between PGE_1 (anti-inflammatory) and PGE_2 (inflammatory) could be due to the difference in the Ca^{2+} signal intensity and that it is mediated through the EP_1 receptor. It will be interesting in the future to stimulate the EP_1 receptor stable cell line with PGE_1 and PGE_2 and perform the microarray analysis to see the difference in upregulation or down regulation of genes involved in inflammation. The EP_1 receptor also appears to be the dominant EP receptor on comparing both the Ca^{2+} and cAMP signal for the two ligands (Figure 23&26). The importance of this lies in the fact that this EP_1 receptor could be used as a potential target for cancer where the EP receptors are co-expressed (Artur et al., 1996; Thorat et al., 2007; Gustafsson et al., 2007; Chang et al., 2005; Shoji et al., 2004; Chell et al., 2006). Various studies have shown the importance of EP receptors individually in cancer cell proliferation or inhibition but none have compared the four EP receptors in terms of the dominant receptor. We have shown that some cancer cells (breast and colon) coexpress all the EP receptors (Figure 21) and that finding antagonists to the EP_1 receptor could be most effective in inhibition of cancer cell signaling.

Calcium has been known to stimulate a variety of cellular functions depending on how it is regulated spatially and temporally (Berridge et al., 2000). In other words the

spatiotemporal shape of the Ca^{2+} signal determines the variety of cellular processes it is a part of. For example, the frequency of Ca^{2+} oscillation determines the gene transcription in T cells (Li et al., 1998; Dolmetsch et al., 1998) and apically-confined Ca^{2+} signals activate exocytosis in pancreatic acinar cells (Maruyama et al., 1993).

Recent data suggests that cAMP also oscillates in a manner similar to Ca^{2+} (Rich and Karpen, 2002) and can be confined to spatially restricted regions of a cell (Gorbunova and Spitzer, 2002). Though the cAMP and Ca^{2+} signaling pathways interact at multiple levels, studies have defined that the molecular location where the two pathways meet is at the level of inositol 1,4,5-trisphosphate (InsP3) generation. Also, data suggests that Ca^{2+} clearance, by the plasma membrane Ca^{2+}-ATPase (PMCA) is also directly modulated by cAMP elevation. Other indirect effects of cAMP on Ca^{2+} signaling are through gap junctions, mitochondrial function, Ca^{2+} influx, and gene expression (Gorbunova and Spitzer, 2002; Rich et al., 2001). However, in an artificially expressed cell system (like a stable cell line) the determination of spatiotemporal association of Ca^{2+} and cAMP is a limitation and has no significance. We also measured the 10 minute cAMP accumulation with PGE_1 and PGE_2 because the shaping of Ca^{2+} signals is achieved by the concomitant activation of additional signal transduction pathways which regulate cAMP concentrations. Usually this is achieved by activating G-protein-coupled receptors (GPCRs) that couple to Gαs (to activate adenylyl cyclase) in addition to those that couple to Gαq, which activates phospholipase C (PLC) and increases InsP3 production. The

cAMP signal was inconclusive in differentiating between the ligands (Figure 26). Similarly, Ca^{2+} can also modulate components of the cAMP signaling machinery by either activating or inhibiting different subtypes of adenylyl cyclase (Giovannucci et al., 2002; Cooper et al., 1995; Mons et al., 1998) and phosphodiesterase (Kakkar et al., 1999). Thus in accordance with the concept that cAMP is regulated in a similar way to Ca^{2+} we postulate that any significant difference in the ratio of Ca^{2+} and cAMP observed could indicate the difference in signaling response or outcome. Therefore we measured the ratio of total Ca^{2+} and cAMP signal generated. This helped us understand that the difference in action of ligands (PGE_1 and PGE_2) can be evaluated by calculating the difference in signal ratio. Here we found that the EP_1 receptor could differentiate between the two ligands at a 100 pM concentration (Figure 23&29).

Similarly, on comparing the binding and signaling of the other EP receptors, we concluded that [^{3}H]PGE_2 has a higher affinity for the EP_1, EP_4 and EP_2 receptors with the highest Ca^{2+} and cAMP signal for EP_1 and EP_2 (with PGE_1 and PGE_2). Here, however, there was a two-log concentration difference between PGE_1 and PGE_2 for the generation of Ca^{2+} signal for the EP_4 receptor (Figure 23). This two-log difference in generation of Ca^{2+} signal could also be contributory to the difference in action between the two ligands but the signal generated is too low as compared to the EP_1 receptor. Both PGE_1 and PGE_2 (bound to the EP_2 receptor) mainly signaled through cAMP and not Ca^{2+}. However, the two ligands did not show any significant difference in binding and

signaling intensity for the EP_2 receptor and thus could not help differentiate their action. PGE_2, being the inflammatory molecule was able to significantly increase the leukotriene C4/D4/E4 levels in the EP_1 stable cell line as compared to PGE_1 (Figure 27B). We suggest that these leukotrienes are likely responsible for differentiating between the actions of PGE_1 and PGE_2. Lipoxins are a group of biologically active eicosanoids detected in a variety of inflammatory conditions. They are typically formed by transcellular lipoxygenase activity. The native lipoxins LXA4 and LXB4 have been shown to demonstrate potent anti-inflammatory and pro-resolution bioactivity such as phagocytic clearance of apoptotic leukocytes. We detected the 20-hydroxy lipoxin B4 peak at 21.441 minutes. We suggest that the anti-inflammatory activity of PGE_1 could be due to the production of Lipoxin B4 (O'Sullivan, 2007; Parkinson, 2006)(Figure 28).

In conclusion, we have tried to identify the changes in Ca^{2+} and cAMP in the EP receptors with common ligands (like PGE_1 and PGE_2) which in turn have opposite actions. Though Ca^{2+} and cAMP interact at multiple levels to effectively form a signaling network we found that it is the EP_1 receptor which could be the dominant receptor among the EP receptors in terms of signaling intensity and that it is also able to differentiate between the two ligands PGE_1 and PGE_2 (Figure 29).

5.4. Establishing a tumor model

The prostanoids metabolized from AA through the COX-pathway, play important roles in balancing hemostasis, vascular functions, inflammation and cancer development. The alteration in the balance of the biosynthesis of different prostanoids is involved in many critical diseases, such as stroke, myocardial infarction, inflammation and cancers (Sheng et al., 2001, Levy, 1997, Reinhart et al., 1983). We have shown in our previous publications using the hybrid enzyme, COX-2-10aa-mPGES-1, that the controlling and re-directing of the prostanoids' biosyntheses in cells through the COX-pathway is a potential approach in redirecting the balance or imbalance towards a particular prostanoid of choice (Ruan et al., 2009). We have established a hybrid enzyme, COX-2-10aa-mPGES-1, in HEK293 cells that produces tumors by redirecting the AA to produce excess PGE_2 (Figure 30). Similarly our especially engineered hybrid enzyme that links COX to PGIS could effectively control and re-direct the AA to be metabolized into PGI_2 for vascular protection (Ruan *et al.*, 2006, 2008a, 2008b). These finding suggest that the COX-pathway in cells could be re-directed and controlled by overexpressing designed hybrid enzymes linking COX to different downstream synthases. The inducible COX-2, when linked to other downstream synthases, such as mPGES-1, mPGES-2 or cytosolic PGES (cPGES), could direct the PGE_2 sysnthesis by the enzyme of our choice. This is important because we chose to link the indicible COX-2 to the inducible mPGES-1, both of which are expressed in response to the critical

physiological processes, including cell proliferation and differentiation, and tissue regeneration and repair (Marnett, 1992; Rao, 1995; Sheng, et al., 1997; Subbaramaiah et al., 1996; Kargman et al., 1995). Since both enzymes are inducible in inflammation and are able to produce tumors, they make an important target-specific tumor model. In our previous publications we have described the engineering of COX-2-10aa-mPGES-1 which has provided evidence to support that COX is an enzyme which can be linked to its downstream substrates and studies have shown that the C-terminus of COX-2 and the N-terminus of mPGES-1 are flexible and could be modified without changing the enzymes' catalytic functions.

Previous studies have described that COX-2 couples to mPGES-1 but not cPGES through the co-expression of the recombinant COX-2 and mPGES-1 in HEK293 cells (Murakami *et al.,* 2002). However, we were able to further demonstrate this favored coupling for tumor production. Here, the evidence of a faster production of tumor suggests that the movement of PGH_2 from COX-2 to mPGES-1, with the help of a linker produces more PGE_2 (Figure 34).

COX-2 and mPGES-1 are important targets for developing anti-inflammatory drugs. The cells expressing the engineered COX-2-10aa-mPGES-1, which specifically convert AA into PGE_2, can be used as an effective model for initial drug screening in search of the effects of the chemical compounds, genetic molecules, and regulators on PGE_2 production.

To date, there have been no tumor animal models designed for testing the anti-cancer activity of COX-2 and mPGES-1. The direct shifting of the results from the lab and non-specific animal studies to human clinical trials has created many risks with damages to the patients during the human use of NSAIDs in the past. In addition, the limited number of participants in the human clinical trials could not precisely evaluate the cardio-toxicity and efficacies involved, which led to unreliable data for mislead FDA approval and later the withdrawal of the drugs, causing a wide range of damages to the public and economy. Vioxx is a typical case of that described above (Konstam et al., 2001). Our proposed BALB/c nu/nu mice that have tumors produced by the hybrid enzyme, COX-2-10aa-mPGES-1, and produce excess PGE_2 (for anti-inflammation efficacy or tumor suppression tests) could be sufficiently sensitive animal models which may be used for establishing a preclinical trial that could greatly reduce the ethical and economic risk for the damages from previous human clinical trials of the selective COX-2 NSAIDs. This would not only benefit the search for a more specific COX-2 or mPGES-1 inhibition treatment of cancers, but could also advance our drugs industrially to a leading position for developing NSAIDs that target COX-2 or mPGES-1 for tumor suppression with target specificity.

The model could help screening for the COX-2 and mPGES-1 inhibitors with different selectivities for their ability to reduce the COX-2-10aa-mPGES-1 -mediated PGE_2 production using the tumors generated on BALB/c nu/nu mice. We believe that the

tumor suppression can be monitored directly by size and by evaluating the kinetic changes in the blood by evaluating the PGE_2 levels (Figure 35). We have shown that there is 100% production of tumors with our hybrid enzyme as compared to the co-transfection group (Figure 34A). We have also shown that the enzyme activity for PGE_2 production is better for the hybrid enzyme than for the co-transfection (Figure 34B). The production of tumors also becomes a very reliable target-specific site which can be monitored for drug discovery. The mouse model is also very convenient, as COX-2 inhibitors and mPGES-1 inhibitors can be given to the mouse through various routes. We also suggest that the high levels of PGE_2 produced by the tumor could also trigger other mechanisms of tumor production in the tumor cells. This sustained high level of PGE_2 acts as a continuous stimulus for tumor production. PGE_2 regulates colon cancer migration via myeloma overexpressed gene (Lawlor et al., 2010) and lung cancer cell migration EP_4, betaArrestin1, and c-Src signalsome (Kim et al., 2010). Prostaglandin E_2 induces CYP1B1 expression via ligand-independent activation of the ERalpha pathway in human breast cancer cells (Han et al., 2010). There is also a suggested association between adenoma risk and genetic variability related to PGE_2, with regard to gene-environment interactions with anti-inflammatory exposures (Poole et al., 2010). This suggests that PGE_2 can enhance tumor growth by interacting with various enzymes, altering gene expression and activating ligand independent pathways. The presence of peripheral tumors with EP_1 and EP_2 stable cell lines suggests that both these receptors

are likely to be involved in cancer growth (Figure 36). Also the hybrid enzyme tumor was able to produce PGE_2 which diffused into the surrounding tissue to activate the EP_1 and EP_2 receptors and produce tumors making it a potentially novel tumor model method (Figure 36 A&B).

This fact suggests that anti-cancer drugs can also be tested on this tumor model for their ability to inhibit the tumors produced by over production of PGE_2.

6. SUMMARY AND CONCLUSIONS

1) Our NMR experiments performed to study the interaction between PGE_2 and the synthetic EP_3 eLP_2 revealed that the residue Serine 211 in an important PGE_2 recognition residue. Site directed mutagenesis of the EP_3 receptor mutant S211L showed a significantly reduced [^{3}H]PGE_2 binding.

2) The mutant S211L was able to elicit a calcium signal with PGE_1 but not with PGE_2. This suggested that a single point mutation was able to differentiate between the common ligands PGE_1 and PGE_2.

3) We identified two residues using NMR in the EP_3 eLP_2 with showed interaction with PGE_2 On comparison of the residues in the sequence alignment of all the eight prostanoid receptors we found that both the residues were in the non conserved region of the eLP_2. We thus concluded that the differences in ligand recognition could lie in the non-conserved residues as S211L and R214L are non-conserved.

4) The calcium signal experiments on the EP receptor revealed that it was the EP_1 receptor that showed a higher calcium signal with PGE1 than PGE at 100mM concentration. We thus suggest that the anti-inflammatory activity of PGE1 at

5) Our LC/MS/MS experiments showed an extra peak at 21.4 mins in the supernatant of the EP_1 stable cell line treated with 100pm PGE_1. The molecular weight of the peak matched with the molecular weight of lipoxin B4. The anti inflammatory activity of PGE_1 could be due to the production of lipoxin B4.

6) Our LC/MS/MS experiments showed multiple peaks with molecular weights similar to leukotrienes, in the supernatant of the EP_1 stable cell line treated with 100pm PGE_2. Thus using the ELISA kit for detection of leukotriene C4/D4/E4 we found a significantly higher leukotriene production in the PGE_2 treated sample than the PGE_1 treated sample. We thus suggest that the inflammatory activity of PGE_2 could be due to production of leukotrienes.

7) Our High throughput mutagenesis experiments using direct PCR product transfection suggest that it is a promising possibility for the future for generation of quick, easy and multiple point mutation assays.

8) We generated 24 point mutations in the EP_1 receptor and expressed them as stable cell lines using direct PCR product transfection. Out of the 24 EP_1 mutants three mutants A104G, P105A, P184A showed reduced binding to [^{3}H]PGE_2.

9) The three residues identified, (A104G, P105A and P184A) could not differentiate between PGE_1 and PGE_2 in the calcium signaling assay.

10) A tumor model was developed by linking inducible COX-2 with mPGES-1 using a 10 amino acid linker (called COX2-10aa-mPGES-1) in BALBc/nu/nu mice. There was a significantly faster tumor growth with the hybrid enzyme using the linker than with the co-transfection of COX2 and mPGES-1 seperately. The enzymes were transfected in HEK293 cells as stable cell lines and injected subcutaneously in BALBc/nu/nu mice. This suggested that the hybrid enzyme was able to produce higher levels of PGE_2 than the co-transection and that this PGE_2 was able to trigger cell proliferation.

11) When we injected the EP receptor stable cell lines around the central PGE_2 producing hybrid enzyme tumor we found that it was the EP_1 and EP_2 stable cell lines that formed peripheral satellite tumors. Thus we concluded that EP_1 and EP_2 receptors are involved in cancer growth using our tumor model.

7. REFERENCES

Abramovitz M and Metters KM (1998) Prostanoid receptors, in *Annual Reports in Medicinal Chemistry*, vol **33** (Bristol JA ed) pp 223–232, Academic Press, NY.

Abramovitz M, Adam A, Boie Y, Godbout C, Lamontagne S, Rochette C, Sawyer N, Tremblay NM, Belley M, Gallant M, et al. (2000) The utilization of recombinant prostanoid receptors to determine the affinities and selectivities of prostaglandins and related analogues. *Biochem Biophys Acta* **1483:**285–293.

Abramovitz M, Boie Y, Nguyen T, Rushmore TH, Bayne MA, Metters KM, Slipetz DM and Grygorczyk R (1994) Cloning and expression of a cDNA for the human prostanoid FP receptor. *J Biol Chem* **269:**2632–2636.

Adam M, Boie Y, Rushmore TH, Müller G, Bastien L, McKee KT, Metters KM, Abramovitz M (1994) Cloning and expression of three isoforms of the human EP_3 prostanoid receptor. *FEBS Lett* **338**:170-174.

An S, Yang J, Xia M, Goetzl E (1993). Cloning and expression of the EP2 subtype of human receptors for prostaglandin E2. *Biochem Biophys Res Commun* **197**: 263–270.

Andus T, Geiger T, Hirano T, Kishimoto T, Tran-Thi TA, Decker K and Heinrich PC (1988) Regulation of synthesis and secretion of major rat acute-phase proteins by recombinant human interleukin-6 (BSF-2/IL-6) in hepatocyte primary cultures. *Eur J Biochem* **173**:287–293.

Anggard E and Larsson C (1971) The sequence of the early steps in the metabolism of prostaglandin E_1. *Eur J Pharmacol* **14**:66–70.

Arosh JA, Banu SK, Chapdelaine P, Emond V, Kim JJ, Maclaren LA et al (2003) Molecular cloning and characterization of bovine prostaglandin E2 receptors EP2 and EP4: expression and regulation in endometrium and myometrium during the estrous cycle and early pregnancy. *Endocrinology* **144**: 3076–3091.

Artur J de B-F, Morisset S, Bkaily G and Patry C (1996) Characterization of the PGE_2 receptor subtype in bovine chondrocytes in culture. *British Journal of Pharmacology* **118**:1597-1604.

Audoly L and Breyer RM (1997) The second extracellular loop of the prostaglandin EP3 receptor is an essential determinant of ligand selectivity. *The Journal Of Biological Chemistry* **272**:13475–13478.

Bastien L, Sawyer N, Grygorczyk R, Metters KM and Adam M (1994) Cloning, functional expression, and characterization of the human prostaglandin E2 receptor EP2 subtype. *J Biol Chem* **269:**11873–11877.

Bek M, Nu Sing R, Kowark P, Henger A, Mundel P And Pavensta H (1999) Characterization of Prostanoid Receptors in Podocytes. *J Am Soc Nephrol* **10**: 2084–2093.

Berridge MJ, Lipp P, Bootman MD (2000) The versatility and universality of calcium signaling. *Nat Rev Mol Cell Biol* **1**:11–21.

Bhattacharya M, Peri K, Almazan G, Ribeiro-da-silva A, Shichi H, Durocher Y et al (1998) Nuclear localization of prostaglandin E2 receptors. *Proc Natl Acad Sci USA* **95**: 15792–15797.

Bhattacharya M, Peri K, Ribeiro-da-silva A, Almazan G, Shichi H, Hou X et al (1999) Localization of functional prostaglandin E2 receptors EP3 and EP4 in the nuclear envelope. *J Biol Chem* **274**: 15719–15724.

Bilson HA, Mitchell DL, Ashby B (2004) Human prostaglandin EP_3 receptor isoforms show different agonist-induced internalization patterns. *FEBS Lett* **572**: 271–275.

Bode J and Heinrich PC (2001) Interleukin-6 signaling during the acute-phase response of the liver. In The Liver: *Biology and Pathobiology* (Arias IM, Boyer JL, Chisari F V, Fausto N, Schachter D and Shafritz DA eds) pp. 565–580, Lippincott Williams Wilkins, Philadelphia.

Boie Y, Rushmore TH, Darmon-Goodwin A, Grygorczyk R, Slipetz DM, Metters KM and Abramovitz M (1994) Cloning and expression of a cDNA for the human prostanoid IP receptor. *J Biol Chem* **269:**12173–12178.

Boie Y, Sawyer N, Slipetz DM, Metters KM and Abramovitz M (1995) Molecular cloning and characterization of the human prostanoid DP receptor. *J Biol Chem* **270:**18910–18916.

Boie Y, Stocco R, Sawyer N, Slipetz DM, Ungrin MD, Neuschafer-Rube F, Puschel G, Metters KM and Abramovitz M (1997) Molecular cloning and characterization of

the four rat prostaglandin E2 prostanoid receptor subtypes. *Eur J Pharmacol* **340:**227–241.

Boxma GC, Custer RP, Bosma MJ (1983) A severe combined immunodeficiencymutation in the mouse. *Nature* **301**:527–530.

Breyer RM, Emeson RB, Breyer MD, Abromson RM, Davis LS, Ferrenbach SM (1994) Alternative splicing generates multiple isoforms of a rabbit prostaglandin E2 receptor. *J Biol Chem* **269**: 6163–6169.

Callihan D, West J, Kumar S, Schweitzer BI and Loga TM (1996) Simple, distortion-free homonuclear spectra of peptides and nucleic acids in water using excitation sculpting. *J Magn Reson B* **112**:82-85.

Campbell WB (1990) in Goodman and Gilman's *The Pharmacological Basis of Therapeutics,* 8th ed (Gilman AG, Rall TW, Nies AS, and Taylor P eds) pp 600–617, Pergamon Press, New York.

Castellone MD, Teramoto H, Williams BO, Druey KM, Gutkind JS (2005) Prostaglandin E_2 promotes colon cancer cell growth through a Gs-axin-beta-catenin signaling axis. *Science* **310**: 1504–1510.

Chang SH, Ai Y, Breyer RM, Lane TF, Hla T (2005) The prostaglandin E_2 receptor EP_2 is required for cyclooxygenase 2-mediated mammary hyperplasia. *Cancer Res* **65**:4496-4499.

Chell SD, Witherden IR, Dobson RR, Moorghen M, Herman AA, Qualtrough D, Williams AC, Paraskeva C (2006) Increased EP_4 receptor expression in colorectal cancer progression promotes cell growth and anchorage independence. *Cancer Res* **66**:3106-3113.

Chen L, Zhang W, Yue H, Han Q, Chen B, Shi M, Li J, Li B, You S, Shi Y And Zhao RC (2007) Effects of Human Mesenchymal Stem Cells on the Differentiation of Dendritic Cells from CD34 Cells. *Stem Cells And Development* **16**:719–731.

Chiang N, Kan WM and Tai HH (1996) Site-directed mutagenesis of cysteinyl and serine residues of human thromboxane $a_2$receptor in insect cells.*Arch. Biochem. Biophys* **334**:9–17.

Chillar A, Wu J, So SP, Ruan KH (2008) Involvement of non-conserved residues important for PGE_2 binding to the constrained EP_3 eLP_2 using NMR and site-directed mutagenesis. *FEBS Letters* **582**: 2863-2868.

Cianfarani F, Tommasi R, Failla CM, Viviano MT, Annessi G, Papi M, Zambruno G, Odorisio T (2006) Granulocyte/macrophage colony- stimulating factor treatment of human chronic ulcers promotes angiogenesis associated with de novo vascular endothelial growth factor transcription in the ulcer bed. *Br J Dermatol* **154**:34–41.

Coleman RA, Kennedy I, Humphrey PPA, Bunce K and Lumley P (1989) Prostanoids and their receptors, in *Comprehensive Medicinal Chemistry*, vol. **3** (Emmet JC ed), pp 643–714, Pergamon Press, Oxford.

Coleman RA, Smith WL and Narumiya S (1994) VIII International union of pharmacology classification of prostanoid receptors: Properties, distribution, and structure of the receptors and their subtypes. *Pharmacol Rev* **46:**205–229.

Cooper DM, Mons N, Karpen JW (1995) Adenylyl cyclases and the interaction between calcium and cAMP signaling. *Nature* **374**: 421–424.

Crooke ST (1992) Therapeutic applications of oligonucleotides. *Annu Rev Pharmacol Toxicol* **44**:329–376.

D'Angelo D D, Eubank JJ, Davis MG and Dorn GW (1996) Mutagenic analysis of platelet thromboxane receptor cysteines. *J Biol Chem* **271**:6233–6240.

Davies P and MacIntyre DE (1992) in Inflammation: *Basic Principles and Clinical Correlates,* 2nd ed (Gallin JI, Goldstein IM, and Snyderman R, eds) pp 123–138, Raven Press, New York.

Deng H, Huang A, So SP, Lin YZ and Ruan KH (2002) Substrate access channel topology in membrane-bound prostacyclin synthase. *Biochem J* **362**:545-551.

Deng H, Wu J, So SP and Ruan KH (2003) Identification of the residues in the helix F/G loop important to catalytic function of membrane-bound prostacyclin synthase. *Biochemistry* **42**:5609-5617.

Desai S, April H, Nwaneshiudu C, Ashby B (2000) Comparison of agonist-induced internalization of the human EP_2 and EP_4 prostaglandin receptors: role of the carboxyl terminus in EP_4 receptor sequestration. *Mol Pharmacol* **58**: 1279–1286.

Dey I, Lejeune M and Chadee K (2006) Prostaglandin E_2 receptor distribution and function in the gastrointestinal tract. *British Journal of Pharmacology* **149**:611–623.

Dolmetsch RE, Xu K, Lewis RS (1998) Calcium oscillations increase the efficiency and specificity of gene expression. *Nature* **392**:933–936.

Filion F, Bouchard N, Goff AK, Lussier JG and Sirois J (2001) Molecular cloning and induction of bovine prostaglandin E synthase by gonadotropins in ovarian follicles prior to ovulation in vivo. *J Biol Chem* **276**:34323-34330.

Fisher RA (1922) "On the interpretation of χ^2 from contingency tables, and the calculation of P". *Journal of the Royal Statistical Society* **85**:87–94.

Fujino H, Salvi S, Regan JW (2005) Differential regulation of phosphorylation of the cAMP response element-binding protein after activation of EP_2 and EP_4 prostanoid receptors by prostaglandin E_2. *Mol Pharmacol* **68**: 251–259.

Fujino H, Xu W, Regan JW (2003) Prostaglandin E_2 induced functional expression of early growth response factor-1 by EP_4, but not EP_2, prostanoid receptors via the phosphatidylinositol 3-kinase and extracellular signal-regulated kinases. *J Biol Chem* **278**: 12151–12156.

Funk CD, Furci L, FitzGerald GA, Grygorczyk R, Rochette C, Bayne MA, Abramovitz M, Adam M and Metters KM (1993) Cloning and expression of a cDNA for the human prostaglandin E receptor EP1 subtype. *J Biol Chem* **268:**26767–26772.

Funk CD, Furci L, Moran N and Fitzgerald GA (1993) Point mutation in the seventh hydrophobic domain of the human thromboxane A_2 receptor allows discrimination between agonist and antagonist binding sites. *Mol Pharmacol* **44**: 934–939.

Giovanella BC, Yim SO, Stehlin JS, Williams LJJ (1972) Development of invasive tumors in the ‘‘nude’’ mouse after injection of cultured human melanoma cells. *JNCI* **48**:1531–1533.

Giovannucci DR, Bruce JI, Straub SV, Arreola J, Sneyd J, Shuttleworth TJ, Yule DI (2002) Cytosolic $Ca^{(2+)}$ and $Ca^{(2+)}$-activated $Cl^{(-)}$ current dynamics: insights from two functionally distinct mouse exocrine cells. *J Physiol* **540**:469–484.

Gorbunova YV and Spitzer NC (2002) Dynamic interactions of cyclic AMP transients and spontaneous $Ca^{(2+)}$ spikes. *Nature* **418**:93–96.

Green S, Walter P, Kumar V, Krust A, Bornert JM, Argos P and Chambon P (1986) Human oestrogen receptor cDNA: sequence, expression and homology to v-erb-A. *Nature* **320**:134–139.

Guan Y, Zhang YH, Stillman BA, Schneider A, Saito O, Davis LS et al (1996) Cloning and functional expression of the rabbit prostaglandin EP2 receptor. *J Am Soc Nephrol* **7**: 1646.

Gustafsson A, Hansson E, Kressner U, Nordgren S, Andersson M, Wang W, Lönnroth C, Lundholm K (2007) EP1-4 subtype, COX and PPAR gamma receptor expression in colorectal cancer in prediction of disease-specific mortality. *Int J Cancer* **121**:232-240.

Han C, Wu T (2005) Cyclooxygenase-2-derived prostaglandin E_2 promotes human cholangiocarcinoma cell growth and invasion through EP_1 receptor-mediated activation of the epidermal growth factor receptor and Akt. *J Biol Chem* **280**: 24053–24063.

Han EH, Kim HG, Hwang YP, Song GY, Jeong HG (2010) Prostaglandin E_2 induces CYP1B1 expression via ligand-independent activation of the ERalpha pathway in human breast cancer cells. *Toxicol Sci* **114**:204-216.

Han R, Tsui S and Smith T J (2002) Up-regulation of prostaglandin E_2 synthesis by interleukin-1beta in human orbital fibroblasts involves coordinate induction of prostaglandin-endoperoxide H synthase-2 and glutathione-dependent prostaglandin E_2 synthase expression. *J Biol Chem* **277**:16355-16364.

Hatae N, Yamaoka K, Sugimoto Y, Negishi M and Ichikawa A (2002) Augmentation of receptor-mediated adenylyl cyclase activity by Gi-coupled prostaglandin receptor

subtype EP_3 in a Gbetagamma subunit-independent manner. *Biochem Biophys Res Commun* **290**:162-168.

Hirata M, Hayashi Y, Ushikubi F, Yokota Y, Kageyama R, Nakanishi S and Narumiya S (1991) Cloning and expression of cDNA for a human thromboxane A2 receptor. *Nature (Lond)* **349:**617–620.

Hizaki H, Segi E, Sugimoto Y, Hirose M, Saji T, Ushikubi F, Matsuoka T, Noda Y, Tanaka T, Yoshida N, Narumiya S and Ichikawa A (1999) Abortive expansion of the cumulus and impaired fertility in mice lacking the prostaglandin E receptor subtype EP_2. *Proc Natl Acad Sci U S A* **96**:10501–10506.

Honda A, Sugimoto Y, Namba T, Watabe A, Irie A, Negishi M, Narumiya S and Ichikawa A (1993) Cloning and expression of a cDNA for mouse prostaglandin E receptor EP_2 subtype .*J Biol Chem* **268**:7759–7762.

Honda T, Segi-Nishida E, Miyachi Y, and Narumiya S (2006) Prostacyclin-IP signaling and prostaglandin E_2-EP_2/EP_4 signaling both mediate joint inflammation in mouse collagen-induced arthritis. *J Exp Med* **203**:325–335.

Irie A, Sugimoto Y, Namba A, Harazono A, Honda A, Watabe A, Negishi M, Narumiya S and Ichikawa A (1993) Third isoform of the prostaglandin-E-receptor EP_3 subtype with different C-terminal tail coupling to both stimulation and inhibition of adenylate cyclase. *Eur J Biochem* **217**:313–318.

Jabbour HN, Milne SA, Williams AR, Anderson RA and Boddy SC (2001) Expression of COX-2 and PGE synthase and synthesis of PGE(2)in endometrial adenocarcinoma: a possible autocrine/paracrine regulation of neoplastic cell function via EP_2/EP_4 receptors. *Br J Cancer* **85**:1023-1031.

Jakobsson PJ, Thoren S, Morgenstern R and Samuelsson B (1999) Identification of human prostaglandin E synthase: a microsomal, glutathione-dependent, inducible enzyme, constituting a potential novel drug target. *Proc Natl Acad Sci U S A* **96**:7220-7725.

Jin J, Mao GF and Ashby B (1997) Constitutive activity of human prostaglandin E receptor EP3 isoforms. *Br J Pharmacol* **121:**317–323.

Kakkar R, Raju RV, Sharma RK (1999) Calmodulin-dependent cyclic nucleotide phosphodiesterase (PDE_1). *Cell Mol Life Sci* **55**:1164–1186.

Kamei D , Murakami M, Nakatani Y, Ishikawa Y, Ishii T and Kudo I (2003) Potential Role of Microsomal Prostaglandin E Synthase-1 in Tumorigenesis. *The Journal Of Biological Chemistry* **278**:19396–19405.

Kargman SL, O'Neill GP, Vickers PJ, Evans JF, Mancini JA and Jothy S (1995) Expression of prostaglandin G/H synthase-1 and -2 protein in human colon cancer. *Cancer Res* **55**:2556-2559.

Katoh H, Aoki J, Ichikawa A, Negishi M (1998) P160 RhoA-binding kinase ROKalpha induces neurite retraction. *J Biol Chem* **273**:2489–2492.

Katsuyama M, Nishigaki N, Sugimoto Y, Morimoto K, Negishi M, Narumiya S and Ichikawa A (1995) The mouse prostaglandin E receptor EP_2 subtype: cloning, expression, and Northern blot analysis. *FEBS Lett* **372**:151–156.

Kawamura T, Akira T, Watanabe M, Kagitani Y (1997) Prostaglandin E_1 prevents apoptotic cell death in superficial dorsal horn of rat spinal cord. *Neuropharmacology* **36**: 1023–1030.

Kennedy I, Coleman RA, Humphrey PP, Levy GP and Lumley P (1982) Studies onthe characterization of prostanoid receptors: a proposed classification. *Prostaglandins***24**:667–689.

Kim JI, Lakshmikanthan V, Frilot N, Daaka Y (2010) Prostaglandin E_2 promotes lung cancer cell migration via EP_4-betaArrestin1-c-Src signalsome. *Mol Cancer Res* **8**:569-577.

Kiriyama M, Ushikubi F, Kobayashi T, Hirata M, Sugimoto Y and Narumiya S (1997) Ligand binding specificities of the eight types and subtypes of the mouse prostanoid receptors expressed in Chinese hamster ovary cells. *Br J Pharmacol* **122:**217–224.

Konstam MA, Weir MR, Reicin A, Shapiro D, Sperling RS, Barr E, Gertz BJ (2001) "Cardiovascular thrombotic events in controlled, clinical trials of rofecoxib". *Circulation* **104**:2280–2288.

Kukowska LJF, Bielinska AU, Johnson J, Splinder R, Tomalia DA and Baker JR (1996) Efficient transfer of genetic material into mammalian cells using Starburst polyamidoamine dendrimers. *Proc Natl Acad Sci USA* **93**:4897–4902.

Lawlor G, Doran PP, Macmathuna P, Murray DW (2010) MYEOV (myeloma overexpressed gene) drives colon cancer cell migration and is regulated by PGE_2. *J Exp Clin Cancer Res* **29**:81.

Lawrence RA, Jones RL and Wilson NH (1992) Characterization of receptors involved in the direct and indirect actions of prostaglandins E and I on the guineapig ileum. *Br J Pharmacol* **105:**271–278.

Lazarus M, Munday CJ, Eguchi N, Matsumoto S, Killian GJ, Kubata BK and Urade Y (2002) Immunohistochemical localization of microsomal PGE synthase-1 and cyclooxygenases in male mouse reproductive organs. *Endocrinology* **143**:2410-2419.

Levy GN (1997) Prostaglandin H synthases, nonsteroidal anti-inflammatory drugs, and colon cancer. *FASEB J* **11**: 234–247.

Li W, Llopis J, Whitney M, Zlokarnik G, Tsien RY (1998) Cell-permeant caged InsP3 ester shows that Ca^{2+} spike frequency can optimize gene expression. *Nature* **392**:936–941.

Lin YZ, Deng H and Ruan KH (2000) Topology of catalytic portion of prostaglandin I(2) synthase: identification by molecular modeling-guided site-specific antibodies. Arch Biochem Biophys **379**:188-197.

Liu CH, Chang SH, Narko K, Trifan OC, Wu MT, Smith E, Haudenschild C Lane TF and Hla T (2001) Overexpression of cyclooxygenase-2 is sufficient to induce tumorigenesis in transgenic mice. *J Biol Chem* **276**:18563–18569.

Mancini JA, Blood K, Guay J, Gordon R, Claveau D, Chan C C and Riendeau D (2001) Cloning, expression, and up-regulation of inducible rat prostaglandin e synthase during lipopolysaccharide-induced pyresis and adjuvant-induced arthritis. *J Biol Chem* **276**:4469-4475.

Marion D, Ikura M, Tschudin R, Bax A (1989) Rapid recording of 2D NMR spectra withoutphase cycling. Application to the study of hydrogen exchange in proteins. *J Magn Reson* **85**:393-399.

Marnett LJ (1992) Aspirin and the potential role of prostaglandins in colon cancer. *Cancer Res* **52**:5575-5589.

Maruyama Y, Inooka G, Li YX, Miyashita Y, Kasai H (1993) Agonist-induced localized Ca^{2+} spikes directly triggering exocytotic secretion in exocrine pancreas. *EMBO J* **12**: 3017–3022.

Matsuoka Y, Furuyashiki T, Bito H, Ushikubi F, Tanaka Y, Kobayashi T, Muro S, Satoh N, Kayahara T, Higashi M, Mizoguchi A, Shichi H, Fukuda Y, Nakao K and Narumiya S

(2003) Impaired adrenocorticotropic hormone response to bacterial endotoxin in mice deficient in prostaglandin E receptor EP_1 and EP_3 subtypes. *Proc Natl Acad. Sci U S A* **100**:4132–4137.

Merrifield RB, Vizioli LD, Boman HG (1982) Synthesis of the antibacterial peptide cecropin A. *Biochemistry* **21**: 5020–5031.

Miyauchi Y (1994) Treatment of the peripheral vascular diseases with prostaglandin. *Nippon Rinsho* **52**:2182-2186.

Mizushima Y, Yanagawa A, Hoshi A (1983) Prostaglandin E_1 is more effective, when incorporated in lipid microspheres, for treatment of peripheral vascular diseases in man. *J Pharm Pharmacol* **35**:666–667.

Mons N, Decorte L, Jaffard R, Cooper DM (1998) Ca^{2+} sensitive adenylyl cyclases, key integrators of cellular signaling. *Life Sci* **62**:1647–1652.

Moore WT, Caprioli RM, Villafranca JJ (1991) Techniques in protein chemistry. *Academic Press, New York*, pp. 511–528.

Murakami M and Kudo I (2006) Prostaglandin E synthase: a novel drug target for inflammation and cancer. *Curr Pharm Des* **12**:943-954.

Murakami M, Nakatani Y, Tanioka T and Kudo I (2002) Prostaglandin E synthase. Prostaglandins. *Other Lipid Mediat* **68-69**:383-399.

Murakami M, Naraba H, Tanioka T, Semmyo N, Nakatani Y, Kojima F, Ikeda T, Fueki M, Ueno A, Oh-Ishi S and Kudo I (2000) Regulation of prostaglandin E_2 biosynthesis

by inducible membrane-associated prostaglandin E_2 synthase that acts in concert with cyclooxygenase-2. *J Biol Chem* **275**:32783-32792.

Murota H, Kotobuki Y, Umegaki N, Tani M, Katayama I (2008) New aspect of anti-inflammatory action of lipo-prostaglandin E_1 in the management of collagen diseases-related skin ulcer. *Rheumatol Int* **28**:1127-1135.

Namba T, Sugimoto Y, Negishi M, Irie A, Ushikubi F, Kakizuka A et al. (1993). Alternative splicing of C-terminal tail of prostaglandin E receptor subtype EP3 determines G-protein specificity. *Nature* **365**: 166–170.

Naraba H, Yokoyama C, Tago N, Murakami M, Kudo I, Fueki M, Oh-Ishi S and Tanabe T (2002) Transcriptional regulation of the membrane-associated prostaglandin E_2 synthase gene. Essential role of the transcription factor Egr-1. *J Biol Chem* **277**:28601-28608.

Narumiya S, Sugimoto Y and Ushikubi F. (1999) Prostanoid Receptors: Structures, Properties, and Functions. *Physiol Rev* **79**:1193–1226.

Nemoto K, Pilbeam CC, Bilak S, Raisz L (1997) Molecular cloning and expression of the rat prostaglandin E2 receptor of the EP2 subtype. *Prostaglandins* **54**: 713–725.

Nilsson B, Abrahmsen L and Uhlen M (1985) Immobilization and purification of enzymes with staphylococcal protein A gene fusion vectors. *EMBO J* **4**:1075–1080.

Nishigaki N, Negishi M, Honda A, Sugimoto Y, Namba T, Narumiya S, Ichikawa A (1995) Identification of prostaglandin E receptor 'EP2' cloned from mastocytoma cells EP4 subtype. *FEBS Lett* **364**:339-341.

Nishigaki N, Negishi M, Ichikawa A (1996) Two Gs-coupled prostaglandin E receptor subtypes, EP_2 and EP_4, differ in desensitization and sensitivity to the metabolic inactivation of the agonist. *Mol Pharmacol* **50**: 1031–1037.

Nithipatikom K, Laabs ND, Isbell MA, Campbell WB (2003) Liquid chromatographic-mass spectrometric determination of cyclooxygenase metabolites of arachidonic acid in cultured cells. *J Chromatogr B Analyt Technol Biomed Life Sci* **785**:135−145.

North TE, Goessling W, Walkley CR, Lengerke C, Kopani KR, Lord AM, Weber GJ, Bowman TV, Jang IH, Grosser T, Fitzgerald GA, Daley GQ, Orkin SH, Zon LI (2007) Prostaglandin E_2 regulates vertebrate haematopoietic stem cell homeostasis. *Nature* **447**:1007-1011.

Okuda AE, Sakamoto K, Ezashi T, Miwa K, Ito S, Hayaishi O (1996) Suppression of prostaglandin E receptor signaling by the variant form of EP1 subtype. *J Biol Chem* **271**: 31255–31261.

Okuyama T, Ishihara S, Sato H, Rumi MA, Kawashima K, Miyaoka Y, Suetsugu H, Kazumori H, Cava CF, Kadowaki Y, Fukuda R, Kinoshita Y (2002) Activation of prostaglandin E_2-receptor EP_2 and EP_4 pathways induces growth inhibition in human gastric carcinoma cell lines. *J Lab Clin Med* **140**:92–102.

Oldfield S, Grubb BD, Donaldson LF (2001). Identification of a prostaglandin E2 receptor splice variant and its expression in rat tissues. *Prostaglandins Other Lipid Mediat* **63**: 165–173.

Oshima M, Dinchuk JE, Kargman SL, Oshima H, Hancock B, Kwong E, Trzaskos JM, Evans JF and Taketo MM (1996) Suppression of intestinal polyposis in Apc delta716 knockout mice by inhibition of cyclooxygenase 2 (COX-2). *Cell* **87**:803-809.

O'Sullivan TP, Vallin KS, Shah ST, Fakhry J, Maderna P, Scannell M, Sampaio AL, Perretti M, Godson C, Guiry PJ (2007) Aromatic lipoxin A_4 and lipoxin B_4 analogues display potent biological activities. *J Med Chem* **50**:5894-902.

Papps PJ, Fallek SR, Gracia A, Anaki CT, Back TL, Duran WK, Hobson RW 2nd (1995) Role of leukocyte activation in patients with venous stasis ulcers. *J Surg Res* **59**:553–559.

Parkinson JF (2006) Lipoxin and synthetic lipoxin analogs: an overview of anti-inflammatory functions and new concepts in immunomodulation. Inflamm Allergy Drug Targets. *Review* **5**:91-106.

Penolazzi L, Facciolo MC, Aguiari G, Senno LD, Piva R (1997) Direct transfection of polymerase chain reaction-generated DNA fragments into mammalian cells employing ethidium bromide indicator and ultrafiltration. *Anal Biochem* **248**:190-193.

Pierce KL and Regan JW (1998) Prostanoid receptor heterogeneity through alternative

Piva R, Bianchi N, Aguiari GL, Gambari R and del Senno L (1993) Sequencing of an RNA transcript of the human estrogen receptor gene: evidence for a new transcriptional event. *J Steroid Biochem Mol Biol* **46**:531–538.

Piva R, Lambertini E, Penolazzi L, Facciolo MC, Lodi A, Aguiari G, Nastruzzi C, del Senno L (1998) In vitro stability of polymerase chain reaction-generated DNA fragments in serum and cell extracts. *Biochem Pharmacol* **56**:703-708.

Poole EM, Hsu L, Xiao L, Kulmacz RJ, Carlson CS, Rabinovitch PS, Makar KW, Potter JD, Ulrich CM (2010) Genetic variation in prostaglandin E_2 synthesis and signaling, prostaglandin dehydrogenase, and the risk of colorectal adenoma. *Cancer Epidemiol Biomarkers Prev* **19**:547-557.

Rao CV, Rivenson A, Simi B, Zang E, Kelloff G, Steele V and Reddy BS (1995) Chemoprevention of colon carcinogenesis by sulindac, a nonsteroidal anti-inflammatory agent. *Cancer Res* **55**:1464-1472.

Rasmussen SG, Choi HJ, Rosenbaum DM, Kobilka TS, Thian FS, Edwards PC, Burghammer M, Ratnala VR, Sanishvili R, Fischetti RF, Schertler GF, Weis WI, Kobilka BK (2007) Crystal structure of human adrenergic beta 2 G-protein coupled receptor. *Nature* **450**:383–387.

Regan JW, Bailey TJ, Pepperl DJ, Pierce KL, Bogardus AM, Donello JE, Fairbairn CE, Kedzie KM, Woodward DF, Gil DW (1994) Cloning of a novel human prostaglandin

receptor with characteristics of the pharmacologically defined EP2 subtype. *Mol Pharmacol* **46**:213-220.

Reinhart WH, Muller O and Halter F (1983) Influence of long-term 16,16-dimethyl prostaglandin E2 treatment on the rat gastrointestinal mucosa. *Gastroenterology* **85**:1003-10010.

Rich TC and Karpen JW (2002) Review article: cyclic AMP sensors in living cells: what signals can they actually measure? *Ann Biomed Eng* **30**: 1088–1099.

Rich TC, Fagan KA, Tse TE, Schaack J, Cooper DM, Karpen JW (2001) A uniform extracellular stimulus triggers distinct cAMP signals in different compartments of a simple cell. *Proc Natl Acad Sci USA* **98**:13049–13054.

Ruan KH (2004) Advance in understanding the biosynthesis of prostacyclin and thromboxane A_2 in the endoplasmic reticulum membrane via the cyclooxygenase pathway. *Mini Rev Med Chem* **4**:639-647.

Ruan KH and Dogne´JM (2006) Implications of the molecular basis of prostacyclin biosynthesis and signaling in pharmaceutical designs. *Curr Pharm Des* **12**:925-41.

Ruan KH, Cervantes V and So SP (2009) Engineering of a novel hybrid enzyme: an anti-inflammatory drug target with triple catalytic activities directly converting arachidonic acid into the inflammatory prostaglandin E_2. *Protein Engineering Design & Selection* pp. 1–8.

Ruan KH, Deng H and So SP (2006) Engineering of a protein with cyclooxygenase and prostacyclin synthase activities that converts arachidonic acid to prostacyclin. *Biochemistry* **44**:14003-14011.

Ruan KH, Deng H, Wu J and So SP (2005) The N-terminal membrane anchor domain of the membrane-bound prostacyclin synthase involved in the substrate presentation of the coupling reaction with cyclooxygenase. *Arch Biochem Biophys* **435**:372-81.

Ruan KH, So SP, Cervantes V, Wu H , Wijaya C and Jentzen RR (2008) An active triple-catalytic hybrid enzyme engineered by linking cyclo-oxygenase isoform-1 to prostacyclin synthase that can constantly biosynthesize prostacyclin, the vascular protector. *FEBS J* **275**:5820-5829.

Ruan KH, So SP, Wu H and Cervantes V (2008) Large-scale expression, purification, and characterization of an engineered prostacyclin-synthesizing enzyme with therapeutic potential. *Arch Biochem Biophys* **480**:41-50.

Ruan KH, So SP, Wu J, Li D, Huang A, Kung J (2001) Solution structure of the second extracellular loop of human thromboxane A_2 receptor. *Biochemistry* **40**:275–280.

Ruan KH, Stiles BG, Atassi MZ (1991) The short-neurotoxin-binding regions on the alpha-chain of human and Torpedo californica acetylcholine receptors. *Biochem J* **274**: 849– 854.

Rygaard J, Povlsen CO (1969) Heterotransplantation of a human malignant tumour to the mouse mutant ‘‘nude’’. *Acta Pathology Microbiol Scand* **77**:758–760.

Sambrook J, Fritsch EF and Maniatis T (1989) MolecularCloning: A Laboratory Manual, *ColdSpring Harbor Laboratory Press*, Plainview, NY, **2nd ed., pp**. 16.30–16.55.

Santori MI, Gonzalez C, Serrano L, Isalan M (2006) Localized transfection with magnetic beads coated with PCR products and other nucleic acids. *Nat Protoc* **1**:526-531.

Satoh K, Nagano Y, Shimomura C, Suzuki N, Saeki Y and Yokota H (2000) Expression of prostaglandin E synthase mRNA is induced in beta-amyloid treated rat astrocytes. *Neurosci Lett* **283**:221-223.

Scanlon KJ, Ohta Y, Ishida H, Kijima H, Ohkawa T, Kaminski A, Tsai J, Horng G and Kashani-Sabet M (1995) Oligonucleotide-mediated modulation of mammalian gene expression. *FASEB J* **9**:1288-1296.

Schmid A, Thierauch K, Schleuning W, Dinter H (1995) Splice variants of the human EP3 receptor for prostaglandin E2. *Eur J Biochem* **15**: 23–30.

Sheng H, Shao J, Kirkland SC, Isakson P, Coffey RJ, Morrow J, Beauchamp RD and DuBois, RN (1997) Inhibition of human colon cancer cell growth by selective inhibition of cyclooxygenase-2. *J Clin Invest* **99**:2254-2259.

Sheng H, Shao J, Washington MK and DuBois RN (2001) Prostaglandin E_2 increases growth and motility of colorectal carcinoma cells. *J Biol Chem* **276**:18075-18081.

Shoji Y, Takahashi M, Kitamura T, Watanabe K, Kawamori T, Maruyama T, Sugimoto Y, Negishi M, Narumiya S, Sugimura T, Wakabayashi K (2004) Downregulation of prostaglandin E receptor subtype EP3 during colon cancer development. *Gut* **53**:1151-1158.

So SP, Wu J, Huang G, Huang A, Li D and Ruan KH (2003) Identification of residues important for ligand binding of thromboxane A_2 receptor in the second extracellular loop using the nmr experiment-guided mutagenesis approach. *The Journal Of Biological Chemistry* **278**:10922–10927.

Sobota RM, Müller PJ, Heinrich PC, Schaper F (2008) Prostaglandin E_1 inhibits IL-6-induced MCP-1 expression by interfering specifically in IL-6-dependent ERK1/2, but not STAT3, activation. *Biochem J* **412**:65-72.

Steel GG, Courtenay VD, Peckham MJ (1983) The response to chemotherapy of a variety of human tumour xenografts. *British Journal of Cancer* **47**:1–13.

Stichtenoth DO, Thoren S, Bian H, Peters-Golden M, Jakobsson PJ and Crofford LJ (2001) Microsomal prostaglandin E synthase is regulated by pro-inflammatory cytokines and glucocorticoids in primary rheumatoid synovial cells. *J Immunol* **167**:469-474.

Stillman BA, Breyer MD, Breyer RM (1999) Importance of the extracellular domain for prostaglandin EP (2) receptor function. *Mol Pharmacol* **56**: 545–551.

Su JL, Shih JY, Yen ML, Jeng YM, Chang CC, Hsieh CY (2004) Cyclooxygenase-2 induces EP1- and HER-2/Neu-dependent vascular endothelial growth factor-C up-regulation: a novel mechanism of lymph angiogenesis in lung adenocarcinoma. *Cancer Res* **64**:554–564.

Subbaramaiah K, Telang N, Ramonetti JT, Araki R, DeVito B, Weksler BB and Dannenberg AJ (1996) Transcription of cyclooxygenase-2 is enhanced in transformed mammary epithelial cells. *Cancer Res* **56**:4424-4429.

Sugimoto Y and Narumiya S (2007) Prostaglandin E Receptors. *The Journal Of Biological Chemistry* **282**: 11613–11617.

Sugimoto Y, Nakato T, Kita A, Hatae N, Tabata H, Tanaka S et al (2003) Functional domains essential for Gs activity in prostaglandin EP_2 and EP_3 receptors. *Life Sci* **74**: 135–141.

Sugimoto Y, Nakato T, Kita A, Takahashi Y, Hatae N, Tabata H et al. (2004). A cluster of aromatic amino acids in the i2 loop plays a key role for Gs coupling in prostaglandin EP2 and EP3 receptors. *J Biol Chem* **279**: 11016–11026.

Sugimoto Y, Namba T, Honda A, Hayashi Y, Negishi M, Ichikawa A and Narumiya S (1992) Cloning and expression of a cDNA for mouse prostaglandin E receptor EP_3 subtype. *J Biol Chem* **267**:6463–6466.

Sugimoto Y, Negishi M, Hayashi Y, Namba T, Honda A, Watabe A, Hirata M, Narumiya S, and Ichikawa A (1993) Two isoforms of the EP_3 receptor with different carboxyl-

terminal domains and identical ligand binding properties and different coupling properties with Gi proteins. *J Biol Chem* **268**:2712–2718.

Takiguchi T, Kobayashi M, Nagashima C, Yamaguchi A, Nishihara T, Hasegawa K (1999) Effect of prostaglandin E_2 on recombinant human bone morphogenetic protein-2-stimulated osteoblastic differentiation in human periodontal ligament cells. *J Periodontal Res* **34**:431–436.

Tamma G, Wiesner B, Furkert J, Hahm D, Oksche A, Schaefer M, Valenti G, Rosenthal W, Klussmann E (2003) The prostaglandin E_2 analogue sulprostone antagonizes vasopressin-induced antidiuresis through activation of Rho *J Cell Sci* **116**:285–294.

Tanikawa N, Ohmiya Y, Ohkubo H, Hashimoto K, Kangawa K, Kojima M, Ito S and Watanabe K (2002) Identification and characterization of a novel type of membrane-associated prostaglandin E synthase. *Biochem Biophys Res Commun* **291**:884-889.

Tanioka T, Nakatani Y, Semmyo N, Murakami M and Kudo I (2000) Molecular identification of cytosolic prostaglandin E_2 synthase that is functionally coupled with cyclooxygenase-1 in immediate prostaglandin E_2 biosynthesis. *J Biol Chem* **275**:32775-32782.

Thorat MA, Morimiya A, Mehrotra S, Konger R, Badve SS (2008) Prostanoid receptor EP_1 expression in breast cancer. *Mod Pathol* **21**:15-21.

Toh H, Ichikawa A and Narumiya S (1995) Molecular evolution of receptor for eicosanoids. *FEBS Lett* **361:**17–21.

Toyota T, Hiretea Y, Ikeda Y and Miaush Y& Matsuoka' K, Sakuma A (1993) Lipo-PGE_1, A New Lipid-Encapsulated Preparation Of Prostaglandin E_1: Placebo-And Prostaglandin El-Controlled Multicentbr Trials In Patients With Diabetic Neuropathy And Leg Ulcers .*Prostaglandins* **461**:453-468.

Tsujii M, Kawano S, Tsuji S, Sawaoka H, Hori M and DuBois RN (1998) Cyclooxygenase regulates angiogenesis induced by colon cancer cells. *Cell* **93**:705–716.

Uematsu S, Matsumoto M, Takeda K and Akira S (2002) Lipopolysaccharide-dependent prostaglandin E(2) production is regulated by the glutathione-dependent prostaglandin E(2) synthase gene induced by the Toll-like receptor 4/MyD88/NF-IL6 pathway. *J Immunol* **168**:5811-5816.

Ungrin MD, Carriere M-C, Denis D, Lamontagne S, Sawyer N, Stocco R, Tremblay N, Metters KM and Abramovitz M (2001) Determination of the key structural features of prostaglandin E_2 and prostanoid analogs involved in binding and activation of the human EP_1 prostanoid receptor. *Mol Pharmacol* **59**:1446-1456.

Ushikubi F, Segi E, Sugimoto Y, Murata T, Matsuoka T, Kobayashi T, Hizaki H, Tuboi K, Katsuyama M, Ichikawa A, Tanaka T, Yoshida N, and Narumiya S (1998) Impaired febrile response in mice lacking the prostaglandin E receptor subtype EP_3. *Nature* **395**:281–284.

Wagner R (1994) Gene inhibition using antisense oligodeoxynucleotides. Nature **372**:155–163.

Watabe A, Sugimoto Y, Honda A, Irie A, Namba T, Negishi M, Ito S, Narumiya S and Ichikawa A (1993) Cloning and expression of cDNA for a mouse EP_1 subtype of prostaglandin E receptor. *J Biol Chem* **268**:20175–20178.

Watanabe K, Kawamori T, Nakatsugi S, Ohta T, Ohuchida S, Yamamoto H (1999) Role of the prostaglandin E receptor subtype EP_1 in colon carcinogenesis. *Cancer Res* **59**:5093–5096.

Williams CS, Mann M and DuBois RN (1999) The role of cyclooxygenases in inflammation, cancer, and development. *Oncogene* **18**:7908–7991.

Yamagata K, Matsumura K, Inoue W, Shiraki T, Suzuki K, Yasuda S, Sugiura H, Cao C, Watanabe Y and Kobayashi S (2001) Coexpression of microsomal-type prostaglandin E synthase with cyclooxygenase-2 in brain endothelial cells of rats during endotoxin-induced fever. *J Neurosci* **21**:2669–2677.

Yamamoto Y and Imai YN (1996) Modelling of thromboxane A2 and prostaglandin receptors: analysis of receptor-ligand interactions and application to drug design, in Structure and Function of 7TM Receptors (Schwartz TW, Hjorth SA and Sandholm Kastrup J eds) pp 328–338, Munksgaard, Copenhagen.

Yang J, Xia M, Goetzl E, Songzhu A (1994) Cloning and expression of the EP3-subtype of human receptors for prostaglandin E2. *Biochem Biophys Res Commun* **198**: 999–1006.

Yang P, Felix E, Madden T, Fischer SM, Newman RA (2002) Quantitative high-performance liquid chromatography/electrospray ionization tandem mass spectrometric analysis of 2- and 3-series prostaglandins in cultured tumor cells. *Anal Biochem* **308**:168−177.

Yano T, Zissel G, Muller QJ, Jae SS, Satoh H, Ichikawa T (2002) Prostaglandin E_2 reinforces the activation of Ras signal pathway in lung adenocarcinoma cells via EP_3. *FEBS Lett* **518**:154–158.

Yoshimatsu K, Altorki NK, Golijanin D, Zhang F, Jakobsson PJ, Dannenberg AJ and Subbaramaiah K (2001) Inducible prostaglandin E synthase is overexpressed in non-small cell lung cancer. *Clin Cancer Res* **7**:2669-2674.

Yoshimatsu K, Golijanin D, Paty PB, Soslow RA, Jakobsson PJ, DeLellis RA, Subbaramaiah, K and Dannenberg AJ (2001) Inducible microsomal prostaglandin E synthase is overexpressed in colorectal adenomas and cancer. *Clin Cancer Res* **7**:3971-3976.

Zhang L, Huang G, Wu J, Ruan KH (2005) A profile of the residues in the first intracellular loop critical for Gs-mediated signaling of human prostacyclin receptor characterized by an integrative approach of NMR-experiment and mutagenesis. *Biochemistry* **44**:11389-11401.